ERYTHRO-9-(2-HYDROXY-3-NONYL)ADENINE (EHNA) BLOCKS DIFFERENTIATION AND MAINTAINS THE EXPRESSION OF PLURIPOTENCY MARKERS IN HUMAN EMBRYONIC STEM CELLS

Peter Burton[1], David R. Adams[2], Achamma Abraham[2], Robert W. Allcock[2], Zhong Jiang[2], Angela McCahill[1], Jane Gilmour[1], John McAbney[1], Alexandra Kaupisch[1], Nicole M. Kane[3], George S. Baillie[1], Andrew H. Baker[3], Graeme Milligan[1], Miles D. Houslay[1] and Joanne C. Mountford[1].

From [1]Neuroscience and Molecular Pharmacology, Faculty of Biomedical and Life Sciences (FBLS), and [3]Glasgow Cardiovascular Research Centre, Faculty of Medicine, University of Glasgow, Glasgow G12 8QQ, Scotland, UK; [2]Department of Chemistry, Heriot-Watt University, Riccarton Campus, Edinburgh EH14 4AS, Scotland, UK

Short title: EHNA maintains hESC pluripotency

Address correspondence to Dr J C Mountford, Neuroscience and Molecular Pharmacology, Faculty of Biomedical and Life Sciences (FBLS), University of Glasgow, Glasgow G12 8QQ Scotland, UK. Email : j.mountford@bio.gla.ac.uk; Phone : +44 141 330 7212

Abbreviations: hESCs, Human embryonic stem cells; EHNA, *erythro*-9-(2-hydroxy-3-nonyl)adenine; bFGF, basic fibroblast growth factor; ADA, Adenosine deaminase; LIF, leukaemia inhibitory factor; GSK3β, glycogen synthase kinase 3 beta; PDE**,** phosphodiesterases; IBMX, isobutylmethylxanthine; AICAR, 5-aminoimidazole-4-carboxamide riboside; ABT-702, 4-amino-5-(3-bromophenyl)-7-(6-morpholinopyridin-3-yl)pyrido[2,3-*d*]pyrimidine; NECA, 5'-*N*-ethylcarboxamidoadenosine, THEO, theophylline; NF, exogenous FGF-free medium; NFE, exogenous FGF-free medium containing 10uM EHNA.

Keywords: Human embryonic stem cells; EHNA; Differentiation; ell culture; Adenosine Deaminase; Fibroblast Growth Factor

SYNOPSIS

Human embryonic stem cells (hESCs) have enormous potential for use in pharmaceutical development and therapeutics, however to realise this potential there is a requirement for simple and reproducible cell culture methods that provide adequate numbers of cells of suitable quality. We have discovered a novel way of blocking the spontaneous differentiation of hESCs in the absence of exogenous cytokines by supplementing feeder-free conditions with *erythro*-9-(2-hydroxy-3-nonyl)adenine (EHNA), an established inhibitor of adenosine deaminase (ADA) and cyclic nucleotide phosphodiesterase- 2 (PDE2). hESCs maintained in feeder-free conditions with EHNA for more than 10 passages showed no reduction in hESC associated markers including NANOG, POU5F1 and SSEA 4 compared to cells maintained in feeder-free conditions containing basic fibroblast growth factor (bFGF). Spontaneous differentiation was reversibly suppressed by the addition of EHNA, but upon removing EHNA hESC populations underwent efficient spontaneous, multi-lineage and directed differentiation. EHNA also acts as a strong blocker of directed neuronal differentiation. Chemically distinct inhibitors of ADA and PDE2 lacked the capacity of EHNA to suppress hESC differentiation, suggesting that the effect is not driven by inhibition of either ADA or PDE2. Preliminary structure activity relationship analysis found the differentiation blocking properties of EHNA to reside in a pharmacophore comprised of a close adenine mimetic with an extended hydrophobic substituent in the 8- or 9-position. We conclude that EHNA and simple 9-alkyladenines can block directed neuronal and spontaneous differentiation in the absence of exogenous cytokine addition, and may provide a useful replacement for bFGF in large scale or cGMP compliant processes.

INTRODUCTION

Human embryonic stem cells (hESCs) can be maintained in an undifferentiated state whilst remaining capable of differentiating to all cell types in the body [1, 2], as such, they have huge potential both as research tools and for cell therapies. In order to fully exploit this potential we must understand how to efficiently maintain hESCs in this self-renewing, pluripotent state. A large body of evidence indicates that the three transcription factors POU5F1, NANOG and SOX2 constitute the core transcriptional regulatory circuit that determines the fate of ESCs [3-7]. Expression levels of POU5F1/NANOG/SOX2 and their target genes are crucial in imposing stem cell identity and controlling differentiation [8], and therefore it is critical for any culture system to maintain appropriate expression of this network. Methods to suppress spontaneous differentiation and maintain pluripotent hESCs vary greatly and utilise either feeder cells, feeder-conditioned media [9] or different combinations of cytokines (including high concentrations of bFGF [10, 11], TGF-β/NODAL/ACTIVIN signalling molecules [12-14] or bone morphogenic protein (BMP) suppressors such as noggin [10, 15]).

Small-molecule chemicals have been used in attempts to replace exogenous cytokines, in particular glycogen synthase kinase 3 beta (GSK3β) inhibitors, which stimulate the canonical Wnt/β-catenin axis, have been widely used to maintain pluripotency in mESC and in some hESC studies [16]. Additionally, Ying *et al* found that stimulation of cells by exogenous growth factors was not required for the maintenance of pluripotency in mouse ESCs, instead suppression of pro-differentiation signals – by inhibiting mitogen-activated protein kinase (MAPK), GSK-3β and FGF signaling – was sufficient to maintain self-renewal and pluripotency [17]. Thus, rather than using combinations of complex growth factors to stimulate self-renewal, protecting the cells from pro-differentiation factors or using small-molecule inhibitors of differentiation may provide viable alternatives for the maintenance of hESCs. Given the importance of the core transcriptional network in both maintaining and inducing pluripotency, the discovery of small molecules that can maintain the expression of these transcription factors, either in the presence of differentiation cues or in the absence of maintenance factors such as exogenous FGF, would be a valuable asset to the field and a further step towards unraveling the mechanisms of pluripotency.

Cyclic nucleotides are pivotal second messengers that influence a number of critical events including cell cycle and differentiation processes. Cyclic nucleotide phosphodiesterases (PDEs) provide the sole means of degrading cAMP and cGMP in cells with selective inhibitors shown to provide powerful reagents to manipulate specific cellular events and act as therapeutic agents [18]. With this in mind we analysed the effect of a range of inhibitors selective for major PDE families on hESC differentiation. From this we discovered that *erythro*-9-(2-hydroxy-3-nonyl)adenine (EHNA), an inhibitor of both the dual specificity cAMP/cGMP-phosphodiesterase, PDE2 [19] and adenosine deaminase (ADA) [20], maintains the expression of hESC pluripotency markers even when cells are cultured under differentiating conditions. Moreover, EHNA also prevents differentiation and maintains pluripotency when exogenous FGF is removed from a supportive culture system. It thus provides a simple chemical entity that is capable of blocking the differentiation of hESCs.

EXPERIMENTAL

Cell culture and differentiation

The SA121 hES cell line [21], (Cellartis AB, Dundee, UK) was cultured in feeder-free conditions on fibronectin and enzymatically passaged with TrypLE Select (Invitrogen). The fully supportive media used to maintain the hESCs was a 1:1 mixture of defined media [22] and conditioned VitrohES (VitroLife, Gothenburg, Sweden). VitrohES was conditioned for 24 h on mitotically inactivated mouse embryonic fibroblasts (MEF) with no addition of FGF. SA461 hES cells [21] (Cellartis AB) were maintained on MEFs and used to test whether EHNA supports the change from feeders to feeder-free

culture (Figure 1a). Routine maintenance used bFGF (Invitrogen) at a final concentration of 10 ng/ml unless stated otherwise. For passive differentiation cells were passaged onto Matrigel (BD Biosciences, Oxford, UK) in fully supportive media, changed to defined medium supplemented with experimental components 24 h later and thence changed daily. Cytogenetic analyses confirmed a normal karyotype in cells grown in the presence of EHNA for either 10 or 20 passages, or with HWC57 or HWC64 for 22 passages (Supplemental Figure 7).

Erythro-9-(2-hydroxy-3-nonyl)adenine (EHNA) was used at 10 μM unless otherwise stated (Merck Chemicals Ltd., Nottingham, UK). Other compounds were purchased from Merck or Sigma-Aldrich except BAY-60-7550 (Axxora). A range of EHNA analogues were synthesized; compound structures and synthetic procedures are detailed in the Supplemental Chemistry section. Neuronal differentiation was carried out as described previously [23]. Briefly, cells were seeded onto Matrigel (BD Biosciences) in 1:1 mix of Advanced D-MEM/F12 containing N2 supplement, and Neurobasal supplemented with B27 (all Invitrogen) containing 100 ng/ml mouse recombinant Noggin (R&D Systems). Cells were allowed to reach confluence and passaged using collagenase (Invitrogen) after 2 weeks.

Quantitative PCR

RNA was extracted and cDNA prepared as previously described [24]. Gene-specific assays were used for DNMT3b, KLF4, TEAD4 and POU5F1 (Applied Biosystems (AB)); other primer and probe sets were from MWG (Ebersberg, Germany). Biological and technical triplicates were performed for each sample, standardised to GAPDH and relative expression values calculated. The human stem cell pluripotency Taqman Low Density Array (TLDA) was also used with the 7900HT system (AB).

Immunocytochemistry

Cells were incubated at 4°C overnight with the following antibodies in 10% goat serum (Sigma-Aldrich)/PBS: mouse anti-POU5F1 (1:250) (Santa Cruz Biotech., California, USA), rabbit anti-PAX6 (1:1000) (Millipore Ltd, Herts, UK), mouse anti β-tubulin III (1:1000), mouse anti-Alpha-feta-protein (AFP) (1:400) (Sigma-Aldrich), mouse anti-muscle-specific actin (SMA) (1:50) (Dako, Denmark), SSEA1 (1:5), SSEA3 (1:5) (Hybridoma Bank University of Iowa), SSEA4 (1:5) (Hybridoma Bank University of Iowa), Tra1-60 (1:200) and Tra1-80 (1:200) (Santa Cruz Biotech.). Secondary antibodies were Alexa fluor 555 goat anti-rabbit IgG (1:400) or Alexa fluor 488 goat anti-mouse IgG (1:400) and cells were mounted using Prolong Gold containing DAPI (all Invitrogen). All immunofluorescence was visualised and captured using Zeiss Axiovision image analysis system.

RESULTS

EHNA prevents differentiation and maintains the expression of stem cell markers in the absence of exogenous FGF during feeder-free growth.

The capacity of EHNA to maintain stem cell characteristics and block spontaneous differentiation in feeder-free and FGF-free conditions was evaluated by incubating hESCs (Cellartis line SA121) [21] in standard feeder-free conditions without exogenous FGF (including conditioned medium made without the addition of exogenous FGF) but supplemented with 10 μM EHNA (No FGF/+EHNA medium; NFE). Cells were initially seeded from a trypsin passage of a standard, FGF-containing, feeder-free culture. Control cells grown without FGF or EHNA (No FGF medium; NF) had reduced stem cell marker (NANOG and POU5F1) expression by passage 3 and showed clear differentiated morphology by passage 8-10, whereas those grown in the presence of EHNA retained a normal stem cell morphology and marker expression to at least passage 10 (Figure 1a) and, in extended experiments, for as long as 30 passages. In addition to expressing POU5F1, cells maintained in EHNA for 10 passages also expressed the cell surface markers SSEA3, SSEA4, TRA-160 and TRA-180, but were negative for the differentiation marker SSEA1 (Figure 1b). This marker profile strongly indicated the maintenance of a pluripotent phenotype.

To determine if prior adaptation to feeder-free conditions is required for EHNA to block the differentiation of hESCs in the absence of FGF, a culture of the hESC line SA461 was transferred directly from a supportive MEF feeder layer, using manual dissection, to NFE medium. After multiple passages the EHNA-containing cultures were still almost 100% positive for POU5F1 whereas POU5F1 staining in the cultures grown in NF medium was minimal (Figure 1a). This indicates that pre-adaptation to feeder-free conditions was not required for EHNA to block the differentiation of hESCs in the absence of FGF and that the effect of EHNA can be seen in a second hESC line..

Real time qRT-PCR analysis showed that at passage 8 in NF medium cells had greatly down-regulated the expression of NANOG, POU5F1 and SOX2 in comparison to hESCs grown in standard feeder-free culture (containing FGF), or to cells grown with EHNA (NFE) (Figure 1c). The NF-cultured cells also showed an increase in the expression of a variety of differentiation markers from multiple germ layers, particularly those associated with trophoectoderm formation (Supplemental Figure 1). In contrast, EHNA (NFE medium) maintained an expression profile similar to that of cells in standard feeder-free culture and maintained that pattern for at least 30 passages (Supplemental Figure 2).

Cells maintained in EHNA retain the capacity for in vitro differentiation to all three germ layers.
It is important that any component of stem cell medium that maintains a pluripotent phenotype does not permanently block differentiation of the cells. Therefore, to determine if chronic exposure to EHNA still allowed for subsequent differentiation, cells that had been in the EHNA-containing, NFE medium for either 10 passages (Figure 2) or >20 passages (Supplemental Figure 3) were allowed to differentiate passively. After 4 weeks cells were analysed for PAX6 (ectoderm), alpha-feta protein (AFP) (endoderm) and smooth muscle actin (SMA) (mesoderm) in order to detect differentiation to all three germ layers. Cells staining positive for three germ layers were readily detected (Figure 2 and Supplemental Figure 3). This indicates that, at least *in vitro*, cells grown in EHNA for over 10 passages retain functional pluripotency.

In order to understand whether pre-treatment with EHNA has any effect on the dynamics of induced, rather than spontaneous, differentiation cells that had been maintained in either EHNA or FGF for five passages were transferred into neuronal differentiation conditions [23]. Analysis over the time-course demonstrated that expression of PAX6 increased and NANOG decreased similarly in both EHNA-treated and control cultures, although we did observe that there was slight retardation of the NANOG down-regulation in EHNA-maintained cells (Figure 3a-b). Immunofluorescent staining at the 16 day time point also indicated that cells grown previously on EHNA express PAX6 protein and down-regulate POU5F1 (Figure 3c-d).

EHNA maintains the expression of the core stem cell transcriptional factors in differentiating conditions.
In order to test the direct effect of EHNA in maintaining pluripotent genes and blocking differentiation, cells maintained in full feeder-free media were subjected to neuronal differentiation conditions in the presence of various doses of EHNA throughout the neuronal differentiation. As illustrated in Figure 4a, EHNA caused a dose-dependent reduction in the proportion of cells staining positively for PAX6 with 10 μM EHNA completely eliminating PAX6. Additionally, qRT-PCR analysis (Figure 4b-e), showed that the pluripotent markers NANOG, POU5F1 and ZFP42 were all maintained by the presence of EHNA. This ability of EHNA to block differentiation was sustained over at least 6 weeks of neuronal induction (Figure 4f). Thus, EHNA exerts a dramatic anti-differentiation effect even in the presence of established differentiating conditions.

EHNA does not suppress hESC differentiation by inhibition of PDE2.
In order to investigate the basis for EHNA's anti-differentiation effect, we set out to exploit the capacity of EHNA to suppress passive differentiation in defined media. We evaluated the maintenance of NANOG and suppression of PAX6 expression as means of defining whether compounds with related enzyme-inhibitory activity to EHNA acted similarly on hESCs. In this regard, EHNA is an established inhibitor of both adenosine deaminase [20] and PDE2 [19, 25]. In order to evaluate whether the effect of EHNA was due to PDE2 inhibition, the specific PDE2 inhibitor, BAY-60-7550

(BAY) [26, 27] and the pan-cyclic nucleotide PDE inhibitor, 3-isobutyl-1-methylxanthine (IBMX) [25], were each separately added to cultures undergoing passive differentiation (as above). In contrast to EHNA, treatment with neither BAY nor IBMX maintained stem cell marker expression in differentiating conditions (Figure 5a); nor did they inhibit PAX6 induction (Figure 5b). This strongly suggests that PDE2 inhibition is not the mechanism whereby EHNA maintains hESC pluripotency.

EHNA does not suppress hESC differentiation by inhibition of adenosine deaminase.
EHNA is also an established ADA inhibitor and, as such, it causes the accumulation of adenosine and deoxyadenosine, resulting in pleiotropic effects upon the cell [20, 28-32]. To determine whether the effects of EHNA are mediated by phosphorylated metabolites of adenosine, an adenosine kinase inhibitor, ABT-702 (AKI), was used in conjunction with EHNA. After 2 weeks under passive differentiation conditions the effects of EHNA were not reduced by the concurrent inhibition of adenosine kinase (Figure 5c). Additionally, stimulation of AMPK with 5-aminoimidazole-4-carboxamide riboside (AICAR) did not mimic the effect of EHNA. Thus, we concluded that phosphorylation of adenosine is not necessary for the maintenance of pluripotency markers by EHNA.

Accumulation and export of adenosine and deoxyadenosine can, in principle, lead to activation of the adenosine receptors. To investigate whether adenosine receptor activation is responsible for the maintenance of hESC pluripotency markers by EHNA, we evaluated whether 5'-*N*-ethylcarboxamidoadenosine (NECA), a pan-adenosine receptor agonist, and the non-selective PDE inhibitor and adenosine receptor antagonist, theophylline, could ablate the effect of EHNA. Neither agent, had any effect on the expression of hESC pluripotency markers in the presence or absence of EHNA (Figure 5c). Similarly, targeting individual adenosine receptor subtypes with specific antagonists in addition to EHNA had no effect (Figure 5d). Hence, adenosine receptor activity is unlikely to underpin EHNA's action on hESCs.

To further investigate whether the effect of EHNA might still be driven by ADA inhibition, we sourced or synthesised a panel of structurally diverse compounds (Figure 6; Supplemental Figures 4 and 5) known to possess widely varying degrees of ADA-inhibitory activity. Critically, there was no correlation between ADA-inhibitory activity and the capacity of these compounds to maintain pluripotency-associated factors and to suppress PAX6 expression. Some compounds with potent ADA-inhibitory activity failed to show any EHNA-like effect. Pentostatin, an exceptionally potent ADA-inhibitor (K_i = 2.5 pM for ADA) [33], lacked any effect at concentrations of up to 100 μM even in combination with the PDE2 inhibitor, BAY-60-7550 (data not shown). Similarly, *erythro*-1-(2-hydroxynonan-3-yl)-1*H*-imidazole-4-carboxamide (HWC-36), an analogue of EHNA with a truncated adenine ring, showed no capacity to maintain NANOG or to suppress PAX6 expression at a concentration of 10 μM, despite possessing potent ADA-inhibitory action (K_i = 35 nM *vs* 7 nM for EHNA) [34]. However, a series of 2-alkyl-2*H*-pyrazolo[3,4-*d*]pyrimidin-4-amine ADA inhibitors described by Da Settimo *et al.* [35] did exhibit EHNA-like maintenance activity. The octyl, nonyl, decyl and undecyl analogues in this series (Figure 6 and Supplemental Figure 4; respectively HWC-41, HWC-31, HWC-06 and HWC-33), with reported ADA-inhibitory K_i values of 530, 8.1, 0.13 and 0.47 nM, exhibited pronounced maintenance of the pluripotency marker, NANOG, coupled with a suppression of the differentiation marker, PAX6, when tested at 10 μM concentrations. Da Settimo *et al* [35] found the 1-alkyl-substituted isomers of their 2-alkylpyrazolopyrimidine series lacked significant ADA-inhibitory activity. However, we found that the octyl- and nonyl- analogues in the non-ADA-inhibitory 1-alkylpyrazolopyrimidine series (respectively HWC-40 and HWC-30) retained the differentiation-suppressive properties of their 2-alkyl isomers and of EHNA. As shown in Figure 7, HWC-30, like HWC-31 and HWC-33, maintained the expression of pluripotency genes whilst suppressing PAX6. Collectively these data strongly suggest that the action of EHNA on hESCs is not driven by ADA inhibition.

To investigate the possibility that EHNA and other active compounds may act through a protein kinase-inhibitory mode, EHNA, HWC-5 and HWC-6 were evaluated using the Protein Kinase Panel service of the MRC National Centre for Protein Kinase Screening (University of Dundee, UK). When tested at 30 μM, none of these compounds significantly inhibited any of the 80 kinases of the panel

(Supplemental Figure 6). This included GSK-3β[16], a number of ERK/MAPK pathway components [36] and FGF-R1 [37], which have all previously been shown to be important in hESC pluripotency.

Structure activity relationships for the differentiation blocking activity of EHNA

As EHNA did not appear to exert its action on hESCs through inhibition of either PDE2 or ADA, we undertook a preliminary structure activity relationship analysis by evaluating a wider set of EHNA analogues. The compounds assessed, Figure 6 (and detailed in full in the Supplemental Material) show that maintenance of NANOG and suppression of PAX6 requires a compound structure comprising a close adenine mimetic with an extended hydrophobic substituent in the 8- or 9-position. We found that the EHNA structure could be simplified by removal of the hydroxy group from the nonanol side chain, and deoxy-EHNA (HWC-57) retains activity comparable to EHNA itself. As a further step, we replaced the branched hydrocarbon chain of the latter compound with a straight chain *n*-decyl group to provide a compound [9-(decan-1-yl)adenine, HWC-64] that also retained the full action of EHNA on hESCs. In fact cells grown for 10 passages in FGF-free feeder-free conditions, but supplemented with either HWC-57 (10 μM) or HWC-64 (10 μM) show an equivalent morphology (Figure 8a) and gene expression pattern (Figure 8b) to those grown in FGF-containing supportive media. Cells without either FGF or HWC-57/HWC-64 show a strong differentiated morphology by passage 4 (Figure 8a). These data indicate that HWC-57 and HWC-64 are functionally equivalent to EHNA with regard to maintaining the markers of pluripotency in the absence of FGF.

The recently disclosed EHNA-ADA co-crystal structure reveals that its hydroxyl side chain contributes an important hydrogen bond to a histidine residue within the catalytic pocket [38]. The redundancy of this hydroxyl group in regard to the hESC differentiation blocking properties further supports the contention that this activity is not mediated through ADA inhibition. Thus, neither of the two established activities of EHNA, namely ADA inhibition and PDE2 inhibition, appear to be responsible for the maintenance of hESC pluripotency and suppression of differentiation. This implies a novel mechanism of action for which, although currently unidentified, we have provided preliminary structure activity relationships (SAR) by studying a range of EHNA analogues.

DISCUSSION

The regulation and maintenance of pluripotency in hESCs is still far from fully understood and there are multiple methods for cultivating hESCs in a pluripotent state. Traditionally hESCs have been cultivated on a mouse embryonic feeder layer [2] with further recent advances resulting in feeder-free culture systems on extracellular matrix proteins, which may be recombinant or extracted [10-12, 14, 15]. However, hESCs cultured in these feeder-free systems lack the mainly undefined stimuli from the feeder cells that maintain these cells in a self-renewing, pluripotent state and therefore, additional recombinant growth factors must be added to replace the contribution of the feeder cells. The only growth factor that has been shown to be essential for the maintenance of pluripotency in the absence of feeder-layers or conditioned media is basic FGF (bFGF, FGF-2) [10, 37]. However other factors, including TGFβ, are also commonly used to either remove or reduce the need for high concentrations of bFGF and/or conditioned media [12-14]. Such recombinant growth factors have a plethora of effects and, when considering the potential for using pluripotent cell-derived tissues in the clinic, are difficult to obtain from current good manufacturing practice-qualified sources. Simple small molecule alternatives to growth factors for maintaining pluripotent hESCs would not only be more amenable to current good manufacturing practice-compliant use, but are likely to provide powerful new tools for trying to uncover the molecular basis of pluripotency.

We have demonstrated here that the spontaneous differentiation of hESCs in the absence of either feeder cells or exogenous cytokines can be blocked by the addition of EHNA. We have also shown that EHNA is sufficiently supportive in that cells could be directly switched from feeders into feeder-free culture without pre-adaptation to feeder-free culture containing exogenous FGF. Importantly, we found that chronic EHNA treatment did not 'lock' hESCs in an undifferentiated state, as the EHNA-treated cells were capable of multi-lineage differentiation when EHNA was removed. However, suppression of differentiation was sufficiently robust that when cells were switched into neuronal

inducing conditions, the continued addition of EHNA blocked PAX6 expression and maintained the pluripotent morphology and the markers NANOG, POU5F1 and ZPF42. Furthermore, through our structure activity relationship analysis, we discovered that simple 9-alkyladenines, such as HWC-57 and HWC-64, possess activity comparable to EHNA. These robust, stable compounds are readily prepared from commercially available starting materials at low cost in just two synthetic steps, and, as such, offer a very attractive alternative to the use of bFGF in large scale applications.

EHNA has a number of reported effects including the inhibition of PDE2 [19], but as we were unable mimic the effect of EHNA with either a structurally dissimilar PDE2 specific inhibitor (BAY-60-7550) [26] or the non-specific cyclic nucleotide PDE inhibitor IBMX [25] we can conclude that PDE2 inhibition does not account for the effect of EHNA in hESCs. EHNA has also been reported to reduce intracellular trafficking by inhibition of dynein. However, concentrations in the order of 100 μM are typically used for inhibiting dynein, because the EC_{50} value for this lies between 0.23 mM and ~1 mM [39, 40]. As we used EHNA at a maximum concentration of 10 μM and see significant effects at 1 μM, we believe that it is unlikely that EHNA acts through effects on dynein in hESCs. The inhibition of ADA by EHNA was a particularly interesting possibility because a deficiency of ADA can cause a multitude of effects on the cell including apoptosis, the inhibition of transmethylation and an accumulation of adenosine that can subsequently lead to the activation of AMPK and adenosine receptors [30, 41]. We therefore investigated whether the ADA-inhibitory activity of EHNA was essential to its capacity to block differentiation in hESCs via the accumulation of adenosine and autocrine activation of cell-surface receptors, but we could not mimic the effect of EHNA using adenosine receptor agonists. Neither could we ablate the effect of EHNA with adenosine receptor antagonists. A build up of the phosphorylated metabolites of adenosine was also not responsible for the EHNA effect. To further investigate the possibility of ADA inhibition being responsible we used a panel of established adenosine deaminase inhibitors that are chemically distinct from EHNA, and clearly demonstrated (Figures 6 & 7) that there is no link between the two activities. This leads us to believe that EHNA has an unidentified biological activity that is responsible for its ability to prevent hESC differentiation.

It is an interesting proposition that EHNA may be able to maintain pluripotent marker expression by blocking differentiation. Ying *et al.* proposed that mESCs actually exist in a basal self-maintaining state that can be perpetuated if shielded from differentiation-inducing signals [17]. Unlike mESCs, many of the intracellular signalling pathways in hESCs are as yet unidentified. Nevertheless, it is probable that they are conceptually similar to mESCs in that pluripotency can be maintained if the differentiating signals are removed or blocked. Our data show that EHNA is an efficient blocker of induced neuronal differentiation and of other lineages generated as cells differentiate passively after the removal of bFGF. It should also be noted that although feeder-free, the culture system contains a conditioned medium component. Therefore, whilst EHNA is an effective replacement for exogenous bFGF there may be a combinatorial effect with other conditioning factors in the medium.

It is therefore possible that EHNA might be used to maintain hESCs in a self-renewing ground state, regulated by NANOG expression, as has been described for mESCs treated with inhibitors of both GSK-3β and MAPK [17, 42]. This hypothesis is supported by our finding that cells maintained in EHNA retained the expression of the core transcription factors NANOG, POU5F1 and SOX2 to the same degree as those maintained by bFGF, whereas in control cultures from which bFGF was omitted these factors were dramatically down-regulated. Initial reports suggested that GSK3β inhibitors may have the same capacity to maintain self-renewal in hESCs as in mESCs [16]. In order to exclude the possibility that EHNA was acting by directly inhibiting common protein kinase intracellular signalling pathways, we subjected the molecule to a protein kinase screen and found that it did not significantly inhibit any of the kinases evaluated, including GSK-3β, a number of ERK/MAPK pathway components and the FGF receptor, FGF-R1.

In summary, we have found that a small-molecule additive, EHNA, blocks the differentiation of hESCs in the absence of exogenous cytokines or feeder cells and can be used during routine enzymatic passage of the cells without the loss of multi-lineage differentiation potential. We have defined a

pharmacophore for this action of EHNA, which is independent of its established PDE2- and ADA-inhibitory activities, and identified simpler compounds that possess comparable activity. The capacity of EHNA and these derivates to block hESC differentiation may make them useful tools for the manipulation of hESCs and provide an important set of reagents for characterising pathways involved in the maintenance of pluripotency or suppression of differentiation in these cells.

References.

1 Reubinoff, B. E., Pera, M. F., Fong, C. Y., Trounson, A. and Bongso, A. (2000) Embryonic stem cell lines from human blastocysts: somatic differentiation in vitro. Nat Biotechnol. **18**, 399-404

2 Thomson, J. A., Itskovitz-Eldor, J., Shapiro, S. S., Waknitz, M. A., Swiergiel, J. J., Marshall, V. S. and Jones, J. M. (1998) Embryonic stem cell lines derived from human blastocysts. Science. **282**, 1145-1147

3 Avilion, A. A., Nicolis, S. K., Pevny, L. H., Perez, L., Vivian, N. and Lovell-Badge, R. (2003) Multipotent cell lineages in early mouse development depend on SOX2 function. Genes Dev. **17**, 126-140

4 Boyer, L. A., Lee, T. I., Cole, M. F., Johnstone, S. E., Levine, S. S., Zucker, J. P., Guenther, M. G., Kumar, R. M., Murray, H. L., Jenner, R. G., Gifford, D. K., Melton, D. A., Jaenisch, R. and Young, R. A. (2005) Core transcriptional regulatory circuitry in human embryonic stem cells. Cell. **122**, 947-956

5 Chickarmane, V., Troein, C., Nuber, U. A., Sauro, H. M. and Peterson, C. (2006) Transcriptional dynamics of the embryonic stem cell switch. PLoS Comput Biol. **2**, e123

6 Hart, A. H., Hartley, L., Ibrahim, M. and Robb, L. (2004) Identification, cloning and expression analysis of the pluripotency promoting Nanog genes in mouse and human. Dev Dyn. **230**, 187-198

7 Mitsui, K., Tokuzawa, Y., Itoh, H., Segawa, K., Murakami, M., Takahashi, K., Maruyama, M., Maeda, M. and Yamanaka, S. (2003) The homeoprotein Nanog is required for maintenance of pluripotency in mouse epiblast and ES cells. Cell. **113**, 631-642

8 Niwa, H., Miyazaki, J. and Smith, A. G. (2000) Quantitative expression of Oct-3/4 defines differentiation, dedifferentiation or self-renewal of ES cells. Nat Genet. **24**, 372-376

9 Xu, C., Inokuma, M. S., Denham, J., Golds, K., Kundu, P., Gold, J. D. and Carpenter, M. K. (2001) Feeder-free growth of undifferentiated human embryonic stem cells. Nat Biotechnol. **19**, 971-974

10 Xu, R. H., Peck, R. M., Li, D. S., Feng, X., Ludwig, T. and Thomson, J. A. (2005) Basic FGF and suppression of BMP signaling sustain undifferentiated proliferation of human ES cells. Nat Methods. **2**, 185-190

11 Yao, S., Chen, S., Clark, J., Hao, E., Beattie, G. M., Hayek, A. and Ding, S. (2006) Long-term self-renewal and directed differentiation of human embryonic stem cells in chemically defined conditions. Proc Natl Acad Sci U S A. **103**, 6907-6912

12 Beattie, G. M., Lopez, A. D., Bucay, N., Hinton, A., Firpo, M. T., King, C. C. and Hayek, A. (2005) Activin A maintains pluripotency of human embryonic stem cells in the absence of feeder layers. Stem Cells. **23**, 489-495

13 James, D., Levine, A. J., Besser, D. and Hemmati-Brivanlou, A. (2005) TGFbeta/activin/nodal signaling is necessary for the maintenance of pluripotency in human embryonic stem cells. Development. **132**, 1273-1282

14 Vallier, L., Alexander, M. and Pedersen, R. A. (2005) Activin/Nodal and FGF pathways cooperate to maintain pluripotency of human embryonic stem cells. J Cell Sci. **118**, 4495-4509

15 Wang, G., Zhang, H., Zhao, Y., Li, J., Cai, J., Wang, P., Meng, S., Feng, J., Miao, C., Ding, M., Li, D. and Deng, H. (2005) Noggin and bFGF cooperate to maintain the pluripotency of human embryonic stem cells in the absence of feeder layers. Biochem Biophys Res Commun. **330**, 934-942

16 Sato, N., Meijer, L., Skaltsounis, L., Greengard, P. and Brivanlou, A. H. (2004) Maintenance of pluripotency in human and mouse embryonic stem cells through activation of Wnt signaling by a pharmacological GSK-3-specific inhibitor. Nat Med. **10**, 55-63

17 Ying, Q. L., Wray, J., Nichols, J., Batlle-Morera, L., Doble, B., Woodgett, J., Cohen, P. and Smith, A. (2008) The ground state of embryonic stem cell self-renewal. Nature. **453**, 519-523
18 Houslay, M. D. (2009) Underpinning compartmentalised cAMP signalling through targeted cAMP breakdown. Trends Biochem Sci
19 Michie, A. M., Lobban, M., Muller, T., Harnett, M. M. and Houslay, M. D. (1996) Rapid regulation of PDE-2 and PDE-4 cyclic AMP phosphodiesterase activity following ligation of the T cell antigen receptor on thymocytes: analysis using the selective inhibitors erythro-9-(2-hydroxy-3-nonyl)-adenine (EHNA) and rolipram. Cell Signal. **8**, 97-110
20 Carson, D. A. and Seegmiller, J. E. (1976) Effect of adenosine deaminase inhibition upon human lymphocyte blastogenesis. J Clin Invest. **57**, 274-282
21 Heins, N., Englund, M. C., Sjoblom, C., Dahl, U., Tonning, A., Bergh, C., Lindahl, A., Hanson, C. and Semb, H. (2004) Derivation, characterization, and differentiation of human embryonic stem cells. Stem Cells. **22**, 367-376
22 Liu, Y., Song, Z., Zhao, Y., Qin, H., Cai, J., Zhang, H., Yu, T., Jiang, S., Wang, G., Ding, M. and Deng, H. (2006) A novel chemical-defined medium with bFGF and N2B27 supplements supports undifferentiated growth in human embryonic stem cells. Biochem Biophys Res Commun. **346**, 131-139
23 Gerrard, L., Rodgers, L. and Cui, W. (2005) Differentiation of human embryonic stem cells to neural lineages in adherent culture by blocking bone morphogenetic protein signaling. Stem Cells. **23**, 1234-1241
24 Kane, N. M., Meloni, M., Spencer, H. L., Craig, M. A., Strehl, R., Milligan, G., Houslay, M. D., Mountford, J. C., Emanueli, C. and Baker, A. H. (2010) Derivation of endothelial cells from human embryonic stem cells by directed differentiation: analysis of microRNA and angiogenesis in vitro and in vivo. Arterioscler Thromb Vasc Biol. **30**, 1389-1397
25 Lugnier, C. (2006) Cyclic nucleotide phosphodiesterase (PDE) superfamily: a new target for the development of specific therapeutic agents. Pharmacol Ther. **109**, 366-398
26 Boess, F. G., Hendrix, M., van der Staay, F. J., Erb, C., Schreiber, R., van Staveren, W., de Vente, J., Prickaerts, J., Blokland, A. and Koenig, G. (2004) Inhibition of phosphodiesterase 2 increases neuronal cGMP, synaptic plasticity and memory performance. Neuropharmacology. **47**, 1081-1092
27 Castro, L. R., Verde, I., Cooper, D. M. and Fischmeister, R. (2006) Cyclic guanosine monophosphate compartmentation in rat cardiac myocytes. Circulation. **113**, 2221-2228
28 Antonioli, L., Fornai, M., Colucci, R., Ghisu, N., Da Settimo, F., Natale, G., Kastsiuchenka, O., Duranti, E., Virdis, A., Vassalle, C., La Motta, C., Mugnaini, L., Breschi, M. C., Blandizzi, C. and Del Taca, M. (2007) Inhibition of adenosine deaminase attenuates inflammation in experimental colitis. J Pharmacol Exp Ther. **322**, 435-442
29 Hashemi, M., Karami-Tehrani, F., Ghavami, S., Maddika, S. and Los, M. (2005) Adenosine and deoxyadenosine induces apoptosis in oestrogen receptor-positive and -negative human breast cancer cells via the intrinsic pathway. Cell Prolif. **38**, 269-285
30 Hershfield, M. S. (2005) New insights into adenosine-receptor-mediated immunosuppression and the role of adenosine in causing the immunodeficiency associated with adenosine deaminase deficiency. Eur J Immunol. **35**, 25-30
31 Singhal, D. and Anderson, B. D. (1998) Optimization of the local inhibition of intestinal adenosine deaminase (ADA) by erythro-9-(2-hydroxy-3-nonyl)adenine: enhanced oral delivery of an ADA-activated prodrug for anti-HIV therapy. J Pharm Sci. **87**, 578-585
32 Tofovic, S. P., Zacharia, L., Carcillo, J. A. and Jackson, E. K. (2001) Inhibition of adenosine deaminase attenuates endotoxin-induced release of cytokines in vivo in rats. Shock. **16**, 196-202

33 Nabhan, C., Gartenhaus, R. B. and Tallman, M. S. (2004) Purine nucleoside analogues and combination therapies in B-cell chronic lymphocytic leukemia: dawn of a new era. Leuk Res. **28**, 429-442
34 Cristalli, G., Eleuteri, A., Franchetti, P., Grifantini, M., Vittori, S. and Lupidi, G. (1991) Adenosine deaminase inhibitors: synthesis and structure-activity relationships of imidazole analogues of erythro-9-(2-hydroxy-3-nonyl)adenine. J Med Chem. **34**, 1187-1192
35 Da Settimo, F., Primofiore, G., La Motta, C., Taliani, S., Simorini, F., Marini, A. M., Mugnaini, L., Lavecchia, A., Novellino, E., Tuscano, D. and Martini, C. (2005) Novel, highly potent adenosine deaminase inhibitors containing the pyrazolo[3,4-d]pyrimidine ring system. Synthesis, structure-activity relationships, and molecular modeling studies. J Med Chem. **48**, 5162-5174
36 Li, J., Wang, G., Wang, C., Zhao, Y., Zhang, H., Tan, Z., Song, Z., Ding, M. and Deng, H. (2007) MEK/ERK signaling contributes to the maintenance of human embryonic stem cell self-renewal. Differentiation. **75**, 299-307
37 Dvorak, P., Dvorakova, D., Koskova, S., Vodinska, M., Najvirtova, M., Krekac, D. and Hampl, A. (2005) Expression and potential role of fibroblast growth factor 2 and its receptors in human embryonic stem cells. Stem Cells. **23**, 1200-1211
38 Kinoshita, T., Tada, T. and Nakanishi, I. (2008) Conformational change of adenosine deaminase during ligand-exchange in a crystal. Biochem Biophys Res Commun. **373**, 53-57
39 Belles-Isles, M., Chapeau, C., White, D. and Gagnon, C. (1986) Isolation and characterization of dynein ATPase from bull spermatozoa. Biochem J. **240**, 863-869
40 Bouchard, P., Penningroth, S. M., Cheung, A., Gagnon, C. and Bardin, C. W. (1981) erythro-9-[3-(2-Hydroxynonyl)]adenine is an inhibitor of sperm motility that blocks dynein ATPase and protein carboxylmethylase activities. Proc Natl Acad Sci U S A. **78**, 1033-1036
41 Blackburn, M. R. and Kellems, R. E. (2005) Adenosine deaminase deficiency: metabolic basis of immune deficiency and pulmonary inflammation. Adv Immunol. **86**, 1-41
42 Silva, J., Nichols, J., Theunissen, T. W., Guo, G., van Oosten, A. L., Barrandon, O., Wray, J., Yamanaka, S., Chambers, I. and Smith, A. (2009) Nanog is the gateway to the pluripotent ground state. Cell. **138**, 722-737
43 Dravid, G., Ye, Z., Hammond, H., Chen, G., Pyle, A., Donovan, P., Yu, X. and Cheng, L. (2005) Defining the role of Wnt/beta-catenin signaling in the survival, proliferation, and self-renewal of human embryonic stem cells. Stem Cells. **23**, 1489-1501
44 Agarwal, R. P., Sagar, S. M. and Parks, R. E., Jr. (1975) Adenosine deaminase from human erythrocytes: purification and effects of adenosine analogs. Biochem Pharmacol. **24**, 693-701
45 Agarwal, R. P., Spector, T. and Parks, R. E., Jr. (1977) Tight-binding inhibitors--IV. Inhibition of adenosine deaminases by various inhibitors. Biochem Pharmacol. **26**, 359-367
46 Antonini, I., Cristalli, G., Franchetti, P., Grifantini, M., Martelli, S., Lupidi, G. and Riva, F. (1984) Adenosine deaminase inhibitors. Synthesis of deaza analogues of erythro-9-(2-hydroxy-3-nonyl)adenine. J Med Chem. **27**, 274-278
47 Baker, D. C. and Hawkins, L. D. (1982) Synthesis of inhibitors of adenosine-deaminase - A total synthesis of erythro-3-(adenin-9-yl)-2-nonanol and its isomers from chiral precursors. Journal of Organic Chemistry. **47**, 2179-2184
48 Wilson, P. K., Szabados, E., Mulligan, S. P. and Christopherson, R. I. (1998) Comparative effects of cladribine, fludarabine and pentostatin on nucleotide metabolism in T- and B-cell lines. Int J Biochem Cell Biol. **30**, 833-842

FOOTNOTES

This work was funded by the Stem Cell Technologies Programme Grant from ITI Scotland to MDH, GM, JCM, AHB, DRA.

FIGURE LEGENDS

Figure 1. hESC morphology and marker expression is maintained and differentiation blocked by EHNA in the absence of FGF during feeder free growth. (a) (i-ii) SA121 hESCs withdrawn from FGF but grown in the presence of EHNA (10 μM) remain undifferentiated. (iv-v) Cells grown in the absence of FGF and EHNA show strong differentiated morphology by passage 8 (p8). SA461 hES cells taken from feeder supported culture directly into feeder-free conditions remain undifferentiated in the presence (iii) but not absence (vi) of EHNA. (b) Immunofluoresence of SA121 hES cells shows the absence of SSEA1 (i) and presence of stem cell markers SSEA3 (ii), SSEA4 (iii), TRA1-60 (iv), TRA1-80 (v) and POU5F1 (vi). Specific antibodies are in green and DAPI in blue. Scale bars, 100μm. (c) qRT-PCR was used to analyse the samples at p8. Gene expression is relative to expression in normal feeder free cells grown with FGF. Student t tests compared data between experimental groups. Asterisks indicate that cells treated with EHNA are statistically significant in comparison to cells treated with neither EHNA or FGF. *, $P < 0.05$; **, $P < 0.01$; ***, $P < 0.001$.

Figure 2. The ability of EHNA to inhibit differentiation is reversible. After growth for 12 passages in the presence of EHNA (10 μM) instead of FGF SA121 hESCs were transferred to gelatin and differentiated for 4 weeks in 20% fetal calf serum: (a) immunostaining for AFP (green) and DAPI (blue), (b) immunostaining for PAX6 (red) and DAPI (blue), (c) immunostaining for smooth muscle actin (green) and DAPI (blue). Scale bars, 100μm.

Figure 3. Prior growth in EHNA does not block subsequent differentiation. Neuronal differentiations were initiated from SA121 hESCs previously grown with either FGF or EHNA (10 μM) for 5 passages: (a) NANOG expression during neuronal differentiation, (b) PAX6 expression during neuronal differentiation, (c) immunostaining of neuronal differentiation (day 16) after prior growth in EHNA, (d) immunostaining of cells neuronal differentiation (day 16) after prior growth in FGF. All images are representative fields stained for POU5F1 (green), Pax6 (red) and DAPI (blue). Scale bars, 100μm.

Figure 4. Directed differentiation is inhibited by the presence of EHNA. (a) SA121 cells were induced to differentiate towards neural lineages with increasing concentrations of EHNA (0 - 10 μM). Immunostaining is of POU5F1 (green), PAX6 (red) and DAPI (blue). Scale bars, 100μm. qRT-PCR analysis of (b) Nanog, (c) POUF51, (d) ZFP42, and (e) PAX6 expression was analysed throughout a neural differentiation with and without EHNA (10μM) present continually. (f) Expression of NANOG and PAX6 was analysed by qRT-PCR at 4 weeks and 6 weeks post neural differentiation induction. EHNA was either present throughout (+EHNA; 10 μM) or absent (-EHNA) from the differentiations (ND = neural differentiation).

Figure 5. EHNA does not maintain transcription of hESC markers through inhibition of PDE2, increased phosphorylated metabolites of adenosine or adenosine receptor activation. SA121 hESCs underwent passive differentiation for 14 days (with and without compound addition) and were subsequently analysed by qRT-PCR. (a) and (b) Treatment with EHNA and PDE inhibitors. (c) Treatment with adenosine kinase inhibitor, AMPK agonist and adenosine receptor agonist and antagonist. (d) Treatment with EHNA and inhibitors of each specific adenosine receptor. Data represents mean ± SEM from three experiments. For (a) and (b) the value 1 was set to level of expression in undifferentiated hESCS whereas in (c) and (d) the value 1 was set to the expression level in the untreated control samples. All other values were calculated respectively. EHNA – *erythro*-9-(2-hydroxy-3-nonyl)adenine (10 μM); IBMX – 3-isobutyl-1-methylxanthine (100 μM); BAY – BAY-60-7550 (5 μM); AKI – adenosine kinase inhibitor (ABT-702) (5 μM), AICAR – 5-aminoimidazole-4-carboxamide-1-ß-D-ribofuranoside (0.5 mM); NECA – adenosine-5'-*N*-ethylcarboxamide (10 μM), THEO – theophylline (10 μM); CPX – 8-cyclopentyl-1,3-dipropylxanthine (10 μM), SCH – SCH

58261 (10 μM), M3 – MRS3777 (10 μM), M1 – MRS1754 (10 μM). Student t tests compared data between experimental groups. Asterisks indicate that cells treated with EHNA are statistically significant in comparison to the untreated control group. *, $P < 0.05$; **, $P < 0.01$; ***, $P < 0.001$.

Figure 6. The effect of known ADA inhibitors and related compounds on the expression of NANOG and PAX6 in SA121 hESCs under differentiation conditions. Compounds which maintained, after 14 days of differentiation, at least 50% of the level of NANOG-expression in comparison to EHNA and those that inhibited the expression of PAX6 to 50% or less than the value of the untreated controls were considered to have an EHNA-like effect. Those which had a single effect, to these levels, on either PAX6 or NANOG were considered to have a partial-EHNA effect. All compounds were tested at 10 μM. All compound structures are defined in the Supplementary Figure 4. [44-48]**Figure 7. The differentiation blocking effect of EHNA is not associated with adenosine deaminase inhibition.** SA121 hESCs underwent passive differentiation for 14 days (with and without compound addition) and subsequently analysed by qRT-PCR. Data represents mean ± SEM from three experiments. Expression is relative to expression in the untreated control samples. Con – untreated; EHNA – *erythro*-9-(2-hydroxy-3-nonyl)adenine; HWC-57 – deoxy-EHNA; HWC-30 – 2-nonyl-2*H*-pyrazolo[3,4-*d*]pyrimidin-4-amine hydrochloride; HWC-31 – 1-nonyl-1*H*-pyrazolo[3,4-*d*]pyrimidin-4-amine hydrochloride; HWC-33 – 1-undecyl-1*H*-pyrazolo[3,4-*d*]pyrimidin-4-amine hydrochloride; Pento – pentostatin. All compounds were used at 10 μM. Student t tests compared data between experimental groups. Asterisks indicate that cells treated with EHNA are statistically significant in comparison to the untreated control group. *, $P < 0.05$; **, $P < 0.01$; ***, $P < 0.001$.

Figure 8. Standard hESC morphology and expression profile is maintained by HWC-57 and HWC-64 in the absence of FGF for up to 10 passages. (a) Phase images of SA121 hESCs grown for 10 passages in full feeder free media containing FGF (FF), or media containing no FGF (NF), or media containing no FGF but supplemented with either 10 μM HWC-57 or HWC-64. (b) Analysis of gene expression from cells passaged in the conditions referred to in (a). Gene expression is relative to GAPDH. Scale bars, 100μm.

Figure 1.

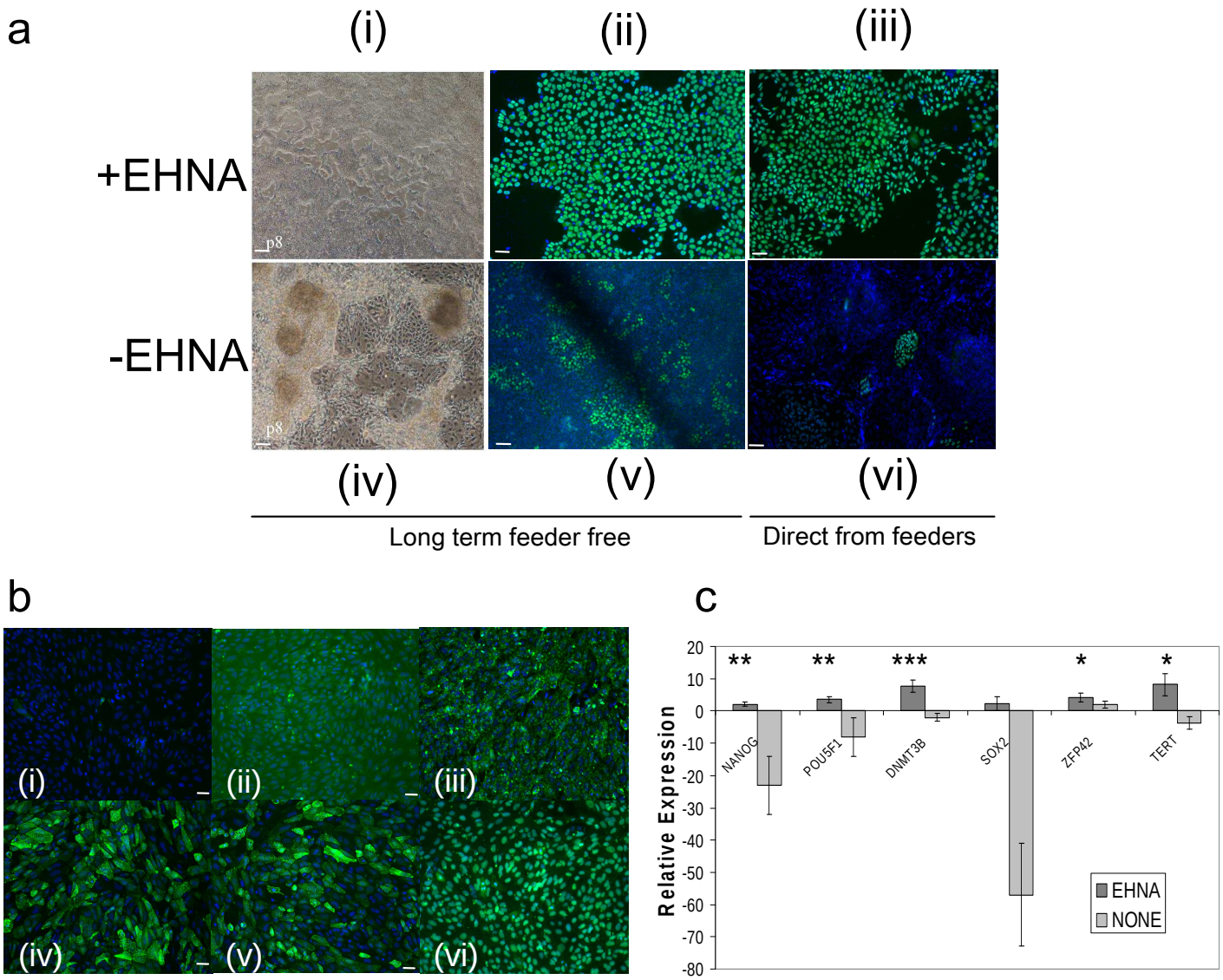
a
(i)
(ii)
(iii)
+EHNA
-EHNA
p8
p8
(iv)
(v)
(vi)
Long term feeder free
Direct from feeders
b
(i)
(ii)
(iii)
(iv)
(v)
(vi)
c
Relative Expression
20
10
0
-10
-20
-30
-40
-50
-60
-70
-80
**
**
***
*
*
NANOG
POU5F1
DNMT3B
SOX2
ZFP42
TERT
EHNA
NONE

Figure 2.

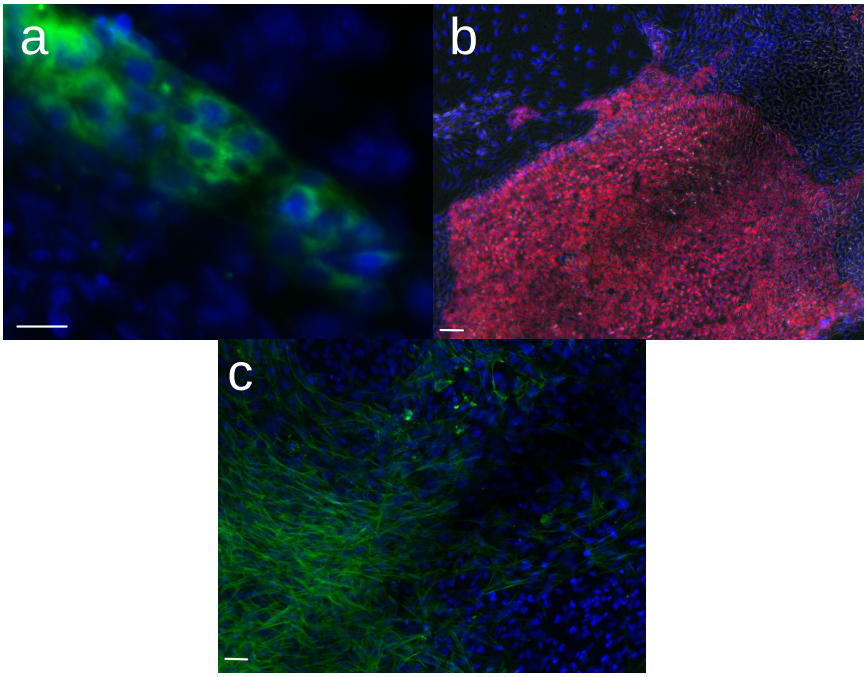

Figure 3.

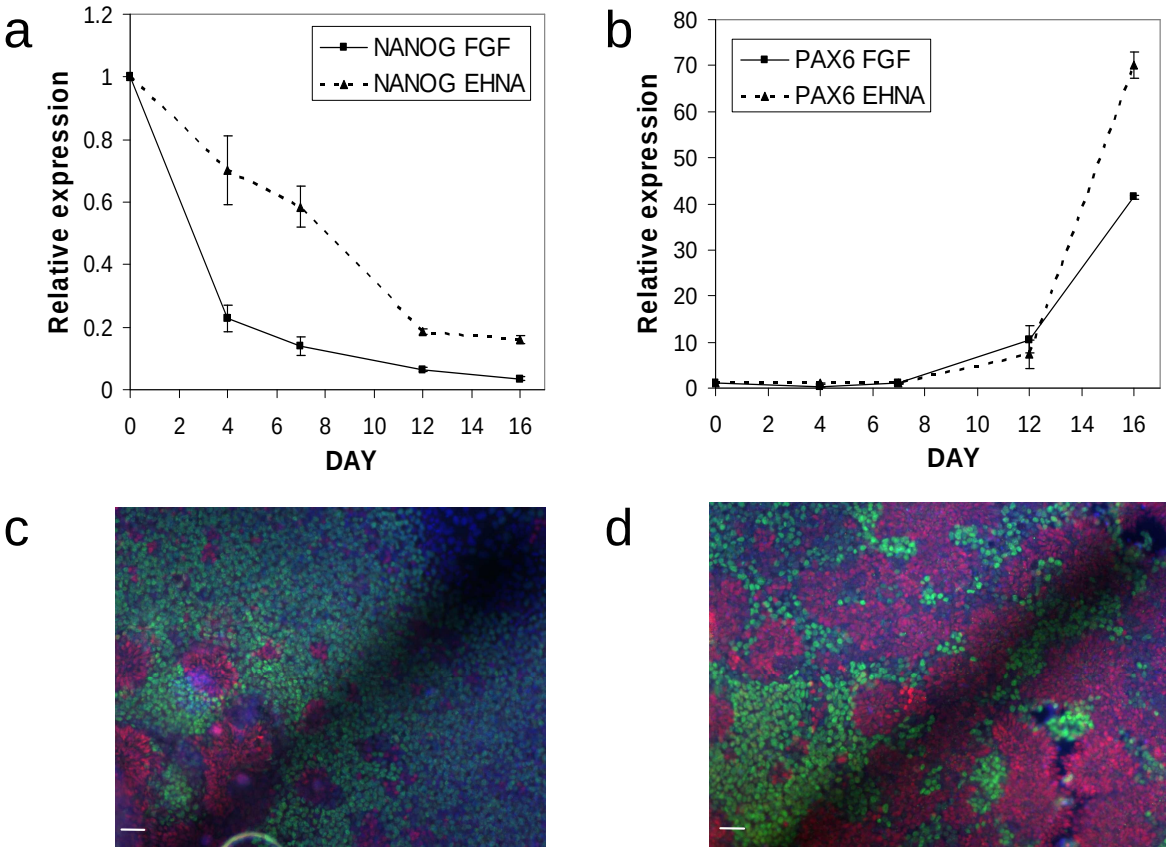
a
Relative expression
DAY
NANOG FGF
NANOG EHNA
b
Relative expression
DAY
PAX6 FGF
PAX6 EHNA
c
d

Figure 4.

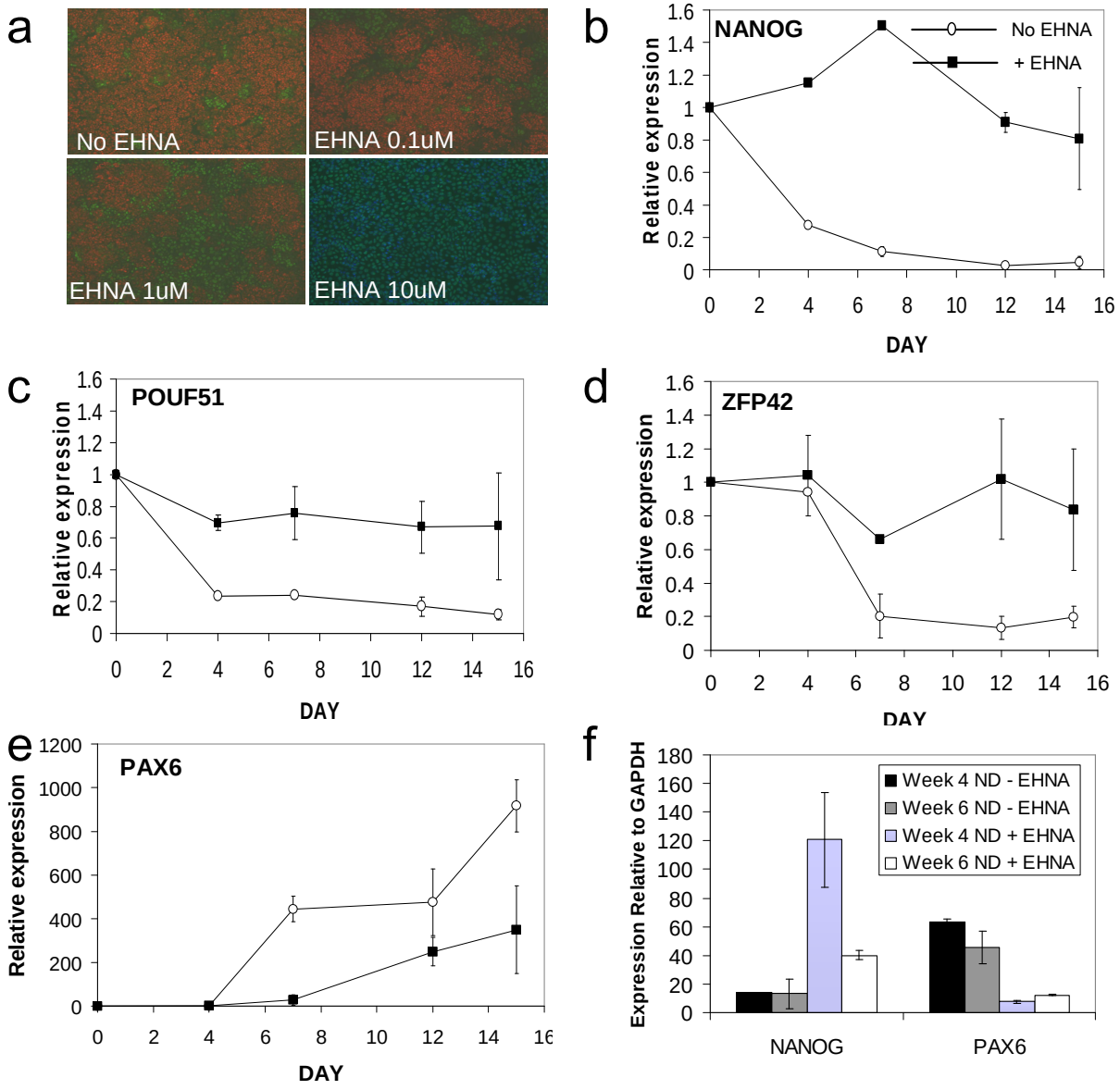
a
No EHNA
EHNA 0.1uM
EHNA 1uM
EHNA 10uM
b
NANOG
No EHNA
+ EHNA
Relative expression
DAY
c
POUF51
Relative expression
DAY
d
ZFP42
Relative expression
DAY
e
PAX6
Relative expression
DAY
f
Week 4 ND - EHNA
Week 6 ND - EHNA
Week 4 ND + EHNA
Week 6 ND + EHNA
Expression Relative to GAPDH
NANOG
PAX6

Figure 5.

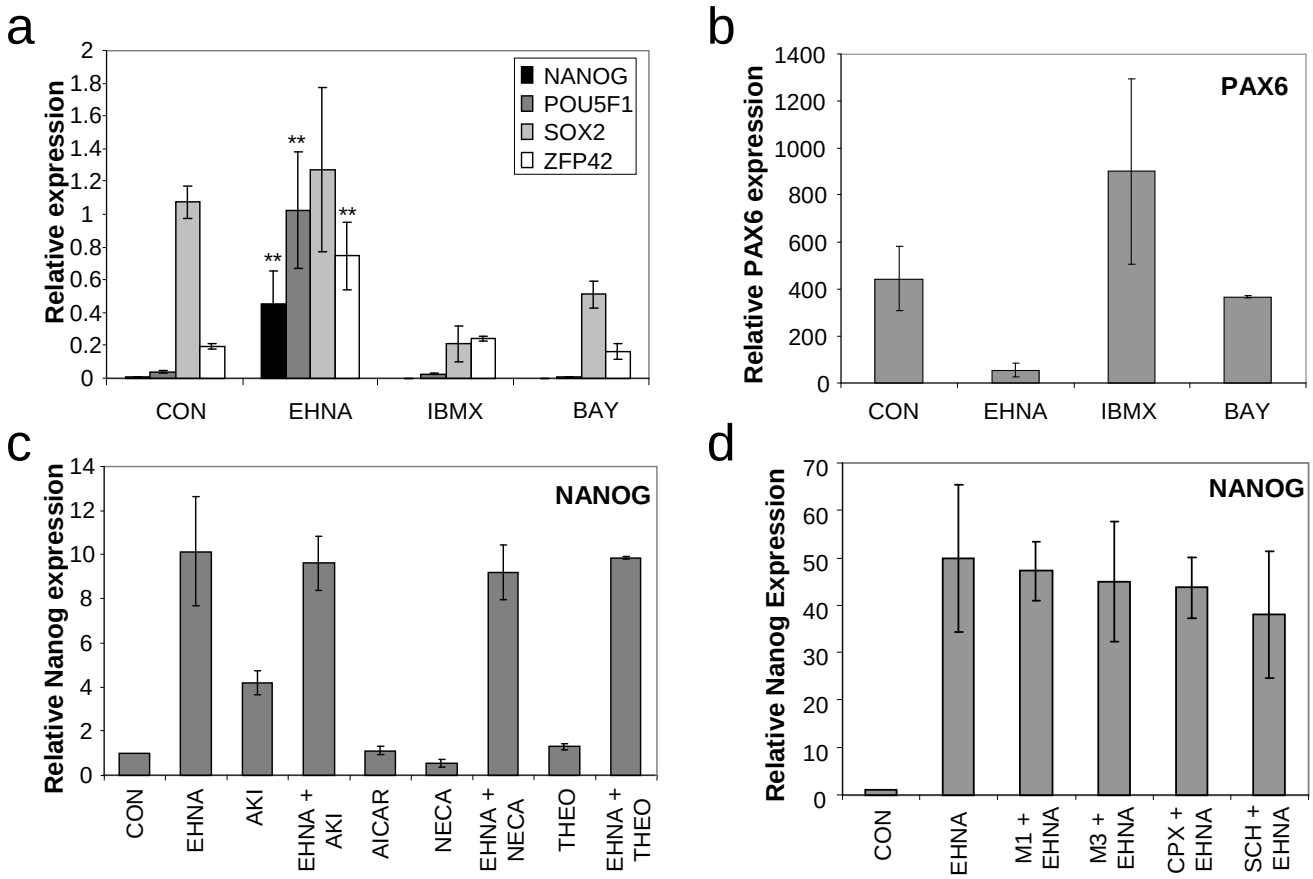
a
Relative expression
NANOG
POU5F1
SOX2
ZFP42
**
**
**
CON
EHNA
IBMX
BAY
b
Relative PAX6 expression
PAX6
CON
EHNA
IBMX
BAY
c
Relative Nanog expression
NANOG
CON
EHNA
AKI
EHNA + AKI
AICAR
NECA
EHNA + NECA
THEO
EHNA + THEO
d
Relative Nanog Expression
NANOG
CON
EHNA
M1 + EHNA
M3 + EHNA
CPX + EHNA
SCH + EHNA

Figure 6.

a

	Full EHNA effect	PARTIAL EHNA EFFECT (NANOG)	PARTIAL EHNA EFFECT (PAX6)	NO EHNA EFFECT	Reported adenosine deaminase inhibition
EHNA	X				K_i 7 nM[34]
HWC-06	X				K_i 0.13 nM[35]
HWC-25	X				ND
HWC-30	X				Inactive[35]
HWC-31	X				K_i 8.1 nM[35]
HWC-33	X				K_i 0.47 nM[35]
HWC-40	X				ND
HWC-41	X				K_i 530 nM[35]
HWC-46	X				K_i 0.76 nM[47]
HWC-57	X				ND
HWC-62	X				ND
HWC-64	X				ND
HWC-08			X		K_i 1.2 uM[46]
HWC-09			X		K_i 10 nM[46]
HWC-10			X		ND
HWC-12			X		K_i 840 nM[46]
HWC-13			X		ND
HWC-16			X		ND
HWC-17			X		ND
HWC-21			X		K_i 73 uM[48]
HWC-24			X		ND
HWC-26			X		ND
HWC-27			X		ND
HWC-34			X		ND
HWC-35			X		ND
HWC-52			X		K_i 62 nM[47]
HWC-05				X	K_i 550 nM[46]
HWC-07				X	K_i 368 nM[34]
HWC-14				X	ND
HWC-15				X	ND
HWC-18				X	K_i 17 uM[44]
HWC-36				X	K_i 35 nM[34]
HWC-44				X	ND
HWC-60				X	ND
pentostatin				X	K_i 2.5 pM[45]; K_i 22 pM[48]

b

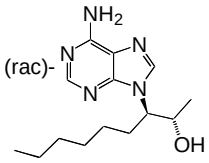

EHNA

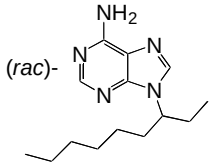

HWC-57

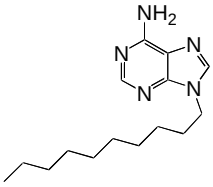

HWC-64

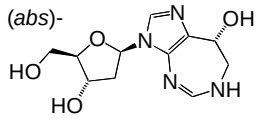

pentostatin
(deoxycoformycin)

Figure 7.

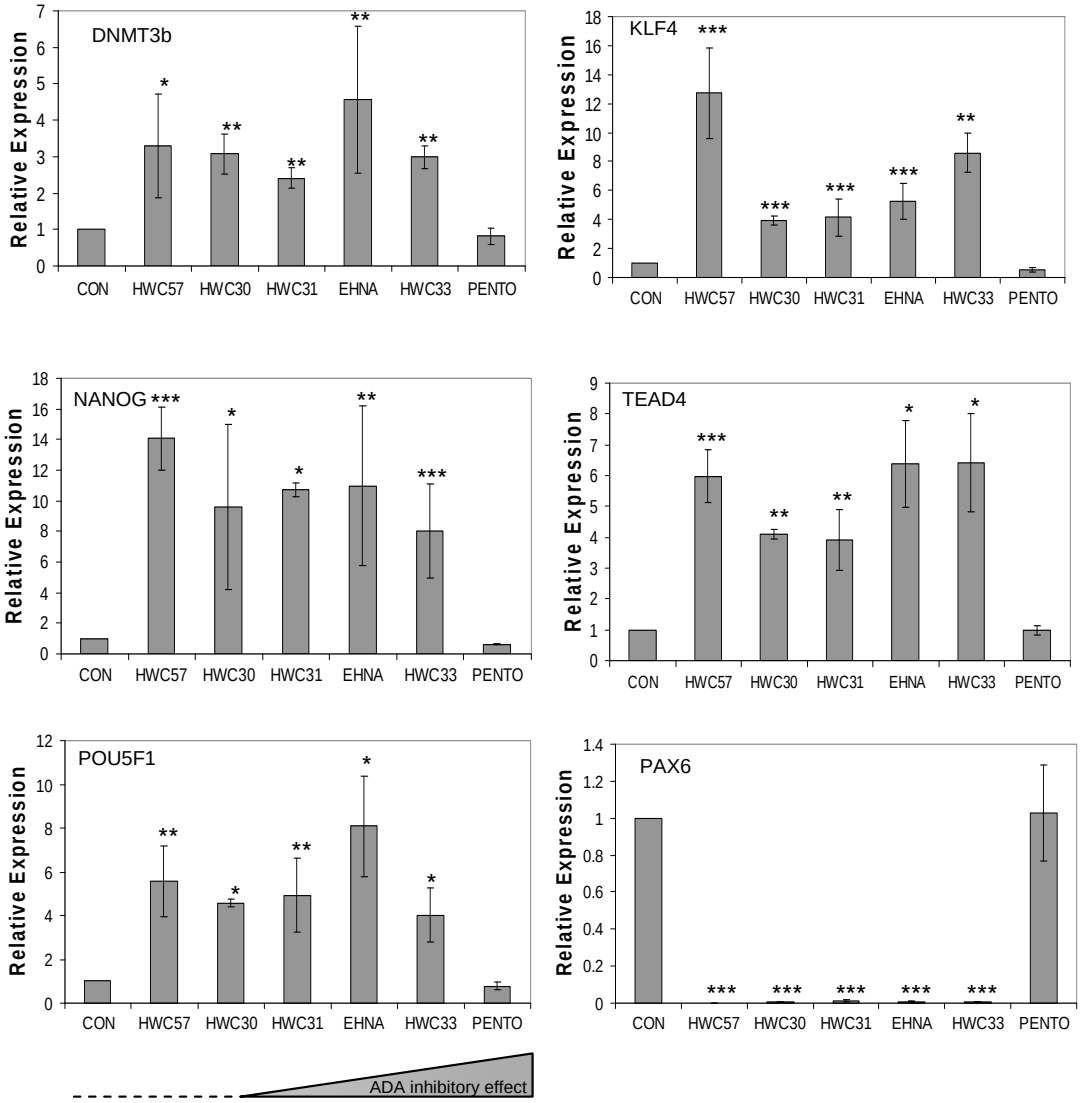
DNMT3b
KLF4
NANOG
TEAD4
POU5F1
PAX6
Relative Expression
CON
HWC57
HWC30
HWC31
EHNA
HWC33
PENTO
ADA inhibitory effect

Figure 8.

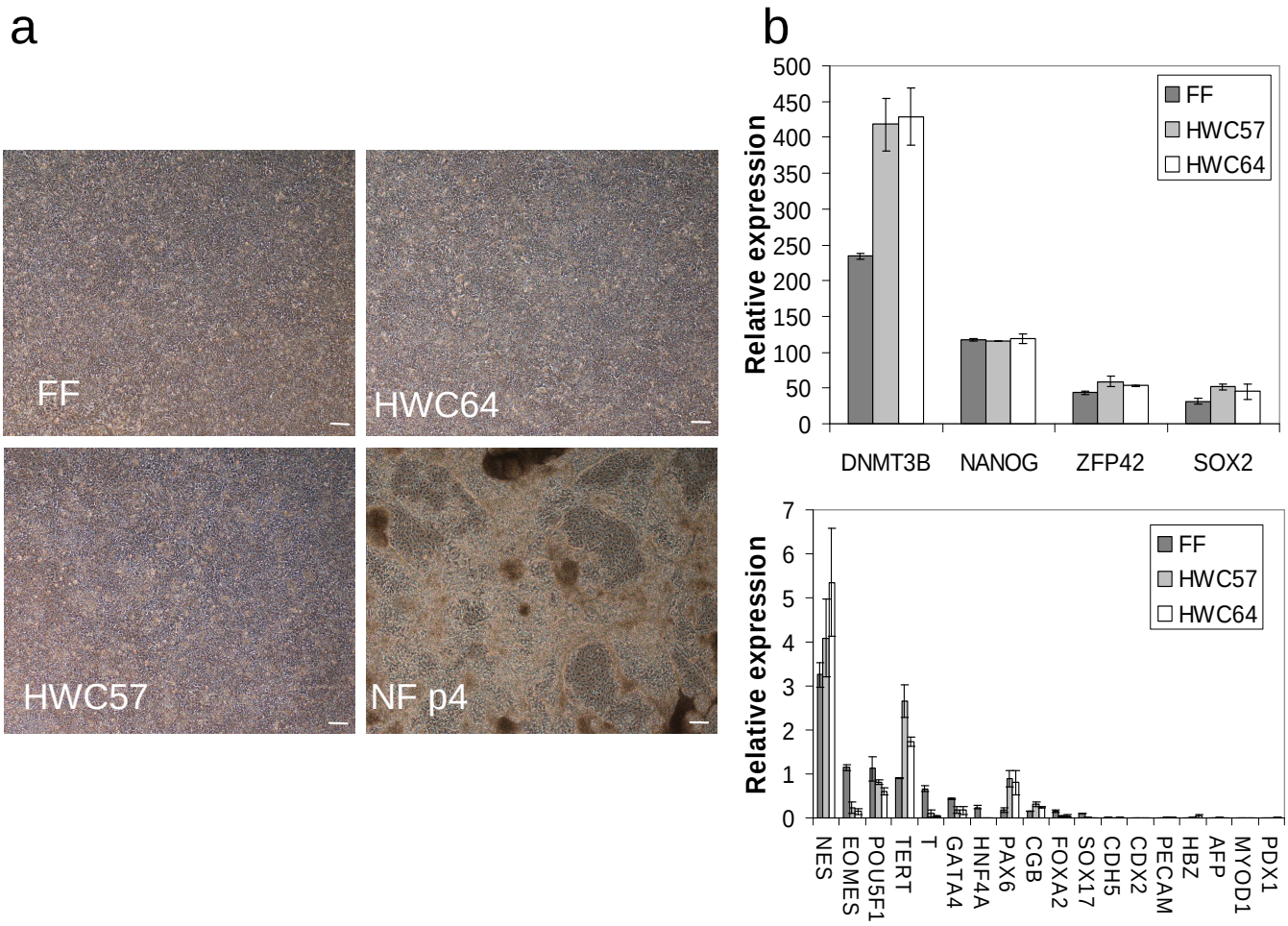
a
FF
HWC64
HWC57
NF p4
b
Relative expression
500
450
400
350
300
250
200
150
100
50
0
FF
HWC57
HWC64
DNMT3B
NANOG
ZFP42
SOX2
Relative expression
7
6
5
4
3
2
1
0
FF
HWC57
HWC64
NES
EOMES
POU5F1
TERT
T
GATA4
HNF4A
PAX6
CGB
FOXA2
SOX17
CDH5
CDX2
PECAM
HBZ
AFP
MYOD1
PDX1

Structure Activity Relationship Commentary

In order to define the structural determinants of EHNA's capacity to suppress hESC differentiation we evaluated a range of structurally variant EHNA analogues. We also included in the test compound set a number of established ADA inhibitors with widely different inhibitory potencies in order to probe the potential contribution of ADA inhibition to EHNA's effects on stem cells.

Removal, replacement or N-substitution of the adenine 6-NH_2 group (as in compounds **2**-**10**, Suppl. Fig. B1) significantly compromised the EHNA stem cell maintenance capacity. In principle, this might be consistent with an ADA-inhibitory mode of action, since the 6-NH_2 group of EHNA makes important contacts within the enzyme's catalytic pocket. Thus, the recently disclosed EHNA-ADA co-crystal structure (PDB: 2Z7G) reveals that the 6-NH_2 engages Asp296 (a residue that binds the protonated substrate N-7 centre) and networks to Glu217 by two hydrogen-bonded bridging water molecules, Suppl. Fig. B2(a)/(b).[1]

In contrast to the N-1, N-9 and 6-NH_2 centres of EHNA, which are all implicated in binding to ADA, the N-3 position makes no contact with the enzyme, Suppl. Fig. B2(b). Consistent with this, the 3-deaza analogue (**11**) of EHNA reportedly possesses comparable ADA-inhibitory potency to EHNA itself.[2] We therefore tested compound **11**, but found that its stem cell maintenance capacity was much reduced compared to EHNA.

It has further been shown that good ADA-inhibitory activity is retained in EHNA analogues where the pyrimidine ring C-2 and N-3 centres are elided. Thus, imidazole carboxamides **12** and **13** are effective ADA inhibitors (K_i 368 nM and 35 nM respectively *vs* K_i 7 nM for EHNA).[3] Co-crystal structures of related compounds (*e.g.* **14**, Suppl. Fig. B2(c); PDB: 1NDW)[4] show that the imidazole carboxamide closely superimposes onto the EHNA adenine bicycle to maintain the same network of interactions with the ADA catalytic pocket. Compounds **12** and **13** lacked any stem cell maintenance effect however. Given the absence of an effect with these compounds, we examined other established ADA inhibitors. Significantly, pentostatin (deoxycoformycin) (**15**), a transition state inhibitor of sub-nanomolar potency,[5] also lacked a stem cell maintenance effect.

In contrast to pentostatin, another established ADA inhibitor, pyrazolopyrimidine **18a** (K_i 0.13 nM),[6] did exhibit a stem cell maintenance effect comparable to EHNA. The ADA inhibitory potency of pyrazolopyrimidines related to **18a** is reportedly strongly dependent on both the length of the hydrocarbon chain and its site of attachment to the core heterocycle. Thus, for a series of 2-alkyl-2*H*-pyrazolo[3,4-*d*]pyrimidin-4-amines (**16a**-**19a**; K_i 530, 8.1, 0.13 & 0.47 nM respectively) optimal ADA inhibition was seen with the *n*-decyl chain and inhibitory potency fell off markedly with truncation to *n*-octyl.[6] The isomeric 1-alkyl-1*H*-pyrazolo[3,4-*d*]pyrimidin-4-amines (**16b**-**19b**) were inactive or only very weakly active as ADA inhibitors.[7] In the ADA-inhibitory 2-substituted series we found the undecyl and nonyl homologues (**17a** and **19a**) to have comparable stem cell maintenance activity to EHNA and **18a**, though the octyl homologue (**16a**) was less effective. Unfortunately, poor solubility characteristics precluded assessment of the longer chain compounds (**18b** and **19b**) in the non-ADA-inhibitory 1-substituted series. The shorter chain homologues **16b** and **17b** were amenable to assessment, however, and compound **17b**, with the nonyl chain, was found to have a stem cell maintenance effect comparable to that of isomer **17a** and to EHNA. The octyl homologue (**16b**) was less active than EHNA, but comparable in activity to isomer **16a**.

Collectively these data strongly suggested that ADA inhibition does not contribute to or is not the sole contributory factor responsible for EHNA's stem cell maintenance properties and that the key structural features required for

---

1 T. Kinoshita, T. Tada and I. Nakanishi, *Biochem. Biophys. Res. Commun.*, 2008, **373**, 53-57.
2 I. Antonini, G. Cristalli, P. Franchetti, M. Grifantini, S. Martelli, G. Lupidi and F. Riva, *J. Med. Chem.*, 1984, **27**, 274-278.
3 G. Cristalli, A. Eleuteri, P. Franchetti, M. Grifantini, S. Vittori and G. Lupidi, *J. Med. Chem.*, 1991, **34**, 1187-1192.
4 T. Terasaka, T. Kinoshita, M. Kuno and I. Nakanishi, *J. Am. Chem. Soc.*, 2004, **126**, 34-35.
5 R. P. Agarwal, T. Spector and R. E. Parks, Jr., *Biochem. Pharmacol.*, 1977, **26**, 359-367.
6 F. Da Settimo, G. Primofiore, C. La Motta, S. Taliani, F. Simorini, A. M. Marini, L. Mugnaini, A. Lavecchia, E. Novellino, D. Tuscano and C. Martini, *J Med Chem*, 2005, **48**, 5162-5174.
7 Only compounds **17b**-**19b** were tested in the work described in Ref. 6; the octyl homologue (**16b**) was not reported.

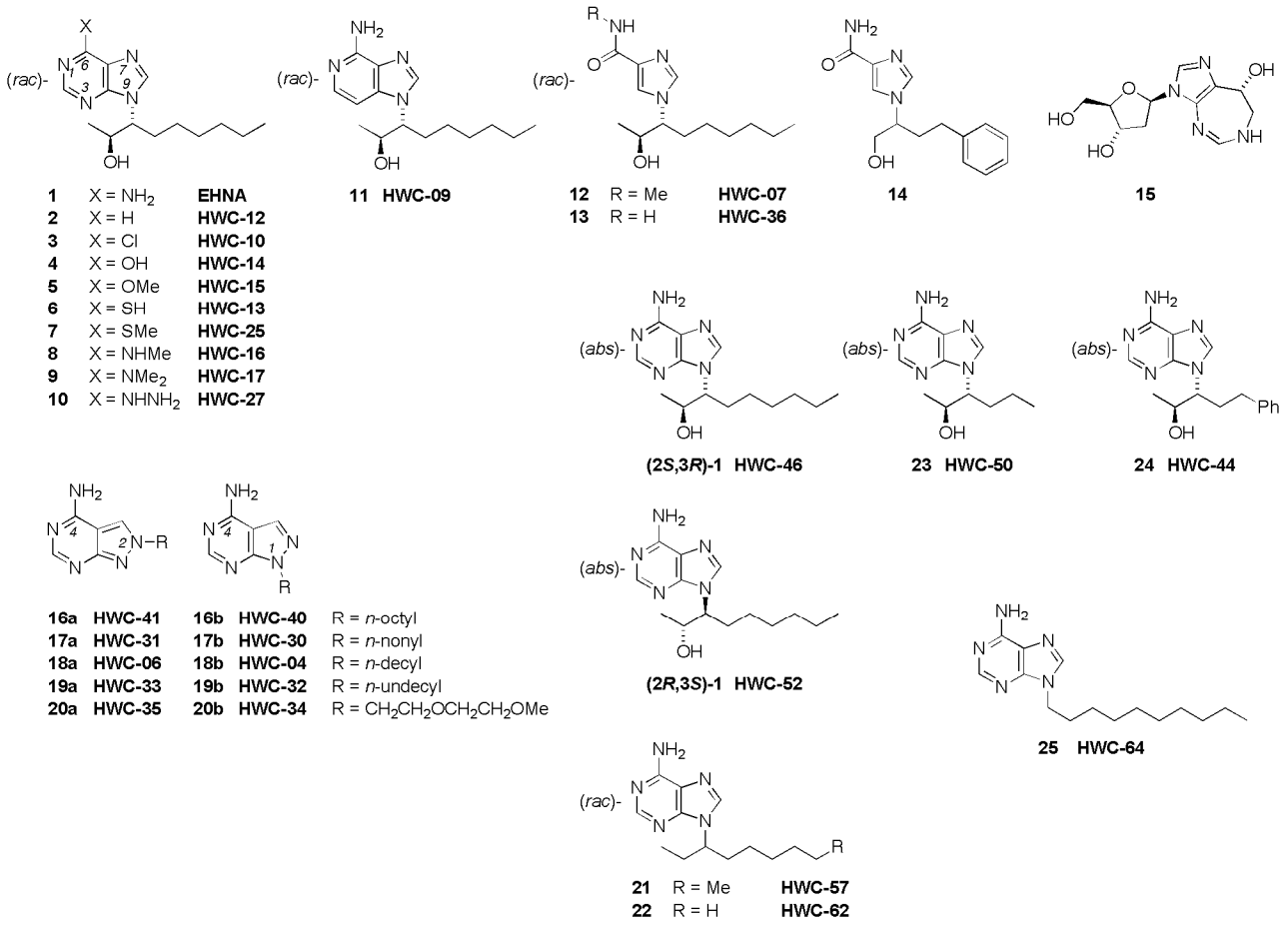

Suuplementary Figure B1

activity are an intact adenine ring (or a close mimetic) together with a long hydrophobic 'tail', though the precise connection of the latter to the 5-membered ring shows some tolerance. The presence of the adenine N-7 nitrogen appears to be non-critical.

The activity of the pyrazolopyrimidine compounds (**17**-**19**) also suggested that the EHNA side chain hydroxyl might be superfluous. Before assessing this, however, we undertook the preparation and separate evaluation of the two *erthyro*-EHNA enantiomers [(+)-EHNA, **(2*S*,3*R*)-1** and (–)-EHNA **(2*R*,3*S*)-1**], Suppl. Fig. B1, since the commercially supplied EHNA was racemic. Of these compounds, **(2*S*,3*R*)-1** is the more potent ADA inhibitor (K_i 0.76 nM *vs* 62 nM for the antipode)[8] and this isomer was also found to be markedly more effective than the enantiomer [**(2*R*,3*S*)-1**] in maintaining stem cell pluripotency. However, deoxy-EHNA (**21**), which was prepared in racemic form, did indeed show comparable activity to (*rac*)-EHNA itself. These data suggest that the hydroxyl in EHNA is merely tolerated in **(2*S*,3*R*)-1** rather than beneficial and that its presence in the enantiomer [**(2*R*,3*S*)-1**] actually compromises activity. The deoxy-EHNA analogue (**22**) with a shortened oct-3-yl side chain also showed similar levels of activity to EHNA itself.

The redundance of the EHNA hydroxyl group for hESC maintenance activity was a significant finding. This group assumes the position of the adenosine substrate 5'-OH and hydrogen bonds to His17 and Asp19 in the ADA catalytic pocket, Suppl. Fig. B2(b), thereby making a significant contribution to the binding of the inhibitor.[9] The

[8] D. C. Baker and L. D. Hawkins, *J Org Chem*, 1982, **47**, 2179-2184.

[9] It will be noted that strong ADA-inhibitory activity in the 2-alkyl-2*H*-pyrazolo[3,4-*d*]pyrimidin-4-amine series (**16a**-**19a**) does not require the hydroxylated side chain of EHNA. This likely reflects the adoption of a distinct but favourable ADA-binding mode by these compounds in which the adenine ring N-1 and 6-NH_2 centres engage Asp296. Connection of the long side chain to the pyrazolopyrimidine N-1 position, as in the 1-alkyl-1*H*-pyrazolo[3,4-*d*]pyrimidin-4-amine series (**16b**-**19b**), would preclude adoption of this arrangement, requiring the compounds to dock in the EHNA-like mode. The absence of the branched hydroxylated EHNA side chain (and the adenine ring N-7 centre) severely compromises the binding affinity in this mode, however, thus accounting for the absent or very weak ADA-inhibitory activity in this series.

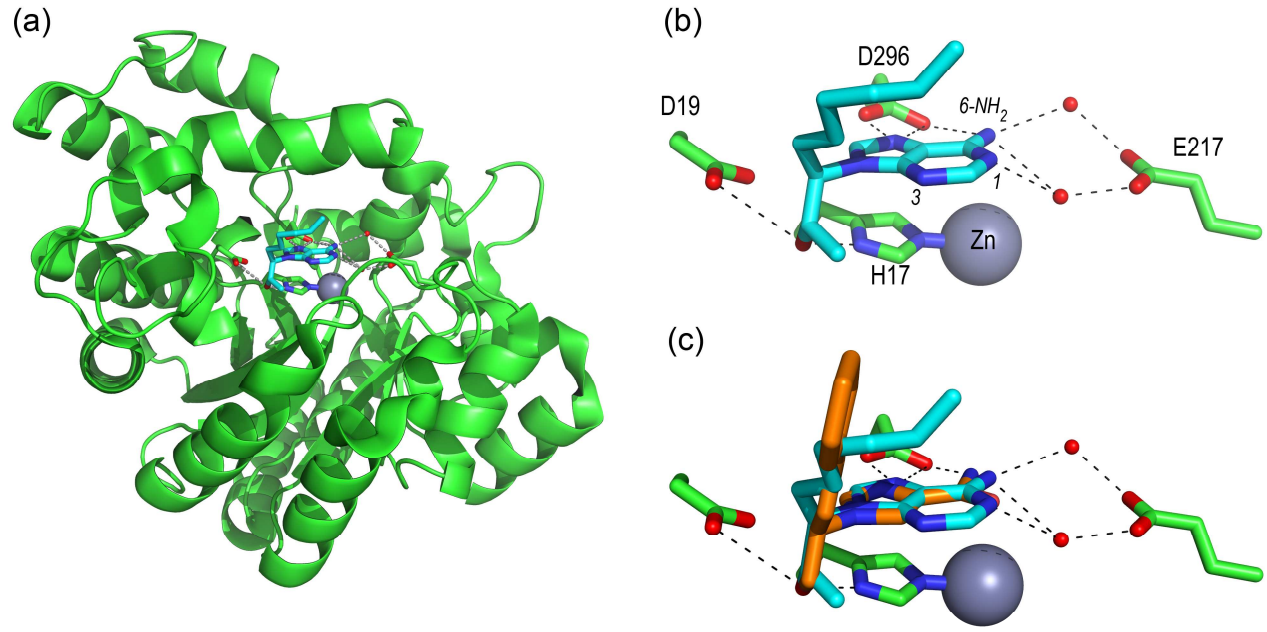

Supplementary Figure B2: (a) EHNA-ADA co-crystal structure (PDB: 2Z7G). **(b)** Detail of EHNA binding mode taken from (a); (*2S*,*3R*)-EHNA is shown as cyan stick. **(c)** Superimposition of imidazole carboxamide **14** (orange stick; taken from its ADA co-crystal structure, PDB: 1NDW) onto EHNA (cyan stick).

efficacy of deoxy-EHNA in the maintenance of stem cell pluripotency therefore further supports the contention that ADA inhibition does not mediate the action of these compounds on stem cells. Although the EHNA hydroxyl group is non-essential for stem cell maintenance activity, the compound's long hydrophobic side chain was found to be critical. Thus, the two methoxyethoxyethyl-substituted pyrazolopyrimidine isomers (**20a/b**), with shortened and more polar side chains, were significantly less active than EHNA or deoxy-EHNA (**21**). Moreover the EHNA analogue (**23**) with a truncated 2-hydroxyhex-3-yl side chain also showed a loss of activity. Interestingly, the activity was not restored by appending a phenyl substituent to the shortened chain of the latter, as in compound **24**. The size and character of the hydrophobic substituent commensurate with stem cell maintenance activity is therefore likely subject to constraints.

As a further simplification to the structure we assessed 9-(1-decyl)adenine (**25**) in order to remove the one remaining stereogenic centre in the deoxy-EHNA analogues **21/22**. In contrast to EHNA, chemical synthesis of compounds **21** and **22** is very readily achieved in simple two-step sequences. The *n*-decyl analogue (**25**) is similarly readily prepared but has the advantage of being achiral. This simple robust compound showed a full stem cell maintenance effect comparable with the activity of the isosteric pyrazolopyrimidine (**18b**) and with that of EHNA itself.

Compound Synthesis

General details

Commercially available reagents from Aldrich and Alfa Aesar chemical companies were generally used as supplied without further purification. Tetrahydrofuran (THF), diethyl ether and toluene were dried by distillation from sodium-benzophenone ketyl under argon. 'Light petroleum' refers to the fraction boiling between 40 ℃ and 60 ℃. Anhydrous *N*,*N*-dimethylformamide (DMF) was purchased from Aldrich and used as supplied from Sure/Seal™ bottles. Reactions were routinely carried out under an inert atmosphere of argon or nitrogen. Analytical thin layer chromatography was carried out using aluminium backed plates coated with Merck Kieselgel 60 GF_{254} (Art. 05554). Developed plates were visualized under ultra-violet light (254 nm) and/or alkaline potassium permanganate dip. Flash chromatography was performed using DAVISIL® silica (60 Å; 35-70 µM) from Fisher (cat. S/0693/60). Fully characterized compounds were chromatographically homogeneous.

Melting points were determined using a Stuart Scientific SMP10 apparatus and are uncorrected. IR spectra were recorded on a Perkin Elmer 1600 FT IR spectrometer. Spectra were recorded as potassium bromide discs, as solutions in $CHCl_3$, or as films between sodium chloride plates. Mass spectra were obtained on Kratos Concept IS EI (electron impact) and Fisons VG Quattro (electrospray) spectrometers. ^{1}H NMR spectra were recorded at 200 and 400 MHz on Bruker AC200 and DPX400 spectrometers; ^{13}C NMR spectra were recorded at 50 and 101 MHz on the same instruments. Chemical shifts are recorded in parts per million (δ in ppm) and are referenced against solvent signals (δ_C 77.16 for chloroform and δ_C 39.52 for methyl sulfoxide) for ^{13}C spectra and solvent residual resonances (δ_H 7.26 for chloroform and δ_H 2.50 methyl sulfoxide) for ^{1}H spectra.[10] Chemical shift values and are accurate to ±0.01 ppm and ±0.1 ppm respectively. *J* values are given in Hz. Multiplicity designations used are: s, d, t, q, sept and m for singlet, doublet, triplet, quartet, septet and multiplet respectively. In ^{13}C NMR spectra, signals corresponding to CH, CH_2, or CH_3 groups are assigned from DEPT. Elemental analyses were carried out by the analytical service of the Chemistry Department at Heriot-Watt University using an Exeter CE-440 Elemental Analyser.

The preparation of HWC-04,[6] HWC-05,[2] HWC-06,[6] HWC-07,[3] HWC-08,[2] HWC-09,[2] HWC-10,[11] HWC-12,[2] HWC-14,[12] HWC-30,[6] HWC-31,[6] HWC-32,[6] HWC-33,[6] HWC-36,[3] HWC-41,[6] HWC-44,[13] (+)-EHNA (HWC-46)[8] and (–)-EHNA (HWC-52)[8] has been described in the literature. *N*^{6}-Methyladenosine (HWC-18) and 2-fluoroadenosine (HWC-20) were procured from Aldrich. Cladribine (HWC-19) and fludarabine (HWC-21) were procured from Sigma.

racemic erythro-3-(6-mercapto-9*H*-purin-9-yl)nonan-2-ol (HWC-13)

A solution of *erythro*-3-(6-chloro-9*H*-purin-9-yl)nonan-2-ol[11] (208 mg, 0.701 mmol) and thiourea (107 mg, 1.40 mmol) in ethanol (7 mL) was heated at 85 ℃ for 2 h. TLC (9:1 CH_2Cl_2 / MeOH) indicated consumption of starting material (R_f 0.53) and formation of a product component (R_f 0.38) (thiourea R_f 0.21). The clear reaction mixture was cooled and the solvent was evaporated. The residue was purified was purified chromatographically on a silica gel column (25 g). Gradient elution with CH_2Cl_2 / MeOH (98:2, 650 mL; 96:4, 200 mL) gave *erythro*-3-(6-mercapto-9*H*-purin-9-yl)nonan-2-ol (134 mg, 0.455 mmol; 65%) as a white powder: δ_H (200 MHz; $CDCl_3$/CD_3OD) 8.25 (1 H, s), 8.12 (1 H, s), 4.47 - 4.35 (1 H, m, chain H-3), 4.07 (1 H, quintet, *J* 6.1, chain H-2), 2.08 (2 H, q, *J* 7.3), 1.45 - 1.12 (8 H, m), 1.10 (3 H, d, *J* 6.4, chain CH_3-1), 0.80 (3 H, approx. t, *J* 6.8, chain CH_3-9); δ_C (50 MHz; $CDCl_3$/CD_3OD) 177.95 (C), 145.74 (CH), 145.45 (C), 143.26 (CH), 136.23 (C), 70.02 (CH), 63.02 (CH), 32.62 (CH_2), 29.72 (2 x CH_2), 27.00 (CH_2), 23.49 (CH_2), 20.34 (CH_3), 14.43 (CH_3). *erythro*-3-(6-Mercapto-9*H*-purin-9-yl)nonan-2-ol was evaluated as its hydrochloride salt**,** formed by treatment with a solution of hydrogen chloride in ether followed by evaporation: (found: C, 50.27; H, 7.08; N, 16.76. $C_{14}H_{22}N_4OS$/1.1 HCl requires C, 50.27; H, 6.96; N, 16.75%).

racemic erythro-3-(6-methoxy-9*H*-purin-9-yl)nonan-2-ol (HWC-15)

A solution of *erythro*-3-(6-chloro-9*H*-purin-9-yl)nonan-2-ol[11] (150 mg, 0.505 mmol) and NaOMe (0.084 mL, 2.02 mmol) in anhydrous MeOH (10 mL) was heated at 70 ℃ for 2 h. TLC (1:2 light petroleum / EtOAc) indicated the transformation of starting material (R_f 0.58) into product (R_f 0.42). The reaction mixture was cooled, adjusted to pH 6 with acetic acid and evaporated. The residual solid was dissolved in water (10 mL) and extracted with CH_2Cl_2 (20 mL) and EtOAc (20 mL). The combined organic layers were dried over Na_2SO_4, filtered and concentrated *in vacuo* to give a crude oil that was purified on a silica gel column (20 g). Elution with CH_2Cl_2 / MeOH (96:4, 150 mL) gave *erythro*-3-(6-methoxy-9*H*-purin-9-yl)nonan-2-ol (142 mg, 0.486 mmol; 96%) as a pale yellow oil: δ_H (200 MHz; $CDCl_3$) 8.44 (1 H, s), 7.89 (1 H, s), 4.78 (1 H, br d, *J* 3.6), 4.38 - 4.19 (2 H, m, chain H-2 and H-3), 4.12 (3 H, s, OMe), 2.10 - 1.87 (2 H, m, chain CH_2-4), 1.27 (3 H, d, *J* 6.5, chain CH_3-1), 1.24 - 1.00 (8 H, m), 0.77 (3 H, approx. t, *J* 6.6, chain CH_3-9); δ_C (50 MHz; $CDCl_3$) 161.16 (C), 151.76 (C), 151.64 (CH), 142.44 (CH), 124.24 (C), 69.41 (CH), 63.30 (CH), 54.42 (OCH_3), 31.65 (CH_2), 28.96 (CH_2), 27.24 (CH_2), 26.28 (CH_2), 22.63 (CH_2), 20.37 (CH_3),

[10] H. E. Gottlieb, V. Kotlyar and A. Nudelman, *J. Org. Chem.*, 1997, **62**, 7512-7515.
[11] H. J. Schaeffer and C. F. Schwender, *J. Med. Chem.*, 1974, **17**, 6-8.
[12] L. N. Simon, . R. Mueller and H. Zutter, *US Pat.*, 4451478, 1984.
[13] E. Abushanab and V. P. Pragnacharyulu Palle, *US Pat.*, 5703084, 1997.

14.13 (CH_3). *erythro*-3-(6-Methoxy-9*H*-purin-9-yl)nonan-2-ol was evaluated as its hydrochloride salt**,** formed by treatment with a solution of hydrogen chloride in ether followed by evaporation.

racemic erythro-3-[6-(methylamino)-9*H*-purin-9-yl]nonan-2-ol (HWC-16)

A stirred mixture of *erythro*-3-(6-chloro-9*H*-purin-9-yl)nonan-2-ol[11] (208 mg, 0.701 mmol) and methylamine (33% w/w in ethanol; 14.0 mL) was heated at 100 ℃ in a heavy-walled sealed flask for 17 h. TLC (9:1 CH_2Cl_2 / MeOH) indicated consumption of starting material (R_f 0.53) and formation of a product component (R_f 0.40). The reaction mixture was evaporated and the residue chromatographed on a silica gel column (25 g). Gradient elution with CH_2Cl_2 / MeOH (98:2, 600 mL; 96:4, 100 mL) gave *erythro*-3-[6-(methylamino)-9*H*-purin-9-yl]nonan-2-ol (191 mg) as a pale yellow oil. ^{1}H NMR indicated the presence of minor impurities and the crude material was re-chromatographed on a silica gel column (20 g). Elution with light petroleum:acetone (2:1, 300 mL) gave *erythro*-3-(6-(methylamino)-9*H*-purin-9-yl)nonan-2-ol (151 mg, 0.518 mmol; 74%): δ_H (200 MHz; $CDCl_3$) 8.32 (1 H, s), 7.67 (1 H, s), 6.17 (1 H, br q, NH), 5.48 (1 H, br s, NH), 4.25 - 4.13 (2 H, m, chain H-2 and H-3), 3.18 (3 H, br d, NMe), 2.09 - 1.77 (2 H, m, chain CH_2-4), 1.25 (3 H, d, *J* 6.5, chain CH_3-1), 1.23 - 1.04 (8 H, m), 0.79 (3 H, approx. t, *J* 6.5, chain CH_3-9); δ_C (50 MHz; $CDCl_3$) 155.83 (C), 152.67 (C), 152.67 (CH), 140.03 (CH), 124.04 (C), 69.78 (CH), 63.93 (CH), 31.72 (CH_2), 29.01 (CH_2), ~28 (br, NMe), 27.43 (CH_2), 26.47 (CH_2), 22.66 (CH_2), 20.49 (CH_3), 14.16 (CH_3).

racemic erythro-3-[6-(dimethylamino)-9*H*-purin-9-yl]nonan-2-ol (HWC-17)

Dimethylamine hydrochloride (3.0 g, 36.8 mmol) was dissolved in water (9 mL) and cooled in an ice-bath. Sodium hydroxide (1.47 g, 36.8 mmol) was added in portions with stirring. The resulting aqueous dimethylamine solution was added to a solution of *erythro*-3-(6-chloro-9*H*-purin-9-yl)nonan-2-ol[11] (215 mg, 0.724 mmol) in ethanol (5 mL) and the mixture heated at 100 ℃ for 17 h in a heavy-walled sealed flask. TLC (1:1 light petroleum / EtOAc) indicated transformation of starting material (R_f 0.28) into product (R_f 0.15). The reaction mixture was concentrated *in vacuo*; the residue diluted with water (10 mL) and extracted with EtOAc (50 mL) and CH_2Cl_2 (2 × 15 mL). The combined extract was dried over Na_2SO_4, filtered and evaporated to give an oily residue that was chromatographed on a silica gel column (25 g). Elution with CH_2Cl_2 / MeOH (96:4, 250 mL) gave *erythro*-3-[6-(dimethylamino)-9*H*-purin-9-yl]nonan-2-ol (220 mg, 0.720 mmol; 99%) as a colourless oil: δ_H (200 MHz; $CDCl_3$) 8.23 (1 H, s), 7.63 (1 H, s), 5.65 (1 H, br s), 4.29 - 4.11 (2 H, m, chain H-2 and H-3), 3.51 (6 H, br s), 2.12 - 1.75 (2 H, m, chain CH_2-4), 1.25 (3 H, d, *J* 6.5, chain CH_3-1), 1.22 - 1.00 (8 H, m), 0.79 (3 H, approx. t, *J* 6.5, chain CH_3-9); δ_C (50 MHz; $CDCl_3$) 155.23 (C), 151.71 (CH), 150.06 (C), 138.78 (CH), 120.88 (C), 69.89 (CH), 64.20 (CH), 38.79 (br, 2 x CH_3), 31.74 (CH_2), 29.05 (CH_2), 27.16 (CH_2), 26.53 (CH_2), 22.69 (CH_2), 20.54 (CH_3), 14.18 (CH_3). *erythro*-3-[6-(Dimethylamino)-9*H*-purin-9-yl]nonan-2-ol was evaluated as its hydrochloride salt**,** formed by treatment with a solution of hydrogen chloride in ether followed by evaporation: (found: C, 50.54; H, 8.07; N, 18.09. $C_{16}H_{27}N_5O$/2.05 HCl requires C, 50.55; H, 7.70; N, 18.42%).

racemic erythro-3-(6-amino-8-methyl-9*H*-purin-9-yl)nonan-2-ol (HWC-24)

racemic erythro-3-(6-Chloro-8-methyl-9*H*-purin-9-yl)nonan-2-ol

Ethanesulfonic acid (8.00 µL, 0.098 mmol) was added to a stirred solution of *erythro*-3-(5-amino-6-chloropyrimidin-4-ylamino)nonan-2-ol[11] (192 mg, 0.669 mmol) in triethyl orthoacetate (3.0 mL) and $CHCl_3$ (1.0 mL). The reaction mixture was stirred at room temperature for 1 h. TLC (1:1 light petroleum / EtOAc) indicated consumption of starting material (R_f 0.35, staining yellow in air) and formation of a product component (R_f 0.30) and a minor component (R_f 0.56). The reaction mixture was diluted with CH_2Cl_2 (50 mL) and washed with saturated sodium bicarbonate solution (3 x 10 mL). The organic layer was dried over Na_2SO_4, filtered and concentrated *in vacuo* to give a pale yellow oily which was chromatographed on a silica gel column (25 g). Gradient elution with light petroleum / EtOAc (3:1, 400 mL; 2:1, 300 mL; 1:1, 200 mL) gave *erythro*-3-(6-chloro-8-methyl-9*H*-purin-9-yl)nonan-2-ol (R_f 0.30) (102 mg, 0.328 mmol; 49%) as a dense colourless oil: δ_H (200 MHz; $CDCl_3$) 8.57 (1 H, s), 4.66 (1 H, s), 4.45 - 4.30 (1 H, m), 4.18 - 4.04 (1 H, m), 2.64 (3 H, s), 2.40 - 1.91 (2 H, m, chain CH_2-4), 1.18 (3 H, d, *J* 6.4,

chain CH_3-1), 1.15 - 0.98 (8 H, m), 0.74 (3 H, approx. t, *J* 6.5, chain CH_3-9); δ_C (50 MHz; $CDCl_3$) 156.04 (C), 152.55 (C), 150.40 (CH), 149.66 (C), 131.23 (C), 69.40 (CH), 64.78 (CH), 31.63 (CH_2), 29.08 (CH_2), 27.72 (CH_2), 26.58 (CH_2), 22.57 (CH_2), 21.26 (CH_3), 15.60 (CH_3), 14.07 (CH_3).

***racemic* erythro-3-(6-Amino-8-methyl-9*H*-purin-9-yl)nonan-2-ol (HWC-24)**

A solution of *erythro*-3-(6-chloro-8-methyl-9*H*-purin-9-yl)nonan-2-ol (97 mg, 0.31 mmol) in ammonia 7 N in MeOH (10 mL) was stirred at 120 ℃ in a heavy-walled sea led tube for 18 h. TLC (95:5 CH_2Cl_2 / MeOH) indicated the starting material (R_f 0.44) was transformed into a minor product (R_f 0.26) and a major product at (R_f 0.12). The reaction mixture was concentrated *in vacuo* to give a light brown residue that was chromatographed on a silica gel column (20 g). Gradient elution with CH_2Cl_2 / MeOH (98:2, 200 mL; 96:4, 200 mL) gave *erythro*-3-(6-amino-8-methyl-9*H*-purin-9-yl)nonan-2-ol (R_f 0.12) (81 mg, 0.278 mmol; 89%) as a white solid: δ_H (200 MHz; $CDCl_3$) 8.14 (1 H, s, H-2), 6.25 (1 H, br s, OH), 4.26 (1 H, qd, *J* 6.5 and 3.0, chain H-2), 3.97 (1 H, dt, *J* 11.1 and 3.0, chain H-3), 2.51 (3 H, s, 8-Me), 2.30 - 1.81 (2 H, m, chain CH_2-4), 1.21 (3 H, d, *J* 6.5, chain CH_3-1), 1.22 - 1.06 (8 H, m), 0.76 (3 H, approx. t, *J* 6.5, chain CH_3-9); δ_C (50 MHz; $CDCl_3$) 154.78 (C), 154.73 (C), 151.22 (CH), 150.02 (C), 149.85 (C), 69.35 (CH), 64.19 (CH), 31.59 (CH_2), 29.08 (CH_2), 27.37 (CH_2), 26.55 (CH_2), 22.52 (CH_2), 21.02 (CH_3), 14.91 (CH_3), 13.98 (CH_3). The minor product component (R_f 0.26; ~10 mg) was identified as 3-(6-methoxy-8-methyl-9*H*-purin-9-yl)nonan-2-ol: δ_H (200 MHz; $CDCl_3$) 8.39 (1 H, s, H-2), 5.67 (1 H, br s, OH), 4.32 (1 H, qd, *J* 6.5 and 2.3, chain H-2), 4.16 (3 H, s, OMe), 4.06 (1 H, dt, *J* 11.1 and 2.7, chain H-3), 2.59 (3 H, s, 8-Me), 2.31 - 1.84 (2 H, m, chain CH_2-4), 1.27 (3 H, d, *J* 6.4, chain CH_3-1), 1.22 - 1.06 (8 H, m), 0.76 (3 H, approx. t, *J* 6.8, chain CH_3-9); δ_C (50 MHz; $CDCl_3$) 160.49 (C), 152.44 (C), 152.05 (C), 150.49 (CH), 121.00 (C), 69.92 (CH), 64.46 (CH), 54.37 (OCH_3), 31.70 (CH_2), 29.23 (CH_2), 27.39 (CH_2), 26.65 (CH_2), 22.66 (CH_2), 21.43 (CH_3), 15.22 (CH_3), 14.14 (CH_3). *erythro*-3-(6-Amino-8-methyl-9*H*-purin-9-yl)nonan-2-ol was evaluated as its hydrochloride salt**,** formed by treatment with a solution of hydrogen chloride in ether followed by evaporation.

***racemic erythro*-3-[6-(methylthio)-9*H*-purin-9-yl]nonan-2-ol (HWC-25)**

Sodium thiomethoxide (71 mg, 1.0 mmol) was added to a stirred solution of *erythro*-3-(6-chloro-9*H*-purin-9-yl)nonan-2-ol[11] (150 mg, 0.505 mmol) in a mixture of DMF (3 mL) and water (1 mL) at 0 ℃. The mixture was allowed to attain room temperature and stirred for 3 h. TLC (9:1 CH_2Cl_2 / MeOH) indicated consumption of starting material (R_f 0.53) and formation of product (R_f 0.60). The reaction mixture was diluted with EtOAc (50 mL) and then washed successively with water (15 mL), saturated sodium bicarbonate solution (15 mL) and brine (15 mL). The organic phase was dried over Na_2SO_4, filtered and evaporated to give a dense colourless oil that was chromatographed on a silica gel column (10 g). Gradient elution with CH_2Cl_2 / MeOH (99:1, 100 mL; 98:2, 100 mL) gave partially purified product (152 mg) that was re-chromatographed on a silica gel column (10 g). Gradient elution with CH_2Cl_2 / MeOH (99:1, 100 mL, 98:2, 100 mL) gave *erythro*-3-[6-(methylthio)-9*H*-purin-9-yl]nonan-2-ol (146 mg, 0.473 mmol; 94%): δ_H (200 MHz; $CDCl_3$) 8.62 (1 H, s), 7.98 (1 H, s), 4.72 (1 H, br d, *J* 4.1, OH), 4.38 (1 H, dt, *J* 10.7 and 3.5, chain H-3), 4.22 (1 H, ~qt, *J* 6.4 and 3.3, chain H-2), 2.62 (3 H, s, SMe), 2.17 - 1.85 (2 H, m, chain CH_2-4), 1.25 (3 H, d, *J* 6.5, chain CH_3-1), 1.20 - 0.95 (8 H, m), 0.76 (3 H, approx. t, *J* 6.5, chain CH_3-9); δ_C (50 MHz; $CDCl_3$) 161.84 (C), 151.47 (CH), 148.06 (C), 142.72 (CH), 131.42 (C), 69.28 (CH), 62.70 (CH), 31.58 (CH_2), 28.90 (CH_2), 27.30 (CH_2), 26.17 (CH_2), 22.56 (CH_2), 20.34 (CH_3), 14.06 (CH_3), 11.86 (CH_3).

***racemic erythro*-3-(7-amino-3*H*-[1,2,3]triazolo[4,5-*d*]pyrimidin-3-yl)nonan-2-ol (HWC-26)**

Sodium nitrite (64 mg, 0.93 mmol) in water (3 mL) was added slowly to a mixture of *erythro*-3-(5-amino-6-chloropyrimidin-4-ylamino)nonan-2-ol[11] (220 mg, 0.767 mmol) in ethanol (5 mL) and hydrochloric acid 1 M (2 mL) at 0 ℃. The mixture was stirred at 0 ℃ for 30 m inutes, treated with conc. ammonium hydroxide (5.0 mL) and refluxed for 30 minutes. The water was reduced by azeotropic distillation of the reaction mixture with toluene and ethanol to give a crude solid (300 mg) that was chromatographed on a silica gel column (20 g). Elution with CH_2Cl_2 / MeOH (95:5, 200 mL) gave *erythro*-3-(7-amino-3*H*-[1,2,3]triazolo[4,5-*d*]pyrimidin-3-yl)nonan-2-ol (185 mg, 0.665 mmol; 87%) as a pale yellow solid: δ_H (400 MHz; $CDCl_3$) 8.45 (1 H, s), 7.20 (2 H, br s, NH_2), 4.89 (1 H, dt, *J* 11.2 and 3.3, chain H-3), 4.58 (1 H, br d, *J* 2.2, OH), 4.37 - 4.30 (1 H, m, chain H-2), 2.32 - 2.19 (1 H, m), 2.08 - 1.99 (1

H, m), 1.32 (3 H, d, *J* 6.4, chain CH_3-1), 1.30 - 1.13 (7 H, m), 1.05 - 0.93 (1 H, m), 0.84 (3 H, approx. t, *J* 6.5, chain CH_3-9); δ_C (101 MHz; $CDCl_3$) 156.26 (C), 156.25 (CH), 149.16 (C), 124.61 (C), 69.57 (CH), 66.23 (CH), 31.49 (CH_2), 28.74 (CH_2), 28.02 (CH_2), 26.05 (CH_2), 22.46 (CH_2), 19.75 (CH_3), 13.97 (CH_3). *erythro*-3-(7-amino-3*H*-[1,2,3]triazolo[4,5-*d*]pyrimidin-3-yl)nonan-2-ol was evaluated as its hydrochloride salt**,** formed by treatment with a solution of hydrogen chloride in ether followed by evaporation: (found: C, 47.60; H, 7.62; N, 25.54. $C_{13}H_{22}N_6O$ /1.0 HCl/0.75 H_2O requires C, 47.56; H, 7.52; N, 25.60%).

***racemic erythro*-3-(6-hydrazinyl-9*H*-purin-9-yl)nonan-2-ol (HWC-27)**

A mixture of *erythro*-3-(6-chloro-9*H*-purin-9-yl)nonan-2-ol[11] (210 mg, 0.708 mmol) and hydrazine hydrate (0.344 mL) in ethanol (7.0 mL) was refluxed at 85 ℃ for 20 h. TLC (9:1 CH_2Cl_2 / MeOH) indicated consumption of starting material (R_f 0.53) and formation of a product component (R_f 0.20, air sensitive). The reaction mixture was evaporated and the residue was chromatographed on a silica gel column (25 g). Gradient elution with CH_2Cl_2 / MeOH (98:2, 200 mL; 95:5, 200 mL; 9:1, 100 mL) gave *erythro*-3-(6-hydrazinyl-9*H*-purin-9-yl)nonan-2-ol (137 mg, 0.469 mmol; 66%) as a white solid: δ_H (400 MHz; DMSO-d_6) 8.87 (1 H, br s, NH), 8.22 (1 H, br s), 8.16 (1 H, s), 5.15 (1 H, d, *J* 5.5, OH), 4.57 (2 H, br s, NH_2), 4.28 - 4.15 (1 H, m, chain H-3), 4.24 (1 H, ~sextet, *J* 6.2, chain H-3), 2.07 - 2.02 (2 H, m, chain CH_2-4), 1.22 - 1.02 (8 H, m), 0.89 (3 H, d, *J* 6.3, chain CH_3-1), 0.78 (3 H, approx. t, *J* 6.5, chain CH_3-9); δ_C (101 MHz; DMSO-d_6) 155.91 (C), 152.44 (CH), 149.69 (C), 140.30 (CH), 118.25 (C), 68.42 (CH), 61.28 (CH), 31.42 (CH_2), 29.21 (CH_2), 28.49 (CH_2), 25.92 (CH_2), 22.33 (CH_2), 20.86 (CH_3), 14.27 (CH_3).

1-[2-(2-methoxyethoxy)ethyl]-1*H*-pyrazolo[3,4-*d*]pyrimidin-4-amine (HWC-34) and 2-[2-(2-methoxyethoxy)ethyl]-2*H*-pyrazolo[3,4-*d*]pyrimidin-4-amine (HWC-35)

3-Amino-1-[2-(2-methoxyethoxy)ethyl]-1*H*-pyrazole-4-carbonitrile & 5-amino-1-[2-(2-methoxyethoxy)ethyl]-1*H*-pyrazole-4-carbonitrile

1-Bromo-2-(2-methoxyethoxy)ethane (753 µL, 5.59 mmol) was added dropwise to a suspension of 3-amino-1*H*-pyrazole-4-carbonitrile (504 mg, 4.66 mmol) and anhydrous potassium carbonate (0.773 g, 5.59 mmol) in DMF (5.0 mL) and the reaction mixture was stirred at 50 ℃ for 20 h. TLC (CH_2Cl_2/MeOH, 9:1) indicated consumption of starting material 3-amino-1*H*-pyrazole-4-carbonitrile (R_f 0.29) and formation of two product components (R_f 0.47 and 0.42). After cooling, the inorganic material was filtered off and the solution was evaporated to dryness under reduced pressure. The residue was chromatographed on a silica gel column (25 g). Gradient elution with CH_2Cl_2 / MeOH (99:1, 100 mL; 98:2, 200 mL; 95:5, 200 mL) gave 5-amino-1-[2-(2-methoxyethoxy)ethyl]-1*H*-pyrazole-4-carbonitrile (225 mg, 1.07 mmol; 23%) (R_f 0.47), 3-amino-1-[2-(2-methoxyethoxy)ethyl]-1*H*-pyrazole-4-carbonitrile (329 mg, 1.56 mmol; 34%) (R_f 0.42) and a 1.8:1 mixture of the two isomers (424 mg; 43%) as colourless oils. 5-Amino-1-[2-(2-methoxyethoxy)ethyl]-1*H*-pyrazole-4-carbonitrile: δ_H (400 MHz; $CDCl_3$) 7.41 (1 H, s, pyrazole H), 4.98 (2 H, br s, NH_2), 4.15 - 4.11 (2 H, m), 3.78 - 3.75 (2 H, m), 3.60 - 3.56 (2 H, m), 3.49 - 3.46 (2 H, m), 3.32 (3 H, s); δ_C (101 MHz; $CDCl_3$) 151.93 (C), 140.09 (CH), 114.61 (C), 76.20 (C), 71.43 (CH_2), 70.85 (CH_2), 70.29 (CH_2), 58.87 (OCH_3), 49.60 (NCH_2). 3-Amino-1-[2-(2-methoxyethoxy)ethyl]-1*H*-pyrazole-4-carbonitrile: δ_H (400 MHz; $CDCl_3$) 7.66 (1 H, s, pyrazole H), 4.18 (2 H, br s, NH_2), 4.12 - 4.09 (2 H, m), 3.80 - 3.7 (2 H, m), 3.60 - 3.57 (2 H, m), 3.52 - 3.49 (2 H, m), 3.38 (3 H, s); δ_C (101 MHz; $CDCl_3$) 156.65 (C), 135.38 (CH), 113.82 (C), 78.89 (C), 71.74 (CH_2), 70.56 (CH_2), 68.83 (CH_2), 59.02 (OCH_3), 52.46 49.60 (NCH_2).

1-[2-(2-Methoxyethoxy)ethyl]-1*H*-pyrazolo[3,4-*d*]pyrimidin-4-amine (HWC-34)

Formamide (0.500 mL, 12.5 mmol) was added to 5-amino-1-[2-(2-methoxyethoxy)ethyl]-1*H*-pyrazole-4-carbonitrile (196 mg, 0.932 mmol) and the reaction mixture was heated at 210 ℃ for 1.5 h. TLC (9:1 CH_2Cl_2 / MeOH) indicated consumption of starting material (R_f 0.47) and formation of a product component (R_f 0.35) with some trace impurities. After cooling, the brown solution was diluted with MeOH, mixed with silica gel and allowed to evaporate for 18 h. The crude sample (dry loaded) was chromatographed on a silica gel column (20 g). Gradient elution with CH_2Cl_2 / MeOH (98:2, 250 mL; 95:5, 250 mL) gave an oil (600 mg). The partially purified oil was dissolved in EtOAc (100 mL) and washed with water (3 x 15). The organic phase was dried over Na_2SO_4, filtered

and concentrated *in vacuo* to give 1-[2-(2-methoxyethoxy)ethyl]-1*H*-pyrazolo[3,4-*d*]pyrimidin-4-amine (165 mg, 0.695 mmol; 75%) as a white solid: δ_H (400 MHz; $CDCl_3$) 8.34 (1 H, s), 8.10 (1 H, s), 6.69 (2 H, br s, NH_2), 4.61 (2 H, t, *J* 5.7), 4.00 (2 H, t, *J* 5.7), 3.65 - 3.60 (2 H, m), 3.51 - 3.46 (2 H, m), 3.31 (3 H, s, OMe); δ_C (101 MHz; $CDCl_3$) 156.36 (C), 153.21 (CH), 153.14 (C), 132.14 (CH), 100.36 (C), 71.77 (CH_2), 70.15 (CH_2), 69.02 (CH_2), 58.89 (OMe), 46.90 (NCH_2).

2-[2-(2-Methoxyethoxy)ethyl]-2*H*-pyrazolo[3,4-*d*]pyrimidin-4-amine (HWC-35)

Formamide (0.700 mL, 17.6 mmol) was added to 3-amino-1-[2-(2-methoxyethoxy)ethyl]-1*H*-pyrazole-4-carbonitrile (304 mg, 1.45 mmol) and the reaction mixture was heated at 210 ℃ for 1.5 h. TLC (9:1 CH_2Cl_2 / MeOH) indicated consumption of starting material (R_f 0.42) and formation of a product component (R_f 0.25) with some trace impurities. After cooling, the brown mixture was diluted with MeOH, mixed with silica gel and allowed to evaporate at room temperature for 18 h. The crude material (dry loaded) was chromatographed on a silica gel column (20 g). Gradient elution with CH_2Cl_2 / MeOH (98:2, 250 mL; 95:5, 250 mL; 9:1, 250 mL) gave 2-[2-(2-methoxyethoxy)ethyl]-2*H*-pyrazolo[3,4-*d*]pyrimidin-4-amine (196 mg, 0.826 mmol; 57%) as a light brown solid: δ_H (400 MHz; $CDCl_3$/CD_3OD) 8.26 (1 H, s), 8.23 (1 H, s), 4.49 - 4.45 (2 H, m), 3.92 - 3.88 (2 H, m), 3.55 - 3.52 (2 H, m), 3.47 - 3.44 (2 H, m), 3.29 (3 H, s, OMe); δ_C (101 MHz; $CDCl_3$/CD_3OD) 159.36 (C), 159.18 (C), 155.51 (CH), 125.87 (CH), 101.64 (C), 71.53 (CH_2), 70.11 (CH_2), 69.00 (CH_2), 58.67 (OMe), 53.74 (NCH_2).

1-octyl-1*H*-pyrazolo[3,4-*d*]pyrimidin-4-amine hydrochloride (HWC-40) and 2-octyl-2*H*-pyrazolo[3,4-*d*]pyrimidin-4-amine hydrochloride (HWC-41)

3-Amino-1-octyl-1*H*-pyrazole-4-carbonitrile and 5-amino-1-octyl-1*H*-pyrazole-4-carbonitrile

1-Bromooctane (1.04 mL, 5.99 mmol) was added dropwise to a suspension of 3-amino-1*H*-pyrazole-4-carbonitrile (540 mg, 5.00 mmol) and anhydrous potassium carbonate (828 mg, 5.99 mmol) in diemtheylformamide (5.0 mL) at room temperature and the reaction mixture was stirred at 50 ℃ for 18 h. TLC (2:1 light petroleum / Et OAc) indicated consumption of starting material 3-amino-1*H*-pyrazole-4-carbonitrile (R_f 0.03) and formation of product (R_f 0.30). After cooling, the inorganic material was filtered off and the solution was evaporated to dryness under reduced pressure. The residue was chromatographed on a silica gel column (20 g). Gradient elution with light petroleum / EtOAc (7:1, 200 mL; 3:1, 200; 1:1, 100 mL) gave a 2.4:1 mixture of 3-amino-1-octyl-1*H*-pyrazole-4-carbonitrile and 5-amino-1-octyl-1*H*-pyrazole-4-carbonitrile (684 mg, 3.11 mmol; 63%). Major product: δ_H (400 MHz; $CDCl_3$) 7.49 (1 H, s), 4.29 (2 H, br s), 3.90 (2 H, t, *J* 7.2), 1.82 (2 H, quintet, *J* 7.1), 1.30 - 1.17 (10 H, m), 0.85 (3 H, approx. t, *J* 6.6); δ_C (101 MHz; $CDCl_3$) 156.69 (C), 133.76 (CH), 113.84 (C), 78.37 (C) 52.68 (CH_2), 31.70 (CH_2), 29.57 (CH_2), 29.06 (CH_2), 28.98 (CH_2), 26.41 (CH_2), 22.58 (CH_2), 14.05 (CH_3).

1-Octyl-1*H*-pyrazolo[3,4-*d*]pyrimidin-4-amine hydrochloride (HWC-40) and 2-octyl-2*H*-pyrazolo[3,4-*d*]pyrimidin-4-amine hydrochloride (HWC-41)

Formamide (0.800 mL, 20.1 mmol) was added to a mixture of 5-amino-1-octyl-1*H*-pyrazole-4-carbonitrile and 3-amino-1-octyl-1*H*-pyrazole-4-carbonitrile (1:2.35; 618 mg, 2.81 mmol) and the reaction mixture was heated at 210 ℃ for 1 h. TLC (9:1 CH_2Cl_2 / MeOH) indicated consumption of starting materials (R_f 0.65) and formation of two product components (R_f 0.31 & 0.24) with some trace impurities. After cooling, water was added to the brown reaction mixture and the separated solid was collected by filtration, washing with water, and dried over P_2O_5 *in vacuo*. The crude material was chromatographed on a silica gel column (25 g). Gradient elution with CH_2Cl_2 / MeOH (98:2, 400 mL; 95:5, 250 mL; 9:1, 175 mL) gave partially purified 1-octyl-1*H*-pyrazolo[3,4-*d*]pyrimidin-4-amine (106 mg) and pure 2-octyl-2*H*-pyrazolo[3,4-*d*]pyrimidin-4-amine (365 mg, 1.48 mmol) (R_f 0.24). The partially purified 1-octyl-1*H*-pyrazolo[3,4-*d*]pyrimidin-4-amine (R_f 0.31) was re-chromatographed on a silica gel column (20 g). Elution with light petroleum / EtOAc (1:1.5, 400 mL) gave 1-octyl-1*H*-pyrazolo[3,4-*d*]pyrimidin-4-amine (91 mg, 0.37 mmol).

1-Octyl-1*H*-pyrazolo[3,4-*d*]pyrimidin-4-amine: δ_H (400 MHz; $CDCl_3$) 8.39 (1 H, s), 7.92 (1 H, s), 6.14 (2 H, br s, NH_2), 4.40 (2 H, t, *J* 7.2), 1.93 (2 H, quintet, *J* 7.3), 1.33 - 1.23 (10 H, m), 0.86 (3 H, approx. t, *J* 6.9); δ_C (101 MHz;

$CDCl_3$) 157.69 (C), 155.52 (CH), 153.23 (C), 130.23 (CH), 100.58 (C), 47.33 (CH_2), 31.71 (CH_2), 29.65 (CH_2), 29.09 (2 x CH_2), 26.64 (CH_2), 22.58 (CH_2), 14.05 (CH_3). 1-Octyl-1*H*-pyrazolo[3,4-*d*]pyrimidin-4-amine was evaluated as its hydrochloride salt**,** formed by treatment with a solution of hydrogen chloride in ether followed by evaporation: (found: C, 53.84; H, 7.95; N, 24.68. $C_{13}H_{21}N_5$/1.12 HCl requires C, 54.18; H, 7.74; N, 24.30%).

2-Octyl-2*H*-pyrazolo[3,4-*d*]pyrimidin-4-amine: δ_H (400 MHz; $CDCl_3$/CD_3OD) 8.29 (1 H, s), 8.18 (1 H, s), 4.26 (2 H, t, *J* 7.2), 1.97 - 1.87 (2 H, m), 1.27 - 1.18 (10 H, m), 0.82 (3 H, approx. t, *J* 6.9); δ_C (101 MHz; $CDCl_3$/CD_3OD) 159.67 (C), 159.36 (C), 155.90 (CH), 124.09 (CH), 101.61 (C), 54.00 (CH_2), 31.65 (CH_2), 30.13 (CH_2), 29.01 (CH_2), 28.97 (CH_2), 26.48 (CH_2), 22.51 (CH_2), 13.95 (CH_3). 2-Octyl-2*H*-pyrazolo[3,4-*d*]pyrimidin-4-amine was evaluated as its hydrochloride salt**,** formed by treatment with a solution of hydrogen chloride in ether followed by evaporation: (found: C, 48.82; H, 7.46; N, 22.20. $C_{13}H_{21}N_5$/1.95 HCl requires C, 49.03; H, 7.26; N, 21.99%).

(2*S*,3*R*)-3-(6-amino-9*H*-purin-9-yl)-5-phenylpentan-2-ol hydrochloride (HWC-44)

(*S*,*E*)-4-(*tert*-Butyldimethylsilyloxy)-1-phenylpent-1-en-3-one

n-Butyllithium (2.5 M in hexane; 8.81 mL, 22.0 mmol) was added dropwise to a solution of (*S*)-dimethyl 3-(*tert*-butyldimethylsilyloxy)-2-oxobutylphosphonate[14] (6.84 g, 22.0 mmol) in THF (100 mL) at -78 ℃. After 25 minutes, benzaldehyde (2.03 mL, 20.0 mmol) was added and the reaction mixture was slowly allowed to attain to room temperature and stirred for 18 h. TLC (light petroleum / EtOAc 95:5) indicated the presence of the starting materials benzaldehyde (R_f 0.31) and phosphonate (R_f 0.05) and a new component (R_f 0.44). The reaction mixture was warmed to 40 ℃ for 16 h after which period TLC indicated the complete consumption of starting material. The reaction mixture was quenched by the slow addition of saturated sodium bicarbonate solution (50 mL) and extracted with CH_2Cl_2 (150 mL). The organic extract was washed with brine (2 x 30 mL), dried with Na_2SO_4, filtered and evaporated to give a crude material **(**6.08 g) as a pale yellow oil. The crude material was chromatographed on a silica gel column (60 g). Elution with light petroleum / EtOAc (95:5, 600 mL) gave (*S*,*E*)-4-(*tert*-butyldimethylsilyloxy)-1-phenylpent-1-en-3-one (5.03 g, 17.3 mmol; 86%): δ_H (200 MHz; $CDCl_3$) 7.71 (1 H, d, *J* 16.1), 7.60 - 7.53 (2 H, m), 7.41 - 7.35 (3 H, m), 7.27 (1 H, d, *J* 16.1), 4.32 (1 H, q, *J* 6.8), 1.35 (3 H, d, *J* 6.8), 0.92 (9 H, s), 0.08 (3 H, s), 0.07 (3 H, s); δ_C (50 MHz; $CDCl_3$) 202.37 (C=O), 144.05 (CH), 135.03 (C), 130.71 (CH), 129.13 (2 x CH), 128.63 (2 x CH), 120.33 (CH), 74.88 (CH), 25.97 (3 x CH_3), 21.46 (CH_3), 18.37 (C), -4.59 (CH_3), -4.75 (CH_3).

(3*S*,4*S*,*E*)-4-(*tert*-Butyldimethylsilyloxy)-1-phenylpent-1-en-3-ol and (2*S*,3*S*,*E*)-3-(*tert*-butyldimethylsilyloxy)-5-phenylpent-4-en-2-ol

L-Selectride (1 M in THF; 20.4 mL, 20.4 mmol) was added dropwise over 30 minutes to a solution of (*S*,*E*)-4-(*tert*-butyldimethylsilyloxy)-1-phenylpent-1-en-3-one (4.94 g, 17.0 mmol) in THF (100 mL) at -78 ℃ and the reaction mixture was stirred for 3 h. TLC (light petroleum / EtOAc 95:5) indicated the consumption of starting material (R_f 0.44) and the presence of two new compounds (R_f 0.24 and 0.18). The reaction mixture was partitioned with a mixture of EtOAc and water (1:1, 30 mL) and the phases then separated. The organic layer was diluted with EtOAc (100 mL), washed with brine, dried with Na_2SO_4, filtered and evaporated to give a mixture 1:1.16 of (2*S*,3*S*,*E*)-3-(*tert*-butyldimethylsilyloxy)-5-phenylpent-4-en-2-ol and (3*S*,4*S*,*E*)-4-(*tert*-butyldimethyl-silyloxy)-1-phenylpent-1-en-3-ol (7.69 g) as a colourless oil.

(3*S*,4*S*)-4-(*tert*-Butyldimethylsilyloxy)-1-phenylpentan-3-ol

A solution of (2*S*,3*S*,*E*)-3-(*tert*-butyldimethylsilyloxy)-5-phenylpent-4-en-2-ol and (3*S*,4*S*,*E*)-4-(*tert*-butyldimethylsilyloxy)-1-phenylpent-1-en-3-ol (1:1.16 mixture; 4.97 g, 17.0 mmol) in ethanol (100 mL) was hydrogenated over 10% palladium on carbon (0.892 g) under hydrogen (1 atm) at 20 ℃ for 20 h. TLC (light petroleum / EtOAc 95:5) indicated consumption of the starting materials and the presence of two new compounds (R_f 0.28 and 0.20). The reaction mixture was flushed with nitrogen and filtered through celite, washing with EtOAc.

[14] G. Shapiro, D. Buechler and S. Hennet, *Tetrahedron Lett.*, 1990, **31**, 5733-5736.

The filtrate was concentrated *in vacuo* and the crude residue chromatographed on a silica gel column (80 g). Gradient elution with light petroleum / EtOAc (99:1~90:1) gave (3*S*,4*S*)-4-(*tert*-butyldimethylsilyloxy)-1-phenylpentan-3-ol (R_f 0.28) (2.01 g, 6.83 mmol; 87%) and (2S,3*S*)-3-(*tert*-butyldimethylsilyloxy)-5-phenylpentan-2-ol (R_f 0.20) (2.46 g, 8.35 mmol; 91%). (3*S*,4*S*)-4-(*tert*-Butyldimethylsilyloxy)-1-phenylpentan-3-ol: δ_H (400 MHz; $CDCl_3$) 7.31 - 7.26 (2 H, m), 7.23 - 7.17 (3 H, m), 3.66 (1 H, qd, *J* 6.2 and 5.2, H-4), 3.33 - 3.29 (1 H, m, H-3), 2.91 - 2.84 (1 H, m, H-1*a*), 2.74 - 2.66 (1 H, m, H-1*b*), 2.39 (1 H, br s), 1.78 - 1.66 (2 H, m, CH_2-2), 1.18 (3 H, d, *J* 6.2), 0.95 (9 H, s), 0.13 (6 H, s); δ_C (101 MHz; $CDCl_3$) 142.31 (C), 128.49 (2 x CH), 128.35 (2 x CH), 125.74 (CH), 75.04 (CH), 71.84 (CH), 35.35 (CH_2), 32.13 (CH_2), 25.85 (3 x CH_3), 20.25 (CH_3), 18.04 (C), -4.12 ($SiCH_3$), -4.81 ($SiCH_3$). (2S,3*S*)-3-(*tert*-Butyldimethylsilyloxy)-5-phenylpentan-2-ol: δ_H (400 MHz; $CDCl_3$) 7.35 - 7.30 (2 H, m), 7.25 - 7.20 (3 H, m), 3.79 (1 H, qd, *J* 6.3 and 4.8, H-4), 3.56 (1 H, dt, *J* 6.0 and 4.8, H-3), 2.77 - 2.63 (2 H, m, CH_2-1), 2.17 (1 H, br s, OH), 1.98 (1 H, ddt, *J* 13.9, 10.4 and 5.9, H-2*a*), 1.79 (1 H, dddd, *J* 4.8, 6.3, 11.0 and 13.9, H-2*b*), 1.21 (3 H, d, *J* 6.4), 0.97 (9 H, s), 0.14 (3 H, s), 0.13 (3 H, s); δ_C (101 MHz; $CDCl_3$) 142.22 (C), 128.43 (2 x CH), 128.28 (2 x CH), 125.84 (CH), 76.19 (CH), 68.98 (CH), 35.55 (CH_2), 31.22 (CH_2), 25.92 (3 x CH_3), 19.56 (CH_3), 18.15 (C), -4.13 ($SiCH_3$), -4.57 ($SiCH_3$).

9-[(3*R*,4*S*)-4-(*tert*-Butyldimethylsilyloxy)-1-phenylpentan-3-yl]-6-chloro-9*H*-purine

Diisopropyl azodicarboxylate (2.52 mL, 12.8 mmol) was added to a stirred solution of (3*S*,4*S*)-4-(*tert*-butyldimethylsilyloxy)-1-phenylpentan-3-ol (1.26 g, 4.27 mmol), 6-chloro-9*H*-purine (667 mg, 4.32 mmol) and triphenylphosphine (2.24 g, 8.54 mmol) in THF (100 mL) at room temperature and the mixture was stirred at room temperature for 48 h. TLC (3:1 light petroleum / EtOAc) indicated almost complete consumption of starting materials (R_f 0.74 and baseline) and formation of product (R_f 0.47). The reaction mixture was filtered through a short silica gel column, washing with light petroleum / EtOAc (2:1, 150 mL), and the filtrate was concentrated *in vacuo* to give an orange oil (4.16 g) that was chromatographed on a silica gel column (80 g). Gradient elution with light petroleum / EtOAc (9:1, 500 mL; 7:1, 800; 5:1, 540 mL) gave 9-[(3*R*,4*S*)-4-(*tert*-butyldimethylsilyloxy)-1-phenylpentan-3-yl]-6-chloro-9*H*-purine (402 mg, 0.933 mmol; 22%) as a white solid: δ_H (200 MHz; $CDCl_3$) 8.70 (1 H, s), 8.13 (1 H, s), 7.34 - 7.19 (3 H, m), 7.01 - 6.91 (2 H, m), 4.59 - 4.49 (1 H, m, chain H-3), 4.19 (1 H, qd, *J* 6.3 and 4.4, chain H-4), 2.58 - 2.32 (4 H, m, chain CH_2-1 and CH_2-2), 1.11 (3 H, d, *J* 6.3, chain CH_3-5), 0.84 (9 H, s), -0.04 (3 H, s), -0.19 (3 H, s); δ_C (50 MHz; $CDCl_3$) 152.15 (C), 151.88 (CH), 151.13 (C), 145.19 (CH), 140.05 (C), 131.77 (C), 128.73 (2 x CH), 128.34 (2 x CH), 126.57 (CH), 70.07 (CH), 61.89 (CH), 32.32 (CH_2), 29.10 (CH_2), 25.95 (3 x CH_3), 20.68 (CH_3), 18.06 (C), -4.17 ($SiCH_3$), -4.90 ($SiCH_3$).

9-[(3*R*,4*S*)-4-(*tert*-Butyldimethylsilyloxy]-1-phenylpentan-3-yl)-9*H*-purin-6-amine

A mixture of 9-[(3*R*,4*S*)-4-(*tert*-butyldimethylsilyloxy)-1-phenylpentan-3-yl]-6-chloro-9*H*-purine (354 mg, 0.821 mmol) and ammonia (7 N in MeOH; 4.50 mL, 31.5 mmol) was heated at 80 ℃ in a sealed pressure tube for 18 h. TLC (95:5 CH_2Cl_2 / MeOH) indicated consumption of starting material (R_f 0.81) and formation of two product components, minor (R_f 0.70) and major (R_f 0.40). The reaction mixture was evaporated to give a crude white solid that was chromatographed on a silica gel column (40 g). Gradient elution with CH_2Cl_2 / MeOH (99:1, 150 mL; 92:2, 200 mL; 95:5, 150 mL) gave 9-[(3*R*,4*S*)-4-(*tert*-butyldimethylsilyloxy]-1-phenylpentan-3-yl)-9*H*-purin-6-amine (R_f 0.40) (228 mg, 0.554 mmol; 67%) as a white solid and 9-[(3*R*,4*S*)-4-(*tert*-butyldimethylsilyloxy)-1-phenylpentan-3-yl]-6-methoxy-*9H*-purine (R_f 0.70) (84 mg, 0.177 mmol; 22%) as a pale yellow dense oil.

9-[(3*R*,4*S*)-4-(*tert*-Butyldimethylsilyloxy)-1-phenylpentan-3-yl]-9*H*-purin-6-amine: δ_H (200 MHz; $CDCl_3$) 8.34 (1 H, s), 7.85 (1 H, s), 7.27 - 7.15 (3 H, m), 7.07 - 6.97 (2 H, m), 5.99 (2 H, br s, NH_2), 4.44 - 4.34 (1 H, m, chain H-3), 4.13 (1 H, qd, *J* 6.2 and 4.6, chain H-4), 2.52 - 2.33 (4 H, m, chain CH_2-1 and CH_2-2), 1.10 (3 H, d, *J* 6.2, chain CH_3-5), 0.85 (9 H, s), -0.05 (3 H, s), -0.20 (3 H, s); δ_C (50 MHz; $CDCl_3$) 155.68 (C), 152.93 (CH), 150.42 (C), 140.71 (CH), 140.39 (C), 128.69 (2 x CH), 128.47 (2 x CH), 126.40 (CH), 120.13 (C), 70.21 (CH), 61.03 (CH), 32.33 (CH_2), 29.28 (CH_2), 25.99 (3 x CH_3), 20.94 (CH_3), 17.84 (C), -4.16 ($SiCH_3$), -4.95 ($SiCH_3$).

9-[(3*R*,4*S*)-4-(*tert*-Butyldimethylsilyloxy)-1-phenylpentan-3-yl]-6-methoxy-9*H*-purine: δ_H (200 MHz; $CDCl_3$) 8.52 (1 H, s), 7.97 (1 H, br s), 7.23 - 7.12 (3 H, m), 7.02 - 6.91 (2 H, m), 4.49 - 4.35 (1 H, m, chain H-3), 4.18 (3 H, s, OMe),

4.12 (1 H, qd, *J* 6.2 and 4.7, chain H-4), 2.55 - 2.26 (4 H, m, chain CH_2-1 and CH_2-2), 1.07 (3 H, d, *J* 6.2, chain CH_3-5), 0.83 (9 H, s), -0.07 (3 H, s), -0.21 (3 H, s); δ_C (50 MHz; $CDCl_3$) 161.19 (C), 151.97 (CH), 149.39 (C), 141.98 (CH), 140.43 (C), 128.63 (2 x CH), 128.37 (2 x CH), 126.36 (CH), 121.73 (C), 70.08 (CH), 61.27 (CH), 54.31 (OCH_3), 32.20 (CH_2), 29.27 (CH_2), 25.91 (3 x CH_3), 20.77 (CH_3), 17.99 (C), -4.26 ($SiCH_3$), -5.00 ($SiCH_3$).

(2*S*,3*R*)-3-(6-Amino-9*H*-purin-9-yl)-5-phenylpentan-2-ol

Tetrabutylammonium fluoride (1 M in THF; 1.07 mL, 1.07 mmol) was added to a solution of 9-[(3*R*,4*S*)-4-(*tert*-butyldimethylsilyloxy)-1-phenylpentan-3-yl]-9*H*-purin-6-amine (220 mg, 0.534 mmol) in THF (15 mL) at room temperature and stirred for 18 h. TLC (95:5 CH_2Cl_2 / MeOH) indicated consumption of starting material (R_f 0.40) and formation of a product component (R_f 0.26). The reaction mixture was evaporated and the residue was dissolved in EtOAc (50 mL), washed with brine (3 x 10 mL), dried over Na_2SO_4, filtered and concentrated *in vacuo* to give a crude white solid. The crude material was chromatographed on a silica gel column (15 g). Gradient elution with CH_2Cl_2 / MeOH (98:2, 150 mL; 95:5, 200 mL; 9:1, 150 mL) gave (2*S*,3*R*)-3-(6-amino-9*H*-purin-9-yl)-5-phenylpentan-2-ol (R_f 0.26) (150 mg, 0.504 mmol; 94%) as a dense colourless oil that solidified upon standing: δ_H (200 MHz; $CDCl_3$) 8.26 (1 H, br s), 7.76 (1 H, br s), 7.23 - 7.12 (3 H, m), 7.02 (2 H, ~d, *J* 7.6), 6.50 (2 H, s, NH_2), 5.55 (1 H, br s, OH), 4.31 - 4.13 (2 H, m, chain H-2 and H-3), 2.56 - 2.21 (4 H, m, chain CH_2-4 and CH_2-5), 1.22 (3 H, d, *J* 6.3, chain CH_3-1); δ_C (50 MHz; $CDCl_3$) 156.02 (C), 152.54 (CH), 149.77 (C), 140.71 (CH), 140.28 (C), 128.72 (2 x CH), 128.41 (2 x CH), 126.47 (CH), 120.19 (C), 69.61 (CH), 62.45 (CH), 32.21 (CH_2), 28.72 (CH_2), 20.32 (CH_3). (2*S*,3*R*)-3-(6-Amino-9*H*-purin-9-yl)-5-phenylpentan-2-ol was evaluated as its hydrochloride salt**,** formed by treatment with a solution of hydrogen chloride in ether followed by evaporation: (found: C, 52.47; H, 5.84; N, 18.97. $C_{16}H_{19}N_5O$/1.9 HCl requires C, 52.42; H, 5.75; N, 19.10%).

(*rac*)-9-(nonan-3-yl)-9*H*-purin-6-amine (HWC-57)

(*rac*)-6-Chloro-9-(nonan-3-yl)-9*H*-purine

Diisopropyl azodicarboxylate (2.33 mL, 12.0 mmol) was added to a mixture of nonan-3-ol (1.26 mL, 7.20 mmol), 6-chloro-9*H*-purine (0.93 g, 6.00 mmol) and triphenylphosphine (2.36 g, 9.00 mmol) in THF (50 mL) at room temperature and stirred for 48 h. TLC (4:1 light petroleum / EtOAc) indicated consumption of nonan-3-ol (R_f 0.59) and formation of a product component (R_f 0.28). The reaction mixture was filtered through a short silica gel column, washing with light petroleum / EtOAc (1:1, 100 mL). Evaporation of the filtrate gave a crude yellow oil that was chromatographed on a silica gel column (80 g). Gradient elution with light petroleum / EtOAc (9:1, 1 L; 7:1, 800 mL; 5:1, 840 mL) gave 6-chloro-9-(nonan-3-yl)-9*H*-purine (1.30 g, 4.63 mmol; 77%) as a dense pale yellow oil: δ_H (200 MHz; $CDCl_3$): 8.70 (1 H, s), 8.08 (1 H, s), 4.47 (1 H, m), 2.07 - 1.88 (4 H, m), 1.27 - 1.10 (8 H, m), 0.83 - 0.72 (6 H, m); δ_C (50 MHz; $CDCl_3$): 152.25 (C), 151.88 (CH), 151.14 (C), 144.15 (CH), 131.91 (C), 59.01 (CH), 34.75 (CH_2), 31.65 (CH_2), 28.90 (CH_2), 28.29 (CH_2), 26.23 (CH_2), 22.63 (CH_2), 14.15 (CH_3), 10.84 (CH_3).

(*rac*)-9-(Nonan-3-yl)-9*H*-purin-6-amine (HWC-57)

A mixture of 6-chloro-9-(nonan-3-yl)-9*H*-purine (560 mg, 1.99 mmol) and ammonia (7 N in MeOH; 4.5 mL, 31 mmol) was heated at 80 ℃ in a 5 mL sealed pressure tube for 18 h. TLC (1:1 light petroleum / EtOAc) indicated remaining starting material (R_f 0.66) and two new product components, minor (R_f 0.41) and major (R_f 0.06). The reaction mixture was evaporated to give a crude white solid that was chromatographed on a silica gel column (20 g). Gradient elution with light petroleum / EtOAc (4:1, 400 mL; 1:1, 200 mL) followed by CH_2Cl_2 / MeOH (9:1, 100 mL) gave starting material 6-chloro-9-(nonan-3-yl)-9*H*-purine (287 mg) and 9-(nonan-3-yl)-9*H*-purin-6-amine (R_f 0.06) (145 mg, 0.56 mmol; 28%) as a white solid: δ_H (200 MHz; $CDCl_3$) 8.30 (1 H, s), 7.76 (1 H, s), 6.33 (2 H, br s), 4.59 - 4.41 (1 H, m), 2.02 - 1.80 (4 H, m), 1.27 - 1.03 (8 H, m), 0.86 - 0.69 (6 H, m); δ_C (50 MHz; $CDCl_3$) 155.89 (C), 152.84 (CH), 150.47 (C), 139.21 (CH), 119.87 (C), 57.88 (CH), 34.94 (CH_2), 31.70 (CH_2), 28.98 (CH_2), 28.45 (CH_2), 26.22 (CH_2), 22.64 (CH_2), 14.16 (CH_3), 10.81 (CH_3). 9-(Nonan-3-yl)-9*H*-purin-6-amine was evaluated as its hydrochloride salt**,** formed by treatment with a solution of hydrogen chloride in ether followed by evaporation: (found: C, 51.03; H, 7.76; N, 21.25. $C_{14}H_{23}N_5$/1.87 HCl requires C, 51.02; H, 7.61; N, 21.34%).

(2*S*,3*S*)-3-(6-amino-9*H*-purin-9-yl)hexan-2-ol (HWC-60)

(*S*,*E*)-2-(*tert*-Butyldimethylsilyloxy)hex-4-en-3-one

Lithium chloride (0.69 g, 16.2 mmol) was added to a solution of (*S*)-dimethyl 3-(*tert*-butyldimethylsilyloxy)-2-oxobutylphosphonate[14] (5.03 g, 16.2 mmol) in acetonitrile (100 mL) under argon at room temperature. *N,N*-Diisoproplyethylamine (2.41 mL, 13.4 mmol) was added and the reaction mixture was stirred for 2 h to give a viscous mixture. Acetaldehyde (0.99 mL, 17.2 mmol) was added and the reaction mixture was stirred for a further 92 h. TLC (10% EtOAc / light petroleum) indicated a new component (R_f 0.52). The reaction mixture was quenched with brine (50 mL), extracted with EtOAc (3 x 40 mL), dried with Na_2SO_4 and evaporated to give a crude colourless oil (2 g). The crude material was chromatographed on a silica gel column (40 g). Elution with 2% EtOAc / light petroleum gave (*S*,*E*)-2-(*tert*-butyldimethylsilyloxy)hex-4-en-3-one (1.92 g, 8.40 mmol; 52%): δ_H (200 MHz; $CDCl_3$) 6.99 (1 H, dq, *J* 15.6 & 6.9), 6.57 (1 H, dt, *J* 15.5 & 1.6), 4.22 (1 H, q, *J* 6.8), 1.89 (3 H, dd, *J* 6.8 & 1.6), 1.27 (3 H, d, *J* 6.8), 0.88 (9 H, s), 0.04 (6 H, s); d_C (50 MHz; $CDCl_3$) 201.91 (CO), 144.35 (CH), 125.88 (CH), 74.50 (CH), 25.91 (3 x CH_3), 21.30 (CH_3), 18.70 (CH_3), 18.33 (C), -4.69 ($SiCH_3$), -4.83 ($SiCH_3$).

(2*S*,3*S*,*E*)-2-(*tert*-Butyldimethylsilyloxy)hex-4-en-3-ol and (2*S*,3*S*,*E*)-3-(*tert*-butyldimethylsilyloxy)hex-4-en-2-ol

Lithium tri-*sec*-butylborohydride (1 M THF solution; 11.2 mL, 11.2 mmol) was added dropwise to a solution of (*S*,*E*)-2-(*tert*-butyldimethylsilyloxy)hex-4-en-3-one (1.71 g, 7.50 mmol) in THF (40 mL) under argon at 0 ℃ over a pe riod of 15 minutes and the reaction mixture was stirred for a further 3 h. TLC (5% EtOAc / light petroleum) indicated formation of a new component (R_f 0.29). The reaction mixture was quenched by the slow addition of a mixture of EtOAc / water (1:1, 20 mL). The organic layer was washed with brine (2 x 10 mL), dried with Na_2SO_4 and evaporated to give a pale brown oil. The crude oil was chromatographed on a silica gel column (30 g). Elution with 2% EtOAc / light petroleum gave a mixture of (2*S*,3*S*,*E*)-2-(*tert*-butyldimethylsilyloxy)hex-4-en-3-ol and (2*S*,3*S*,*E*)-3-(*tert*-butyldimethylsilyloxy)hex-4-en-2-ol (1.70 g, 7.38 mmol; 98%) that was taken forward in the hydrogenation step detailed below.

9-[(2*S*,3*R*)-2-(*tert*-Butyldimethylsilyloxy)hexan-3-yl]-6-chloro-9*H*-purine

10% Palladium on charcoal (100 mg) was added to a mixture of (2*S*,3*S*,*E*)-2-(*tert*-butyldimethylsilyloxy)hex-4-en-3-ol and (2*S*,3*S*,*E*)-3-(*tert*-butyldimethylsilyloxy)hex-4-en-2-ol (1.68 g, 7.29 mmol) dissolved in ethanol (20 mL). The mixture was hydrogenated for 18 h at room temperature under hydrogen (1 atm). TLC (5% EtOAc / light petroleum) indicated consumption of starting material and the reaction mixture was filtered, washing with ethanol (2 x 30 mL). The filtrate was concentrated *in vacuo* to give a mixture of crude (2*S*,3*S*)-2-(*tert*-butyldimethylsilyloxy)hexan-3-ol and (2*S*,3*S*)-3-(*tert*-butyldimethylsilyloxy)hexan-2-ol (1.43 g). To a solution of this mixture in THF (50 mL) was added diisopropyl azodicarboxylate (2.51 mL, 12.9 mmol), triphenylphosphine (2.54 g, 9.68 mmol) and 6-chloro-9*H*-purine (1.30 g, 8.39 mmol). After 18 h at room temperature the reaction mixture was filtered through a short silica pad, washing with petroleum / EtOAc (3:1, 100 mL). The filtrate was evaporated at reduced pressure to give a crude oil that was chromatographed on a silica gel column (80 g). Gradient elution with light petroleum (100 mL) followed by light petroleum / EtOAc (98:2, 200 mL; 96:4, 100 mL; 94:6, 100 mL; 92:8, 100 mL) gave 9-[(2*S*,3*R*)-2-(*tert*-butyldimethylsilyloxy)hexan-3-yl]-6-chloro-9*H*-purine (251 mg, 0.68 mmol) and 9-[(2*S*,3*S*)-3-(*tert*-butyldimethylsilyloxy)hexan-2-yl]-6-chloro-9*H*-purine (171 mg, 0.46 mmol). 9-[(2*S*,3*R*)-2-(*tert*-Butyldimethylsilyloxy)hexan-3-yl]-6-chloro-9*H*-purine: δ_H (200 MHz; $CDCl_3$) 8.71 (1 H, s), 8.17 (1 H, s), 4.56 (1 H, dt, *J* 11.4 & 4.0, chain H-3), 4.10 (1 H, qd, *J* 6.2 & 4.1, chain H-2), 2.24 - 1.89 (2 H, m), 1.21 - 0.99 (2 H, m), 1.18 (3 H, d, *J* 6.3), 0.87 (3 H, t, *J* 6.5), 0.86 (9 H, s), -0.02 (3 H, s), -0.19 (3 H, s). 9-[(2*R*,3*S*)-3-(*tert*-Butyldimethylsilyloxy)hexan-2-yl]-6-chloro-9*H*-purine: δ_H (200 MHz; $CDCl_3$) 8.73 (1 H, s), 8.18 (1 H, s), 4.88 (1 H, qd, *J* 7.1 & 3.1, chain H-2), 4.02 - 3.94 (1 H, m, chain H-3), 1.61 (3 H, d, *J* 7.1), 1.61 - 0.13 (4 H, m), 0.98 (3 H, t, *J* 6.5), 0.84 (9 H, s), -0.09 (3 H, s), -0.51 (3 H, s).

9-[(2*S*,3*R*)-2-(t*ert*-Butyldimethylsilyloxy)hexan-3-yl]-9*H*-purin-6-amine

A mixture of 9-[(2*S*,3*R*)-2-(*tert*-butyldimethylsilyloxy)hexan-3-yl]-6-chloro-9*H*-purine (251 mg, 0.68 mmol) in aqueous ammonia (SG 0.880; 3.0 mL) was heated at 100 ℃ in a sealed tube for 18 h. TLC (5% MeOH / CH_2Cl_2) indicated formation of a new component (R_f 0.24). The reaction mixture was cooled and extracted with EtOAc (3 x 20 mL). The combined organic extracts were washed with brine (15 mL), dried with Na_2SO_4 and evaporated under reduced pressure to give a crude white solid that was chromatographed on a silica gel column (20 g). Gradient elution with CH_2Cl_2 (100 mL); followed by CH_2Cl_2 / MeOH (99:1, 100 mL; 98:2, 100 mL; 97:3, 100 mL) gave 9-[(2*S*,3*R*)-2-(*tert*-butyldimethylsilyloxy)hexan-3-yl]-9*H*-purin-6-amine (186 mg, 0.53 mmol; 78%): δ_H (200 MHz; $CDCl_3$) 8.35 (1 H, s), 7.86 (1 H, s), 5.69 (2 H, br s), 4.45 (1 H, dt, *J* 11.2 & 4.3, chain H-3), 4.11 (1 H, qd, *J* 6.3 & 4.1, chain H-2), 2.20 - 1.87 (2 H, m), 1.19 - 1.04 (2 H, m), 1.17 (3 H, d, *J* 6.3), 0.88 (3 H, t, *J* 6.5), 0.88 (9 H, s), -0.02 (3 H, s), -0.19 (3 H, s).

(2*S*,3*R*)-3-(6-Amino-9*H*-purin-9-yl)hexan-2-ol (HWC-60)

Tetrabutylammonium fluoride (1 M THF solution; 1.03 mL, 1.03 mmol) was added to a solution of 9-[(2*S*,3*R*)-2-(*tert*-butyldimethylsilyloxy)hexan-3-yl]-9*H*-purin-6-amine (180 mg, 0.52 mmol) in THF (10 mL) at room temperature and stirred for 18 h. TLC (1:1 EtOAc / acetone) indicated consumption of starting material (R_f 0.64) and formation of a product component (R_f 0.26). The reaction mixture was evaporated to give a crude residue that was dissolved in EtOAc (50 mL), washed with brine (3 x 10 mL), dried with Na_2SO_4, filtered and concentrated *in vacuo* to give a crude oil. The crude material was chromatographed on a silica gel column (15 g). Gradient elution with CH_2Cl_2 / MeOH (98:2, 250 mL; 95:5, 300 mL) gave partially purified (2*S*,3*R*)-3-(6-amino-9*H*-purin-9-yl)hexan-2-ol (R_f 0.26, 116 mg) as a colourless oil. The partially purified material was re-chromatographed on a silica gel column (15 g). Gradient elution with EtOAc / acetone (1.5:1, 250 mL; 1:1, 200 mL) gave (2*S*,3*R*)-3-(6-amino-9*H*-purin-9-yl)hexan-2-ol (R_f 0.26) (67 mg, 0.29 mmol; 55%) as a white amorphous solid: δ_H (200 MHz; $CDCl_3$) 8.22 (1 H, s), 7.83 (1 H, s), 6.81 (2 H, br s), 5.72 (1 H, br s), 4.35 (1 H, dt, *J* 11.0 & 3.2), 4.18 (1 H, qd, *J* 6.5 & 2.9, chain H-2), 2.15 - 1.77 (2 H, m), 1.22 (3 H, d, *J* 7.1), 1.22 - 0.98 (2 H, m), 0.81 (3 H, t, *J* 7.2); δ_C (50 MHz; $CDCl_3$) 156.10 (C), 152.51 (CH), 149.84 (C), 140.35 (CH), 119.64 (C), 69.37 (CH), 62.39 (CH), 29.71 (CH_2), 20.23 (CH_3), 19.48 (CH_2), 13.71 (CH_3); (found: C, 55.26; H, 7.30; N, 28.79. $C_{11}H_{17}N_5O$/0.29 H_2O requires C, 54.93; H, 7.37; N, 29.12%).

(*rac*)-9-(octan-3-yl)-9*H*-purin-6-amine (HWC-62)

(*rac*)-6-Chloro-9-(octan-3-yl)-9*H*-purine

Diisopropyl azodicarboxylate (1.50 mL, 8.00 mmol) was added to a stirred mixture of octan-3-ol (0.76 mL, 4.8 mmol), 6-chloro-9*H*-purine (618 mg, 4.00 mmol) and triphenylphosphine (1.60 g, 6.00 mmol) in THF (30 mL) at room temperature. After 18 h TLC (80% light petroleum / EtOAc) indicated formation of a product component (R_f 0.35). The reaction mixture was concentrated *in vacuo* and filtered through a short silica gel column, washing with light petroleum / EtOAc (1:1). Evaporation of the filtrate gave a crude yellow oil that was chromatographed on a silica gel column (60 g). Elution with light petroleum / EtOAc (9:1, 1 L; 7:1, 800 mL) gave 6-chloro-9-(decan-3-yl)-9*H*-purine (825 mg, 3.10 mmol; 77%) as a dense yellow oil: δ_H (200 MHz; $CDCl_3$) 8.71 (1 H, s), 8.09 (1 H, s), 4.56 - 4.41 (1 H, m), 2.11 - 1.81 (4 H, m), 1.33 - 0.95 (6 H, m), 0.82 - 0.75 (6 H, m); δ_C (50 MHz; $CDCl_3$) 152.19 (C), 151.80 (CH), 151.08 (C), 144.08 (CH), 131.85 (C), 59.96 (CH), 34.61 (CH_2), 31.30 (CH_2), 28.19 (CH_2), 25.86 (CH_2), 22.42 (CH_2), 13.96 (CH_3), 10.73 (CH_3).

(*rac*)-9-(Octan-3-yl)-9*H*-purin-6-amine (HWC-62)

A mixture of 6-chloro-9-(octan-3-yl)-9*H*-purine (323 mg, 1.21 mmol) and aqueous ammonia (SG 0.880; 4.5 mL) was heated at 100 ℃ in a 5 mL sealed pressure tube for 18 h. TLC (95:5 CH_2Cl_2 / MeOH) indicated conversion of starting material (R_f 0.72) into product (R_f 0.22). The reaction mixture was evaporated to give a crude waxy solid that was chromatographed on a silica gel column (15 g). Elution with CH_2Cl_2 / MeOH (95:5, 100 mL) gave 9-(octan-3-yl)-9*H*-purin-6-amine (R_f 0.22) (286 mg, 1.16 mmol; 96%) as a pale yellow solid: δ_H (200 MHz; $CDCl_3$)

8.31 (1 H, s), 7.62 (1 H, s), 6.51 (2 H, br s), 4.45 - 4.31 (1 H, m), 2.04 - 1.75 (4 H, m), 1.29 - 0.95 (6 H, m), 0.77 (6 H, t, *J* 7.3); δ_C (50 MHz; $CDCl_3$) 155.95 (C), 152.79 (CH), 150.39 (C), 139.06 (CH), 119.83 (C), 57.76 (CH), 34.77 (CH_2), 31.37 (CH_2), 28.32 (CH_2), 25.83 (CH_2), 22.44 (CH_2), 13.97 (CH_3), 10.69 (CH_3). 9-(Octan-3-yl)-9*H*-purin-6-amine was evaluated as its hydrochloride salt**,** formed by treatment with a solution of hydrogen chloride in ether followed by evaporation: (found: C, 49.22; H, 7.81; N, 21.64. $C_{13}H_{21}N_5$/1.63 HCl/0.70 H_2O requires C, 48.89; H, 7.58; N, 21.93%).

Procedure for the preparation of 9-(decan-1-yl)-9*H*-purin-6-amine (HWC-64)

6-Chloro-9-(decan-1-yl)-9*H*-purine

Diisopropyl azodicarboxylate (1.8 mL, 9.3 mmol) was added to a stirred solution of decan-1-ol (1.1 g, 6.9 mmol), 6-chloro-9*H*-purine (720 mg, 4.66 mmol) and triphenylphosphine (1.8 g, 6.9 mmol) in THF (30 mL) at ambient temperature. After 18 h TLC (9:1 light petroleum / EtOAc) indicated formation of a product component (R_f 0.2). The reaction mixture was filtered through a short silica gel column, washing with light petroleum / EtOAc (1:1). The filtrate was evaporated and the resulting red oil was chromatographed on flash silica gel (gradient elution with 15-20% EtOAc / light petroleum) to give 6-chloro-9-(decan-1-yl)-9*H*-purine (1.30 g, 4.41 mmol; 96%) as a pale brown powder: δ_H 8.74 (1 H, s), 8.11 (1 H, s), 4.28 (2 H, t, *J* 7.2), 1.92 (2 H, ~quintet, *J* 7.0), 1.41 - 1.13 (14 H, m), 0.6 (3 H, ~t, *J* 6.4).

9-(Decan-1-yl)-9*H*-purin-6-amine (HWC-64)

A mixture of 6-chloro-9-(decan-1-yl)-9*H*-purine (300 mg, 1.02 mmol) and aqueous ammonia (SG 0.880; 3 mL) was heated at 100 ℃ in a 5 mL sealed pressure tube for 18 h. TLC (2% MeOH / CH_2Cl_2) indicated conversion of starting material (R_f 0.45) to a product component (R_f 0.1). The reaction mixture was extracted with EtOAc; the extract was washed with saturated brine, dried (Na_2SO_4) and evaporated. The resulting crude white solid (282 mg) was chromatographed on a silica gel column. Elution with 2% MeOH / CH_2Cl_2 gave 9-(decan-1-yl)-9*H*-purin-6-amine (203 mg, 0.737 mmol; 72%) as a white solid: δ_H (200 MHz; $CDCl_3$) 8.35 (1 H, s), 7.78 (1 H, s), 6.32 (2 H, br s), 4.16 (2 H, t, *J* 7.1), 1.86 (2 H, ~quintet, *J* 6.5), 1.40 - 1.15 (14 H, m), 0.88 (3 H, ~t, *J* 6.9); δ_C (101 MHz, $CDCl_3$) 155.73 (C), 152.91 (CH), 150.07 (C), 140.32 (CH), 119.68 (C), 43.95 (CH_2), 31.82 (CH_2), 30.08 (CH_2), 29.43 (CH_2), 29.40 (CH_2), 29.21 (CH_2), 29.03 (CH_2), 26.65 (CH_2), 22.63 (CH_2), 14.08 (CH_3). 9-(Decan-1-yl)-9*H*-purin-6-amine was evaluated as its hydrochloride salt**,** formed by treatment with a solution of hydrogen chloride in ether followed by evaporation: (found: C, 56.83; H, 8.39; N, 22.06. $C_{15}H_{25}N_5$/1.15 HCl requires C, 56.78; H, 8.31; N, 22.06%).

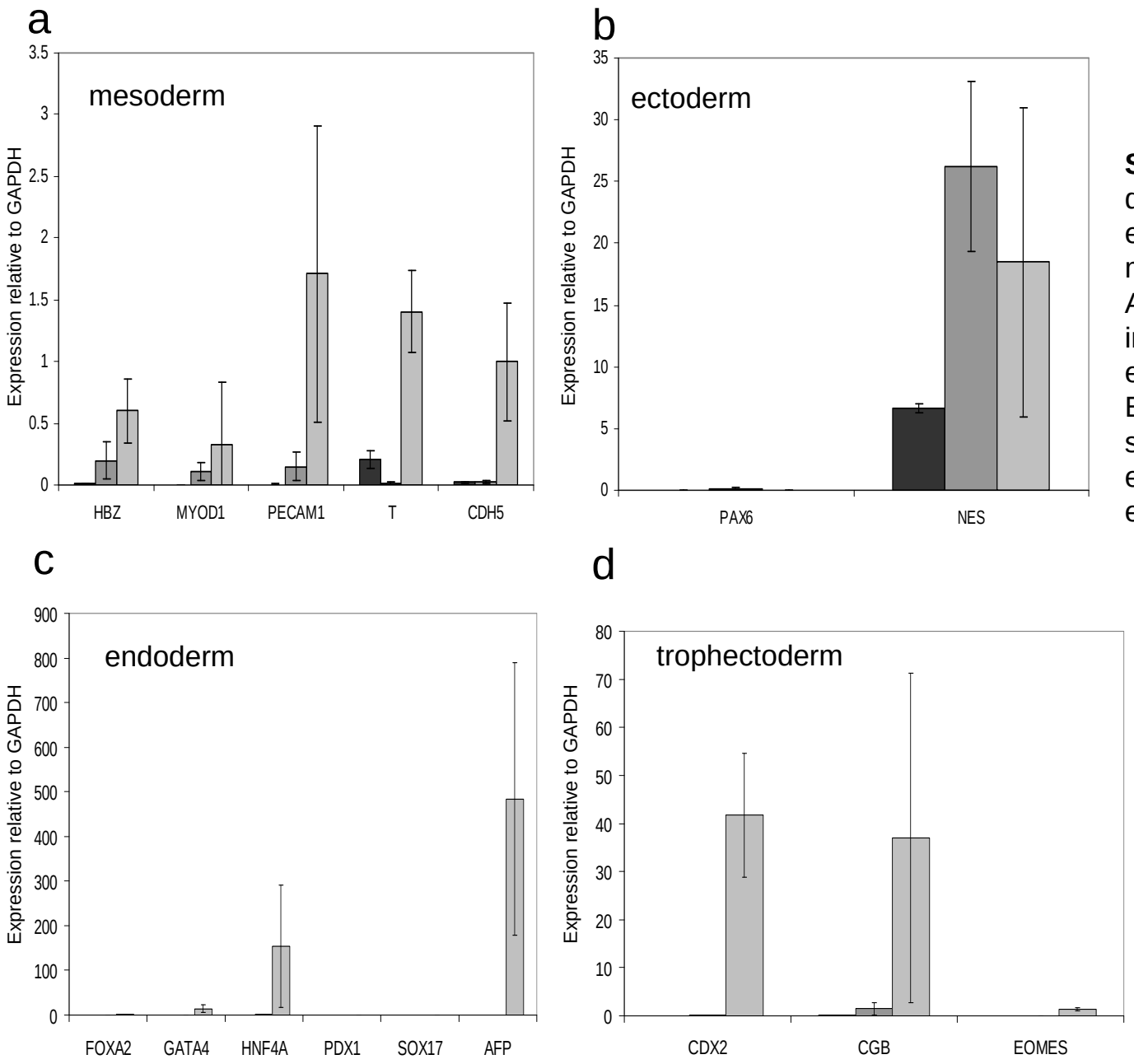

Supplementary Figure 1. EHNA inhibits differentiation to mesoderm (a), ectoderm (b), endoderm (c) or trophectoderm (d) over multiple passages in the absence of FGF. Analysis of mRNA from cells passaged to p8 in standard feeder free media (FF, ■), without exogenous FGF but supplemented with 10μM EHNA (No FGF/+EHNA media (NFE, ▩) and standard feeder free conditions without exogenous FGF and EHNA (NF, □). Gene expression is relative to GAPDH expression

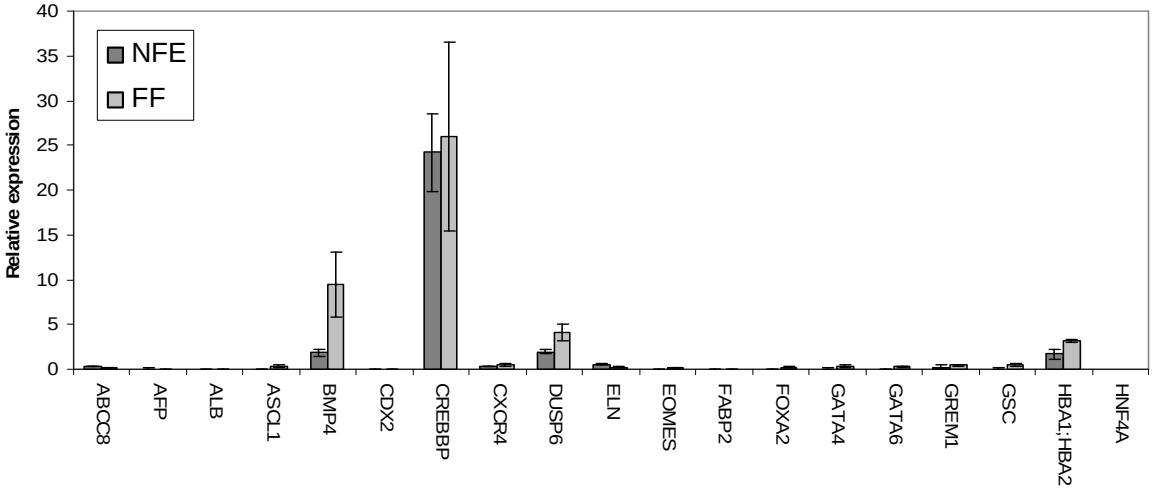

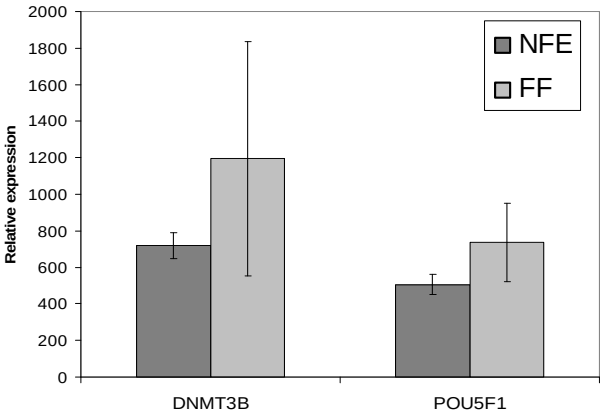

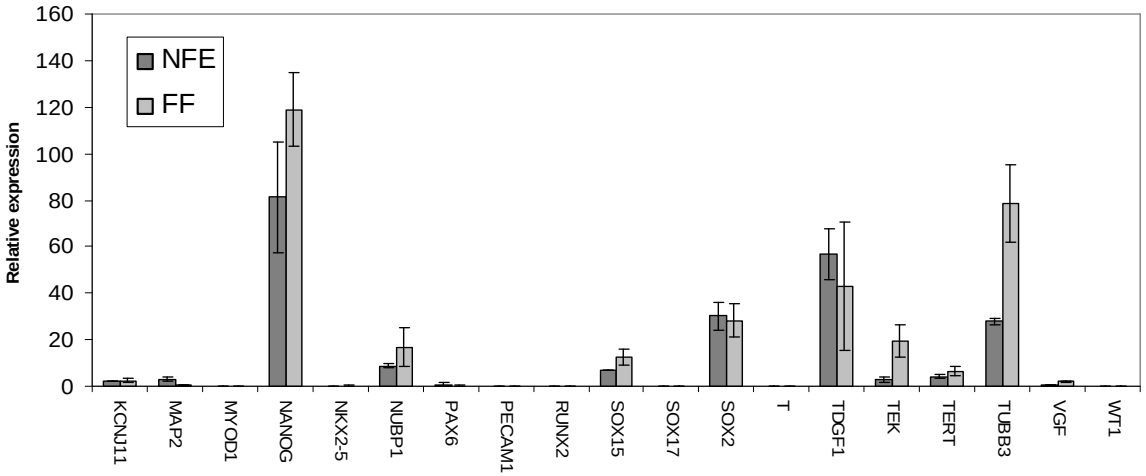

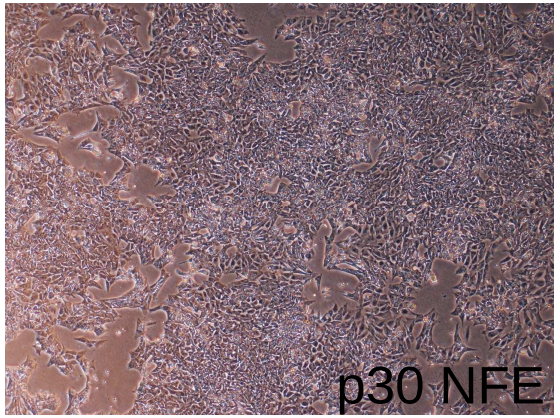

Supplementary Figure 2. Standard hESC expression profile is maintained by EHNA in the absence of FGF for up to 30 passages. Analysis of mRNA from cells passaged in standard feeder free media (FF) or standard feeder free conditions without exogenous FGF but supplemented with 10 μM EHNA (NFE). Gene expression is relative to GAPDH expression. The phase image is of hESCs grown in EHNA (NFE) for 30 passages post FGF withdrawl.

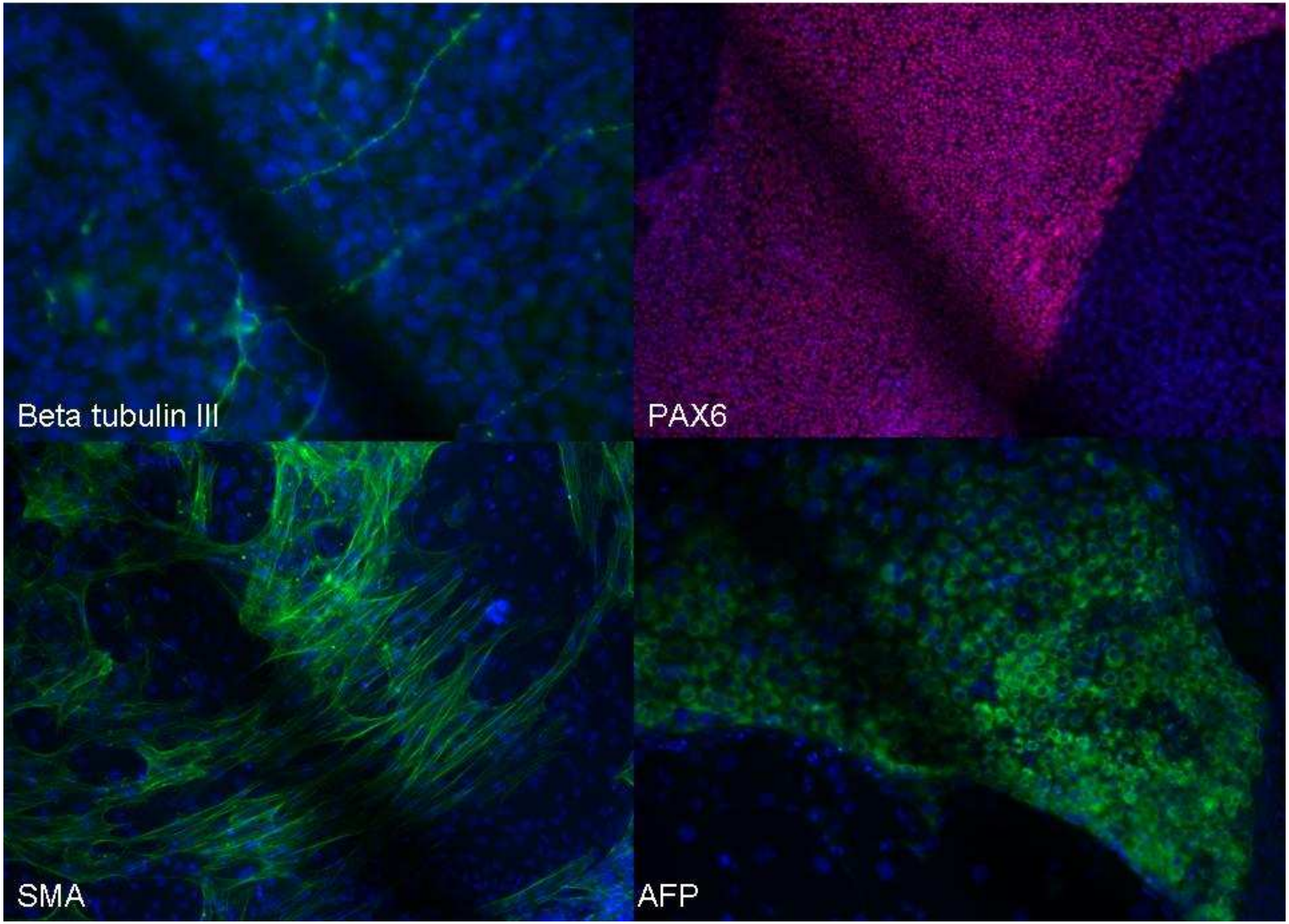

Supplementary Figure 3. Cells grown with EHNA in the absence of exogenous FGF can differentiate into cells expressing markers of all three germ layers after at least 22 passages. After growth for 22 passages in the presence of EHNA instead of FGF hESCs were transferred to matrigel coated dishes or formed into embryoid bodies, and differentiated for 4 weeks in 20% fetal calf serum. Immunostaining for beta tubulin III (ectoderm), PAX6 (ectoderm), smooth muscle actin (SMA) (mesoderm) and AFP (endoderm). Specific antibodies are in either green or red and all cells were also stained with DAPI (blue). Magnification x10.

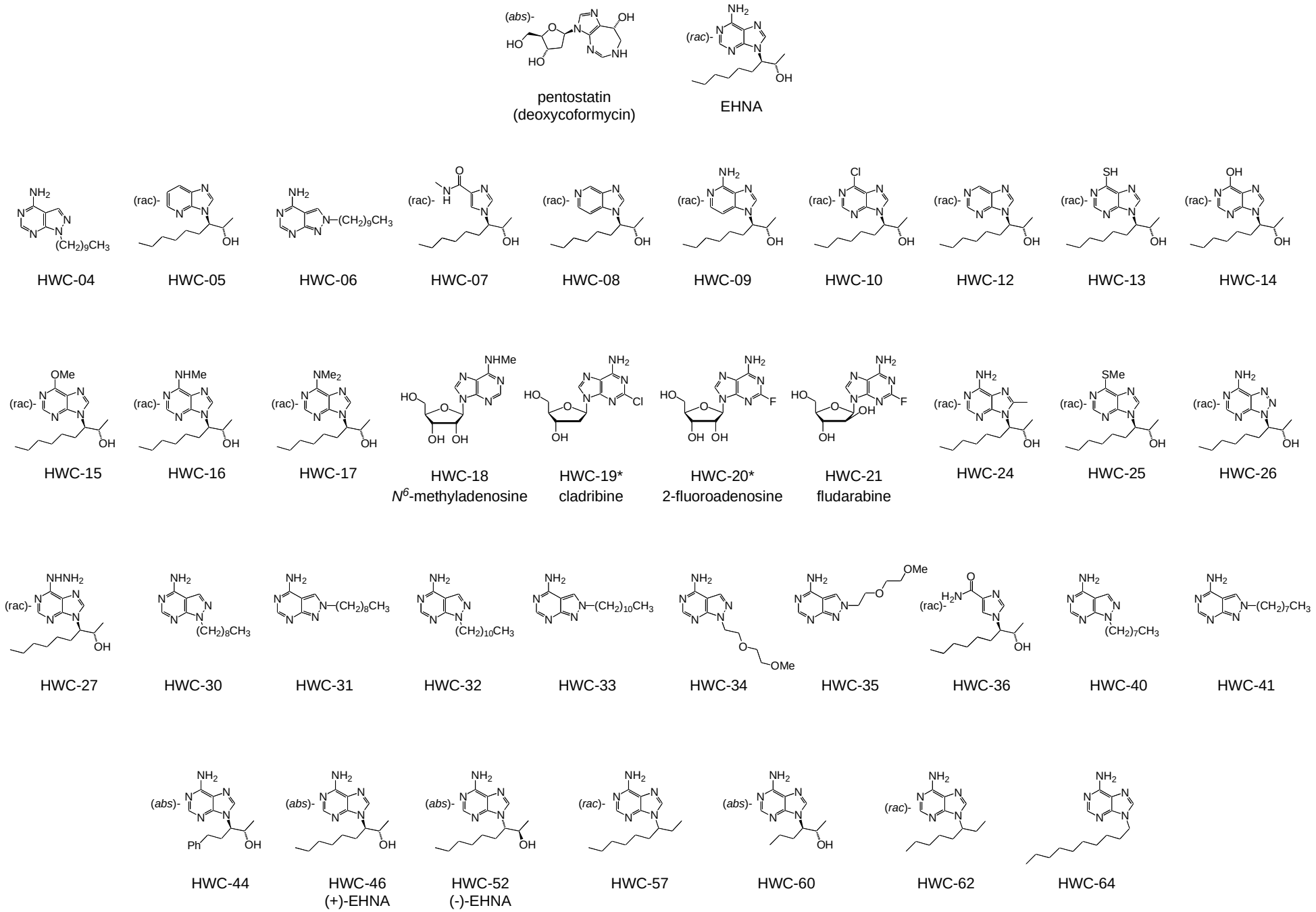

Supplementary Figure 4. Structures of compounds tested for hESC maintenance effect. †The solubility HWC-04 and HWC-32 (even in hydrochloride form) was poor, precluding assessment of these compounds. *Cladribine and 2-fluoroadenosine, nucleoside analogues with modest ADA-inhibitory activity, showed no activity at sub-toxic concentrations (10 µM); their toxicity to hESCs precluded assessment at higher concentrations.

a

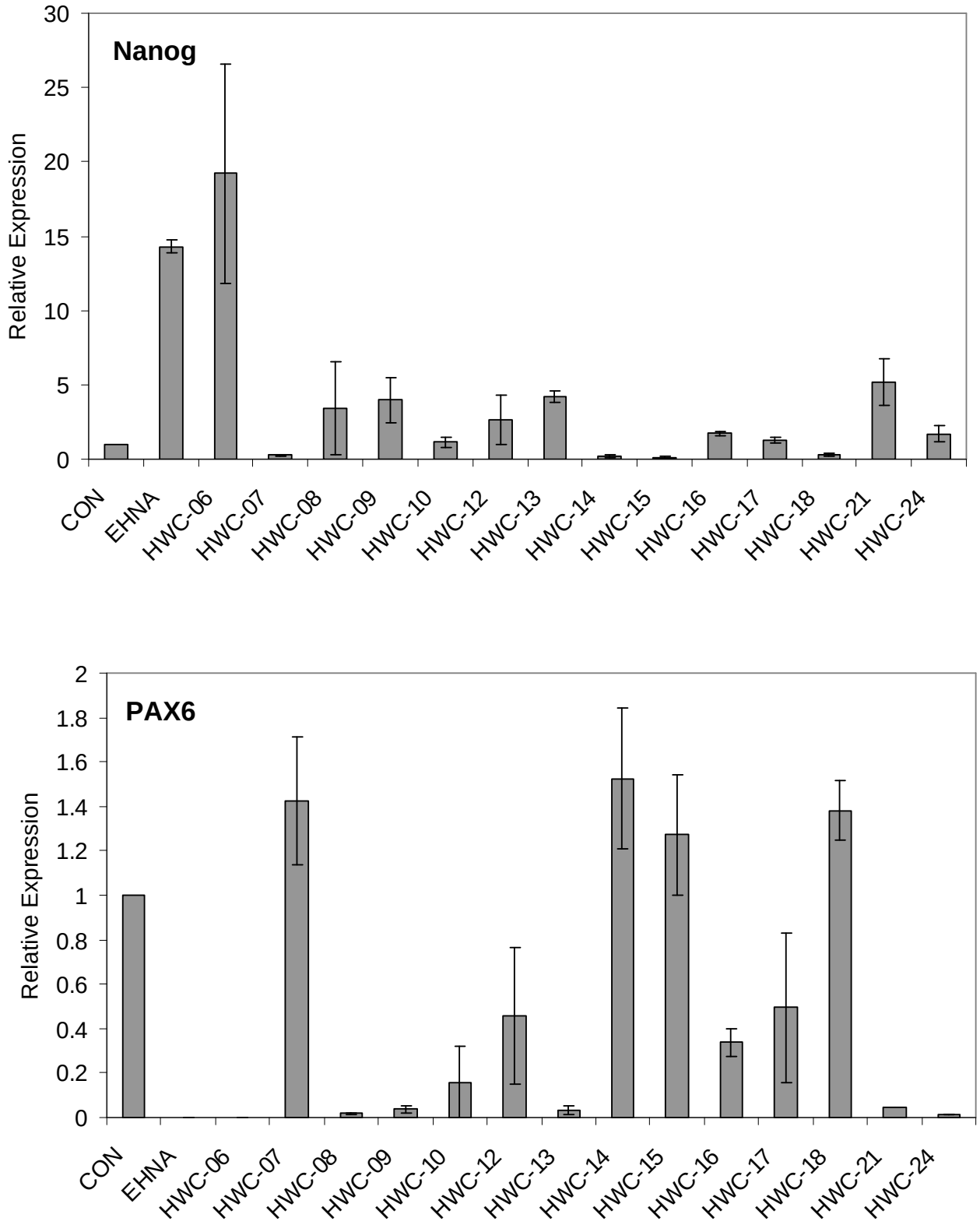

Supplementary Figure 5. Summary of the HWC data. hESCs were plated onto matrigel coated 12 well dishes and differentiated for 14 days in defined media (with and without compound addition) then harvested and analysed by qRT-PCR. Compounds and media were changed every 2 days. Data represents mean ± SEM from three experiments. Expression is relative to expression in the untreated control samples. Each section of the figure represents a separate experiment hence the need for separate controls. **(a) HWC-06 – HWC-24**

b

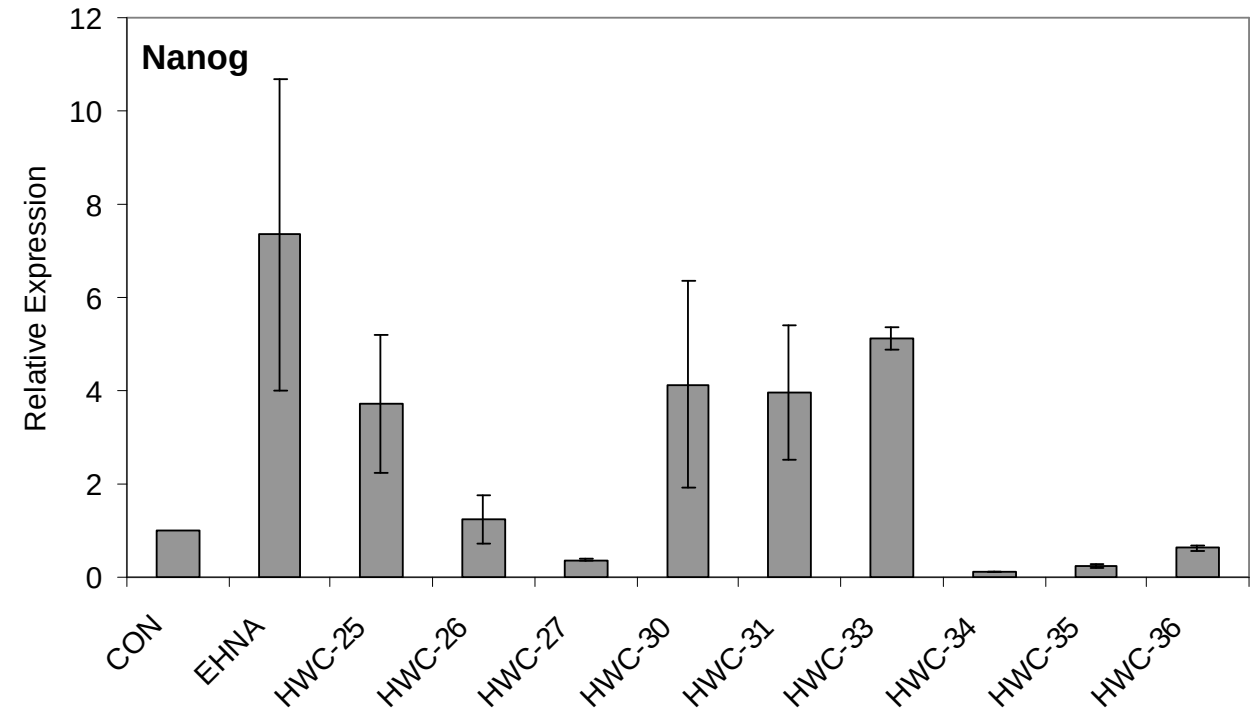

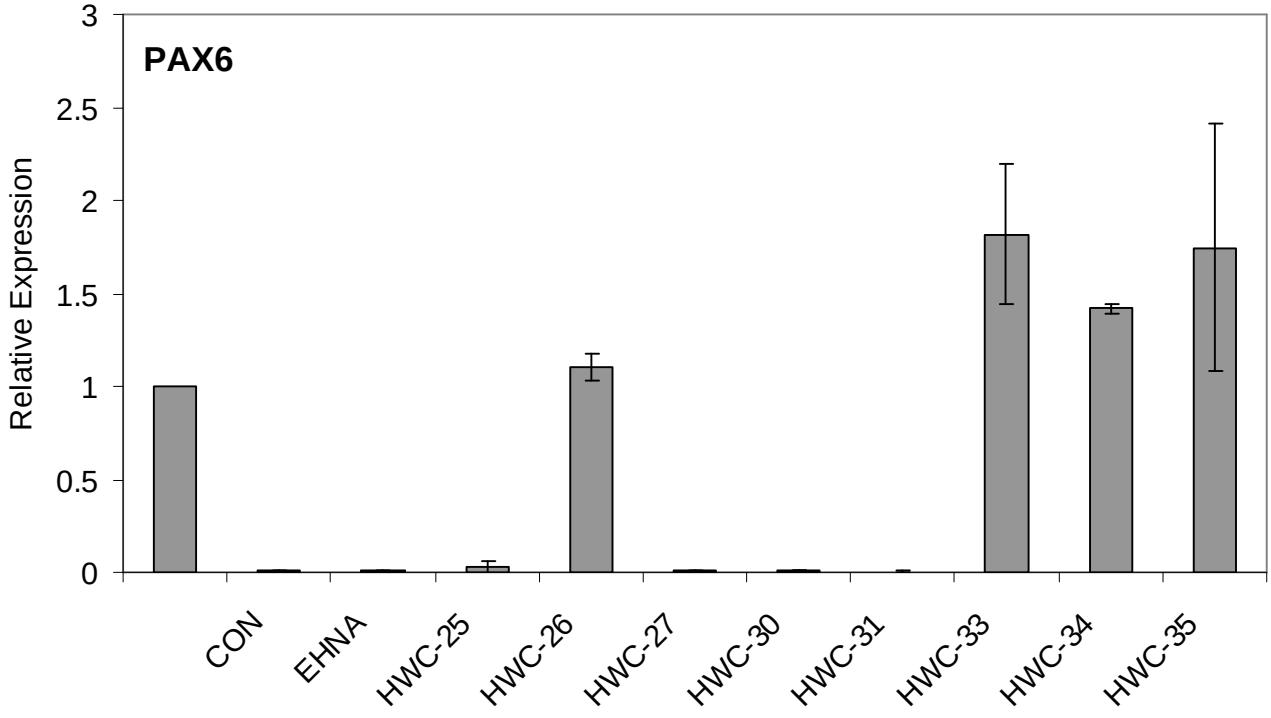

Supplementary Figure 5b. HWC-25 – HWC-36

C

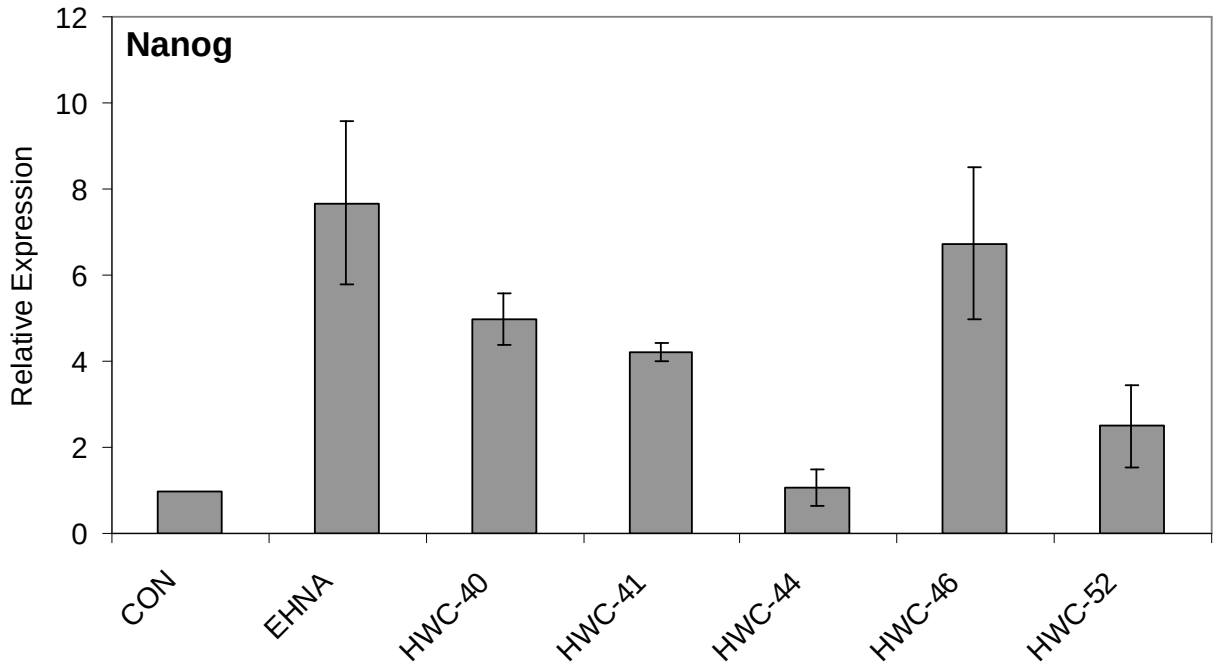

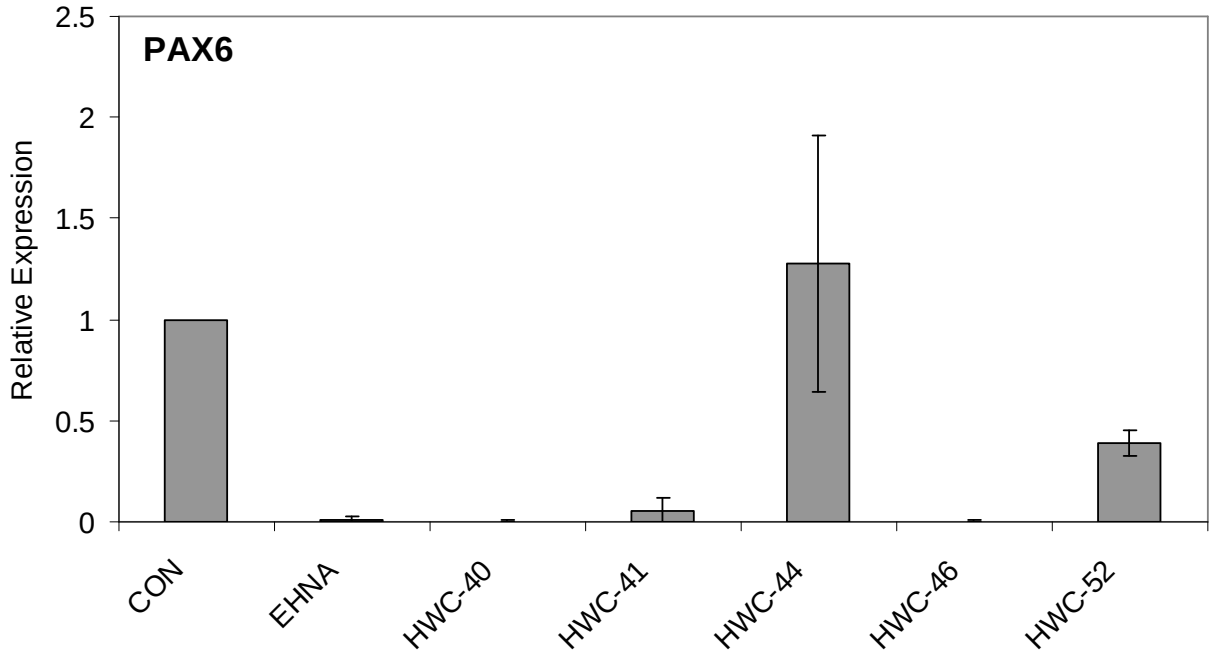

Supplementary Figure 5c. HWC-40 – HWC-52

d

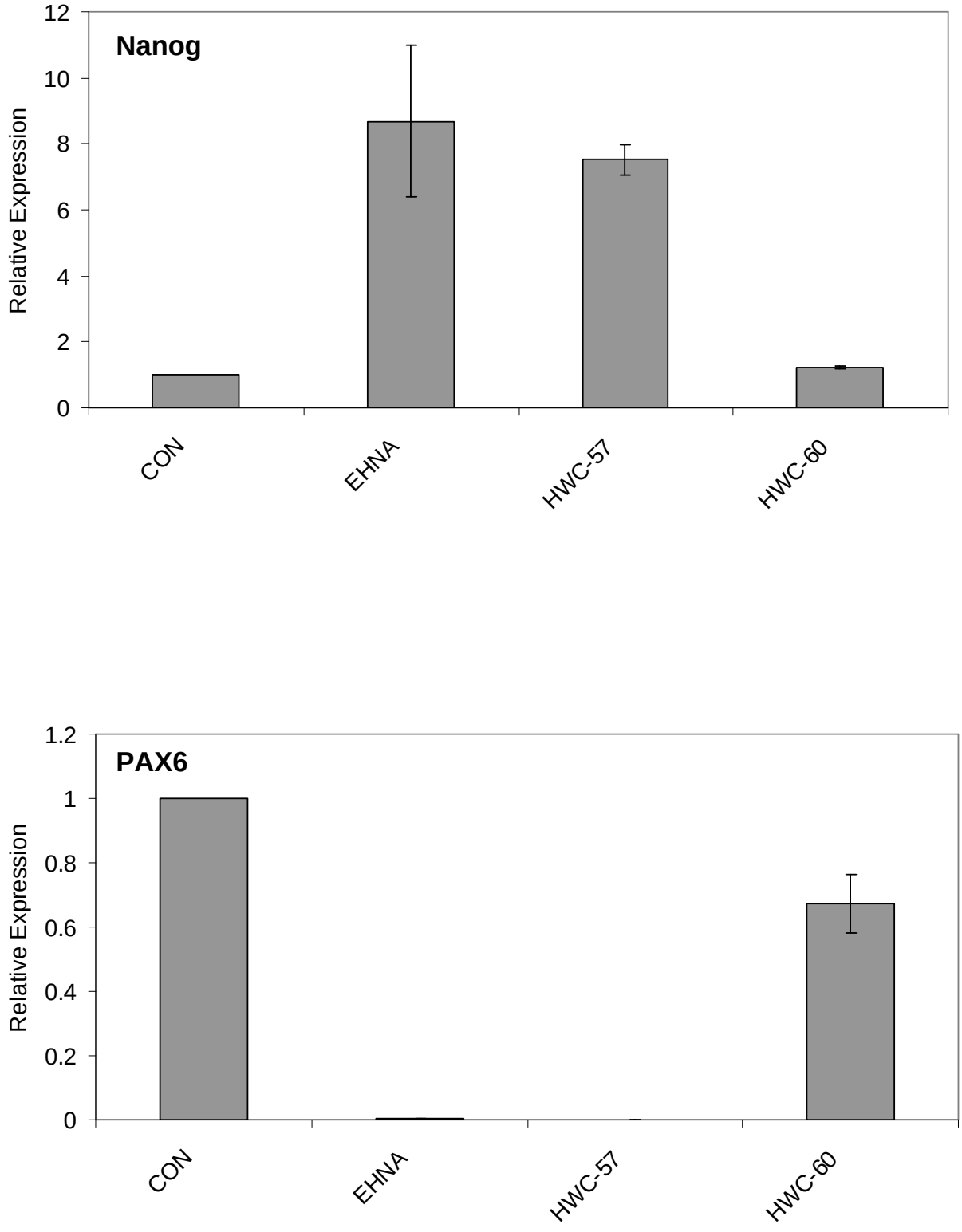

Supplementary Figure 5d. HWC-57 – HWC-60

e

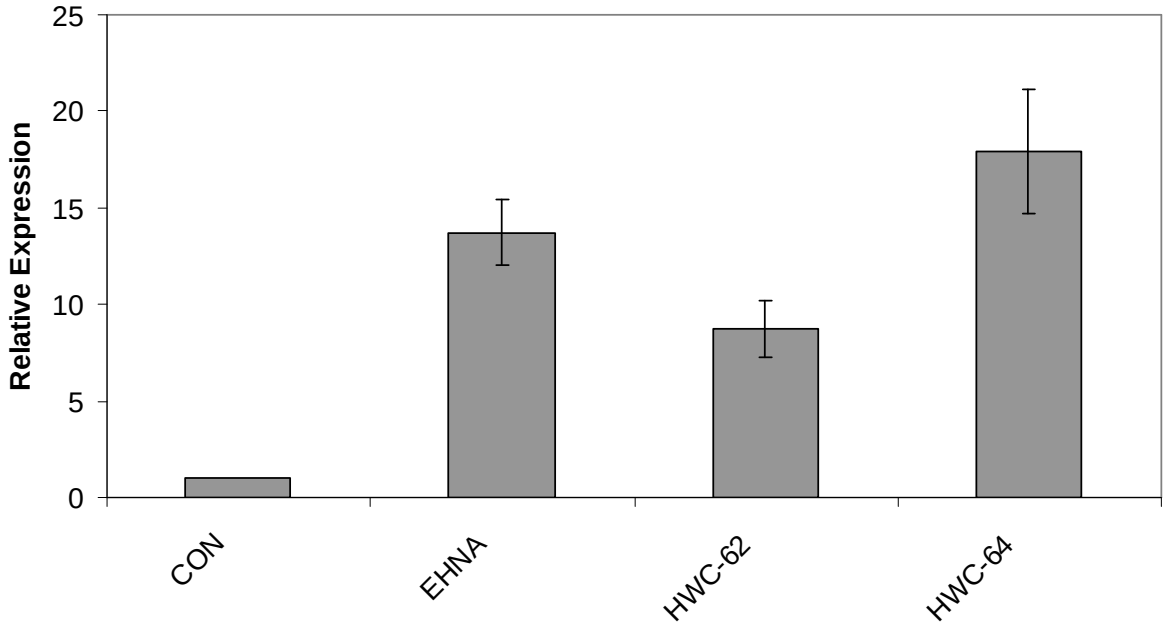

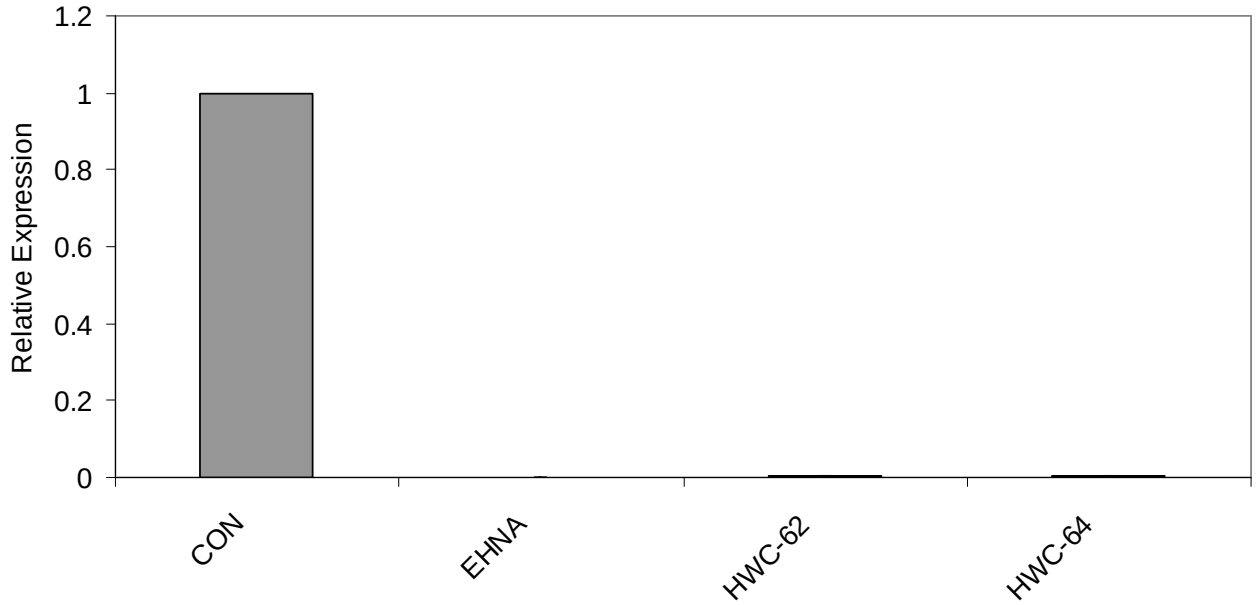

Supplementary Figure 5e. HWC-62 – HWC-64

	hwc5	hwc6	enha	pent
MKK1	73	84	90	94
ERK1	108	92	95	101
ERK2	73	61	84	138
JNK1	101	97	96	100
JNK2	89	83	93	86
p38a MAPK	76	90	77	107
P38b MAPK	110	101	97	112
p38g MAPK	83	80	80	81
p38s MAPK	101	135	90	95
ERK8	81	70	83	82
RSK1	74	90	93	102
RSK2	102	98	104	97
PDK1	92	105	94	92
PKBa	86	80	91	87
PKBb	90	92	118	101
SGK1	98	92	88	98
S6K1	87	68	90	97
PKA	82	90	87	89
ROCK 2	80	68	83	87
PRK2	96	121	101	96
PKCa	95	102	105	109
PKC zeta	87	86	89	92
PKD1	76	61	61	58
MSK1	73	70	88	85
MNK1	103	102	108	98
MNK2	99	92	90	98
MAPKAP-K2	102	96	93	91
PRAK	99	85	96	93
CAMKKb	90	88	97	80
CAMK1	83	74	115	85
SmMLCK	79	82	85	92
PHK	99	94	107	91
CHK1	78	72	83	88
CHK2	84	70	90	94
GSK3b	87	80	96	98
CDK2-Cyclin A	83	86	86	85
PLK1	103	107	115	101
PLK1 (Okadaic Acid)	101	97	98	94
Aurora B	124	106	99	100
AMPK	101	84	88	92

	hwc5	hwc6	enha	pent
MARK3	99	94	102	101
BRSK2	86	82	91	85
MELK	111	101	90	111
CK1	95	94	90	95
CK2	108	101	98	104
DYRK1A	114	104	109	97
DYRK2	85	80	87	99
DYRK3	98	91	101	94
NEK2a	90	88	91	101
NEK6	93	92	90	86
IKKb	94	84	100	94
PIM1	90	71	92	95
PIM2	91	80	92	95
PIM3	79	82	88	83
SRPK1	81	79	91	98
MST2	91	91	95	102
EF2K	90	84	86	93
HIPK2	93	96	96	90
PAK4	90	69	88	95
PAK5	69	66	87	162
PAK6	89	82	95	89
Src	90	63	88	88
Lck	102	73	88	98
CSK	86	83	88	86
FGF-R1	88	79	92	72
IRR	99	90	94	113
EPH A2	111	94	99	96
MST4	87	78	99	83
SYK	102	80	115	99
YES1	100	74	91	81
IKKe	72	91	90	102
TBK1	107	99	88	94
IGF-1R	100	83	115	117
VEG-FR	90	78	89	103
BTK	100	81	108	104
IR-HIS	99	97	100	82
EPH-B3	113	124	101	107
TBK1 (DU12569)	95	96	89	97
IKK epsilon (14231)	92	94	95	113

Supplementary Figure 6. EHNA does not have inhibitory activity against a panel of common kinases.

Kinase screen of EHNA, pentostatin, HWC-05 and HWC-06 all assayed at 30 μM

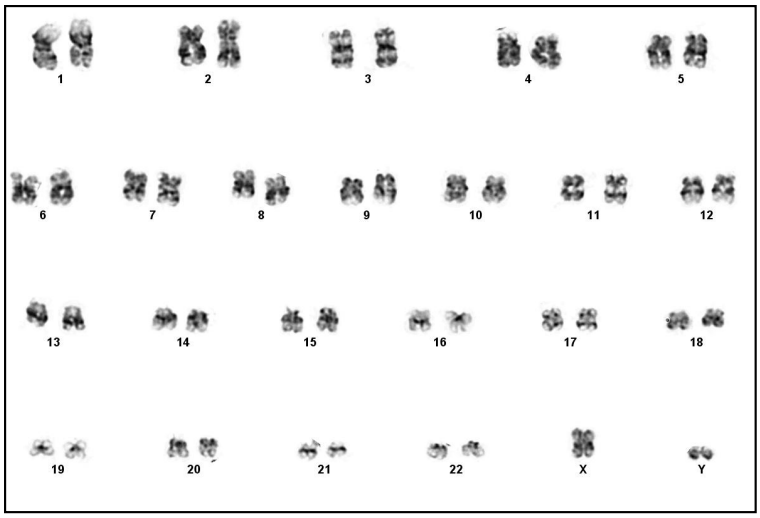

EHNA p10

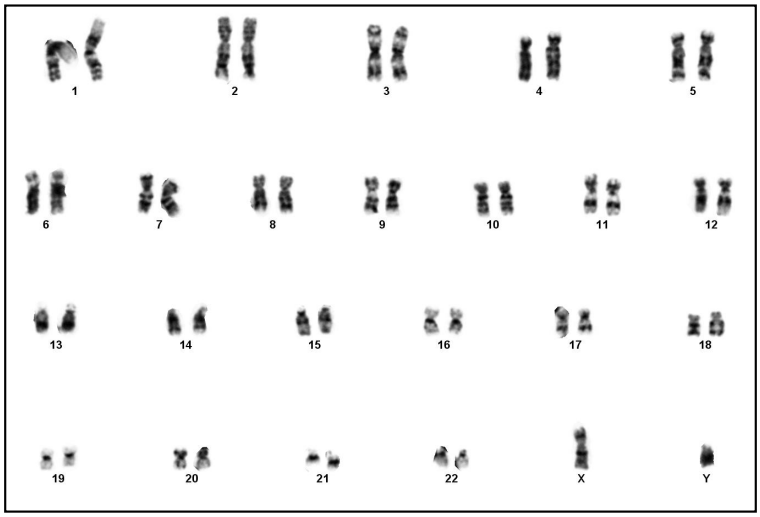

HWC57 p22

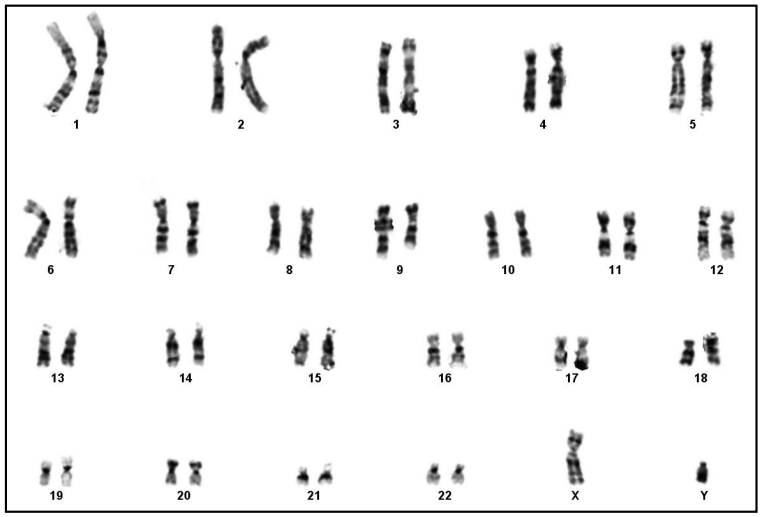

HWC64 p22

Supplementary Figure 7. Cells maintained in EHNA, HWC57 or HWC64 maintain a normal karyotype. A minimum of 15 cells were examined. This excludes greater than 19% mosaicism with 95% confidence limits. Analysis performed by the Cytogenetics Laboratory, Institute of Medical Genetics, Yorkhill Hospital, Glasgow.